N70-18528 — 18536

CR-107927

OAKLAND UNIVERSITY SCHOOL OF ENGINEERING

SECOND QUARTERLY PROGRESS REPORT

on

ERC/NASA
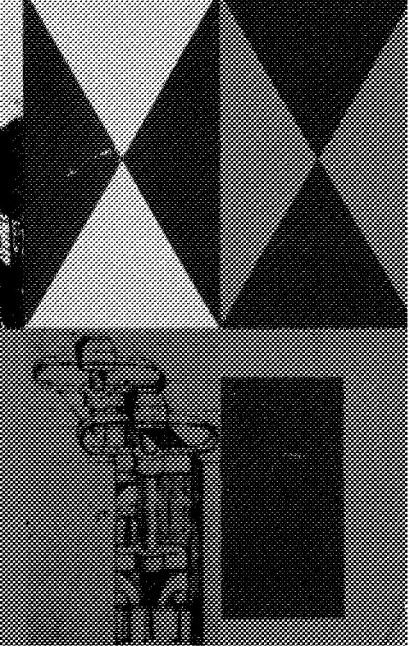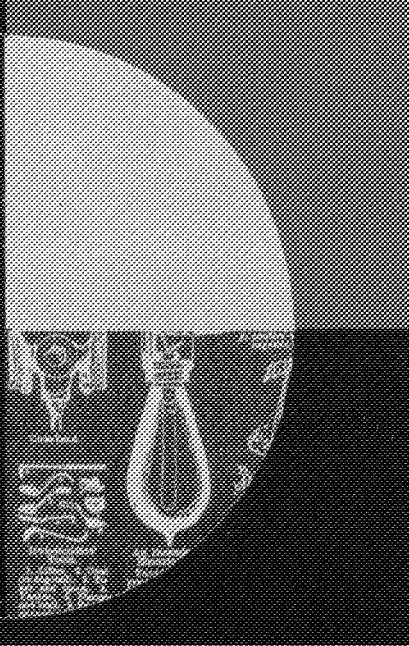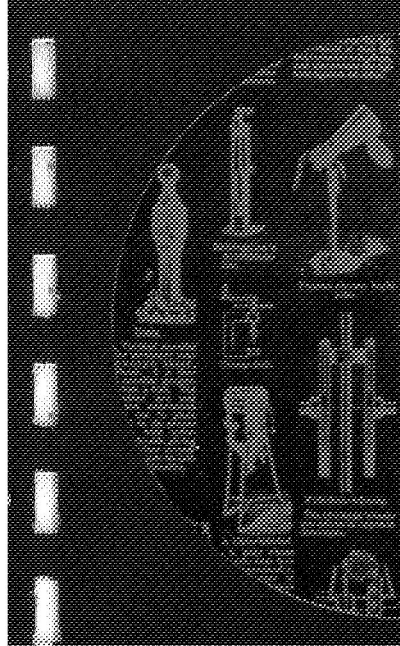
Contract No. NGR 23-054-003
O.U. Account No. 24771

BIOSYSTEMS ENGINEERING RESEARCH

October 30, 1969

SECOND QUARTERLY PROGRESS REPORT

on
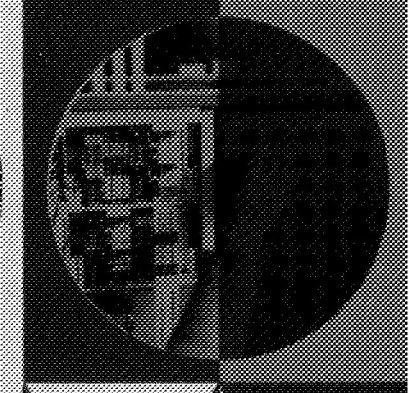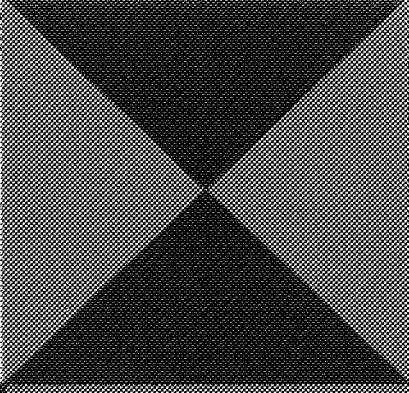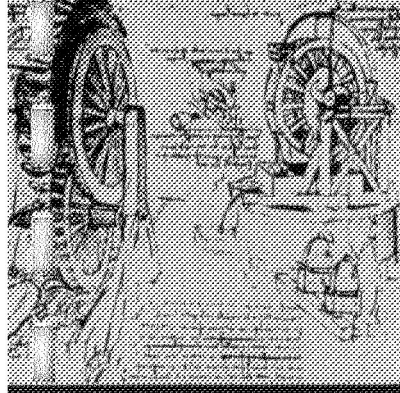
ERC/NASA

Contract No. NGR 23-054-003
O.U. Account No. 24771

BIOSYSTEMS ENGINEERING RESEARCH

· October 30, 1969

School of Engineering
Oakland University
Rochester, Michigan 48063

J. E. Gibson, Principal Investigator
R. H. Edgerton
R. E. Haskell
J. C. Hill

TABLE OF CONTENTS

SECOND QUARTERLY PROGRESS REPORT

ON BIOSYSTEMS ENGINEERING RESEARCH

SECOND QUARTERLY PROGRESS REPORT

on

ERC/NASA

Contract No. NGR 23-054-003

BIOSYSTEMS ENGINEERING RESEARCH

J.E. Gibson, Principal Investigator
J.C. Hill
R.E. Haskell
R.H. Edgerton

School of Engineering
Oakland University
Rochester, Michigan 48063

INTRODUCTION

The postural control work during this quarter has re-
sulted in a working computer model of the stick man. At
the request of OCTA the implications of this work are more
fully explored here than in Progress Report No. 1 (PR 1).
Of some concern to this group is the question posed by OCTA
as to the acceptability of this research to physiologists.
Obviously this depends on the individual but we feel that
close relations are maintained with the latest work in the
field. Here are four specific examples of such relations.

- The Department of Biology at Oakland is housed in
  Dodge Hall of Engineering. Several of the investi-
  gators of this team (Hill, Edgerton, Haskell) are
  in daily contact with Physiologists of the department.

  Item: Hill and Edgerton are jointly teaching
  with the Department of Biology a course in Bioengineering.

1

Item: Haskell works directly with the department on the preparation of slides and interpretation of resulting holograms in the research described herein.

- The Institute of Biological Sciences is housed in Dodge Hall of Engineering and daily contact is maintained. Not only is personnel exchanged but equipment and laboratory space are jointly administered.

- Close relations have been established with neurosurgeons at Pontiac General Hospital and joint research has been initiated in several promising areas.

Thus one may say that the relations and cross discussions with Biology, Medicine and Physiology are deep and continuing at Oakland. This specific research effort is only one of more than a half dozen now ongoing and in preparation. This work is neither an isolated nor singular example of the close ties with the life sciences we have established in the past two years. These comments apply as strongly to any one of the tasks reported here as to any other.

An effort has been made here to illustrate the ties to NASA goals of our Bio optics effort. It is believed that the possible applications will be of significant interest. One is tempted in judging an exploratory effort such as this to fall into either of two clichés. If it's relevant, why don't I see plans for hardware? If there isn't any

hardware then it must be basic physics and OCTA doesn't
support basic physics. Our response to the first would be
that it is valid research precisely because we are not sure
it will be useful to build hardware. And secondly, there
is an interesting physical principle here which may be ap-
plicable. Our effort is goal oriented in that we attempt
to bring the principle to a control application. The prin-
ciple is not being examined simply because of its intrinsic
interest.

The work on pattern recognition using coherent optical
techniques is proceeding well and certain results are in-
cluded in this report.

The effort on the human operator control problem has
gone into high gear. Prior to this period Jackson and his
team were completing work in this area on an NSF contract,
the final report of which is enclosed. Jackson and his group
have no further responsibility to NSF and will be devoting
all their efforts to this OCTA research. We believe that
this arrangement has resulted in a cost effective approach
in which OCTA has had the advantage of taking over a research
effort at its point of maximum effectiveness and with no
starting transient involved.

MUSCULAR COORDINATION AND MULTI-DEGREE OF FREEDOM CONTROL SYSTEMS

I. Introduction

In our First Quarterly Progress Report (July 30, 1969) a set of hand-derived equations for the velocity components of the trunk, thigh, shank, foot, upper arm, forearm, and head of the seven element stick man of Figure 1 was presented. Future work was to have been devoted to finding a digital computer method for reliabily carrying out the formation of the expressions for the kinetic and potential energies and the differentiation operations required to obtain the equations of motion using Lagrange's equations.

This work has been completed, and a digital simulation based on these equations is now under development. Preliminary results from this simulation are presented in this report.

After a short summary of the progress to date under this contract, the prior work and concepts that form a context within which the present research is viewed will be presented, and the tasks that must be carried out to provide a satisfactory conclusion to this work will be outlined.

An estimate of the areas in which discovery of control principles useful to NASA seems probable is provided. It is hoped that this section will serve to clarify the relationship of our research to the concerns and goals of NASA/ERC.

4

A more detailed presentation of the symbolic programming techniques used and the results obtained, followed by an estimate of the direction work will take in the immediate future, completes this chapter.

II. Summary of Progress to Date

1. Derivation of the full nonlinear equations of motion of the seven-element stick man (Figure 1 and Figure 1a) has been completed with the use of a digital symbolic processing language (FORMAC).

2. Small angle approximations have been made leading to a linearized model suitable for small deviations from equilibrium.

3. This small angle model has been simulated digitally, and is producing preliminary results which are being used to verify the validity of the equations of motion. Results from this simulation appear later in this report.

4. Experimentation to date has been with an idealized form of control law, with each joint torqued proportional to the joint angular deflection and proportional to the joint angular rate. It should be noted carefully that we make no assertion that this is the form of control law actually used by human beings; this control law is being used merely for convenience in debugging the small angle simulation.
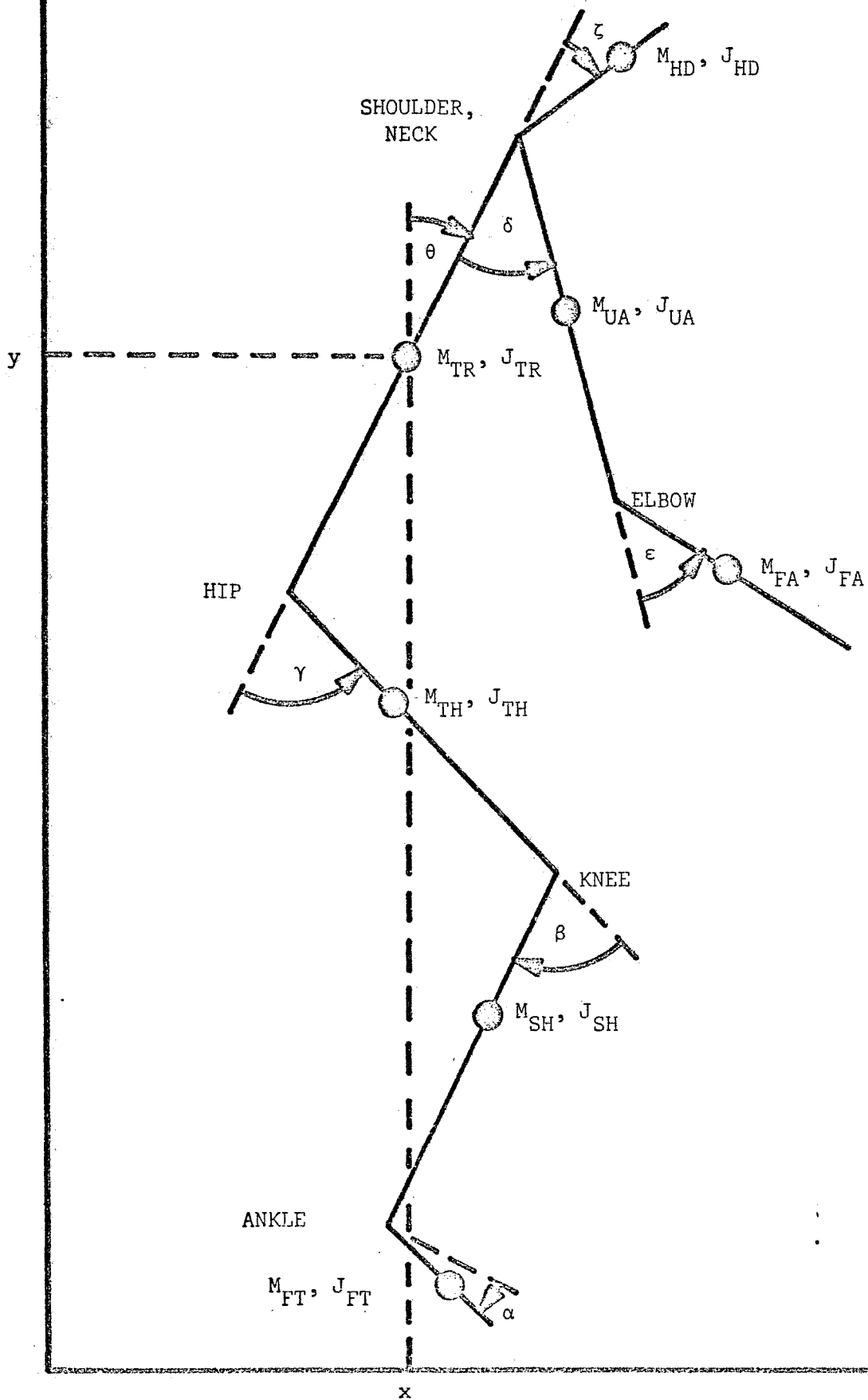
Figure 1.   GENERALIZED COORDINATES
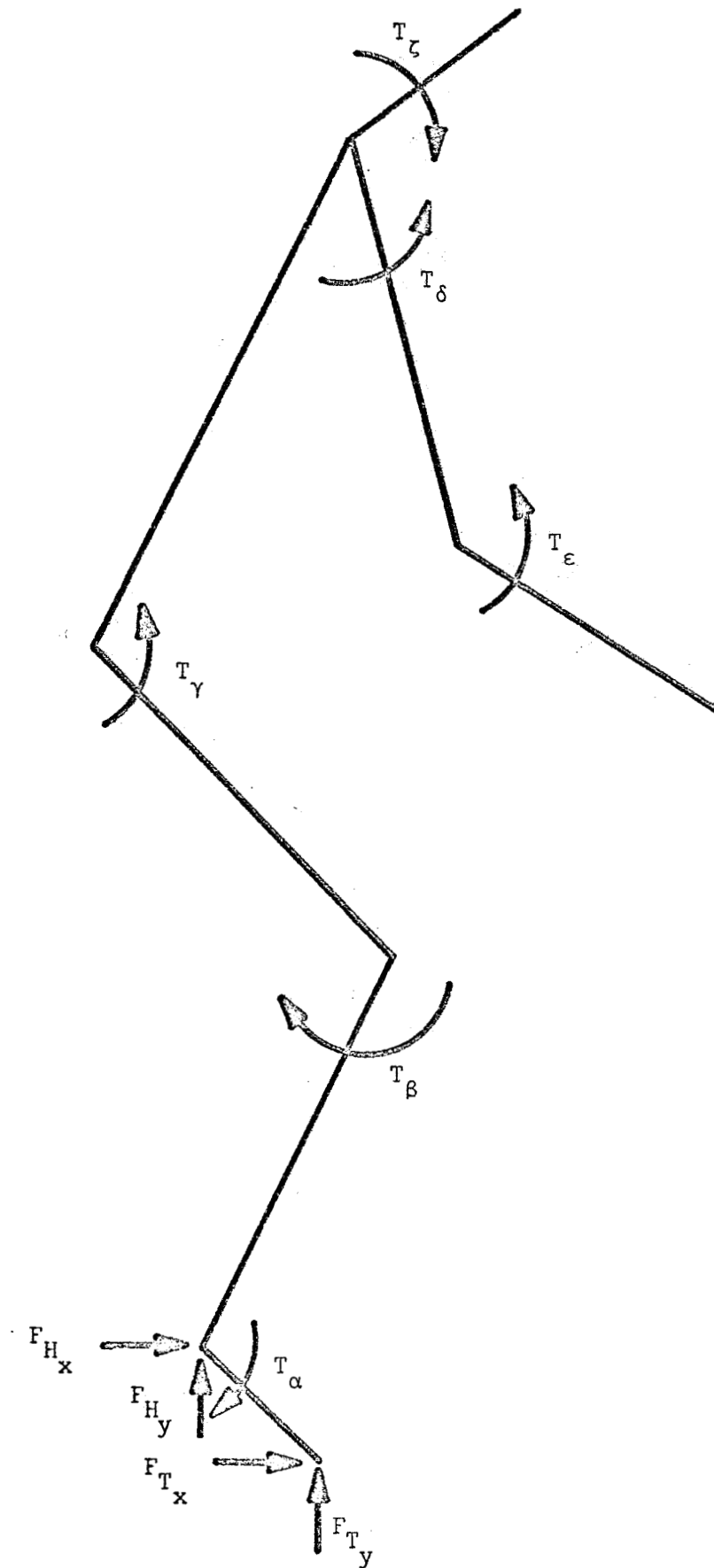
Figure 1a.   FORCES AND TORQUES

5. Professor J. C. Hill presented a paper at the 1969
    I.E.E.E. Systems Science and Cybernetics Conference
    (October 22-24, 1969; Philadelphia) in which the
    analysis and the results presently developed under
    this contract were presented. A reprint of this
    paper is appended to this chapter.

III. Background

In view of the complexity of the nonlinear equations of
motion that have resulted from this analysis, it is desirable
to review the context in which the work is viewed. Accordingly,
the background leading to this particular problem will be dis-
cussed. Next the hypotheses that differentiate this work from
others in the field will be discussed. Finally the broad
outline of this research program in Biomechanics will be given.

Multi-Degree of Freedom Systems

First, it should be clearly in mind that our interest is
in the control of multi-degree-of-freedom systems, and not in
the dynamics of a specific system to be controlled per se. Many
examples of multi-degree of freedom systems of considerable
technological importance can be cited. Businesses receive or
acquire as inputs many types of raw materials, including people,
and produce as outputs a wide variety of finished goods. A
modern petroleum refinery is a dehumanized version of the same
example. A missile guidance and control system receives inputs
from a variety of sensors, including perhaps radars, inertial

platforms, and terminal tracking devices, and is supposed to
coordinate the motion of control surfaces and/or other attitude
controlling devices to steer the missile trajectory through a
desired point in space, such as a target or an orbital insertion
point. Load and distribution scheduling in a large inter-
connected electrical power generation and distribution system
is a problem of much the same kind.

Therefore, basic control principles and techniques de-
veloped for and discovered in one multi-degree of freedom
application have a high probability of finding application in
others.

It is a characteristic of the times that complex control
systems design and analysis techniques, largely developed in
and by the aerospace discipline, are being applied with vigor
in these other areas. The theme of the 1969 I.E.E.E. Systems
Science and Cybernetics Conference was the Modeling and Control
of Natural Systems, which various authors construed as meaning
sociological systems ("Modeling of Criminal Justice System
Operations: An Overview" by R. C. Larson, M.I.T.), natural
resource systems ("Herd Management and Modern Control Theory"
by R. L. Baer, U. of Pennsylvania), learning systems, economic
systems, biological systems, political systems ("Urban Political
Simulation" by Whitehed and Smith), pattern recognition, and
acaptive systems.

Although some of these "applications" appeared to this
attendee to be misdirected, as an indication of the leanings of

a growing segment of the systems science fraternity, the implication is obvious: modern controls research is being directed towards the study of more and more complex systems with less and less well-defined performance indices.

Vertebrate Postural Control

It is generally agreed by workers in the field that the prime example of successful flexible coordination of a multi-degree of freedom system is the vertebrate postural control system, where the term postural control as used by the physiologist refers to all examples of muscular coordination used to control the mechanical position of limbs, trunk, etc. Thus, postural control refers to skeletal muscle systems as opposed to digestive musculature, the diaphragm, and the like.

It is our basic thesis that much can be learned about the control of technological multi-degree of freedom systems by studying the principles that Nature has developed for the vertebrate postural control system. In addition, the vertebrate postural control system is worthy of scientific investigation in its own right.

Overview of Prior Work on Postural Control

A review of the work that has been directed toward the goal of understanding the human postural control system leads to the conclusion that the work may be grouped into five areas (see attached paper by J. C. Hill (Appendix I):

*Analytic Representation of the Force-Velocity Characteristics of Muscle Tissue. [1-8] Aimed toward

characterizing human muscle tissue as an actuator,
this work dates back at least to 1935, with Milhorn's
account of Houk's work a recent example. This work
has been carried out primarily by biologists and
physiologists, with engineering a relative newcomer on
the scene.

*Physiological Sensor Models. [1, 2, 9-11, 20]
Exemplified by the work of Miery and Young on the human
vestibular system and the work on the muscle spindle
receptor by Houk, Gottlieb, Agarwal, and Stark, this work
is aimed at developing transfer functions for the basic
sensory elements that serve to instrument the human "air-
frame." This area has been developed by and for engineers,
and is comparatively recent.

*Human Operator Studies. [12-19] Although physiological
sensory mechanisms are involved in this work also, the
emphasis is less on modeling the sensory organs than it
is on using such models as a guide to the performance of
the human operator in tracking and other control tasks.
An extensive chain of development by McRuer, Graham,
Magdeleno, Shirley and Young, Adams, and Jackson has
served to define and develop this area over the past ten
years. The output of these studies are typically
describing functions explaining the behavior of the human
operator as a function of amplitude and frequency; hence
a rather abstract view of his behavior is taken based on

experimental data, and the emphasis is normally on emperical description of psychological or perceptual factors rather than on mechanical system properties per se.

*Quadruped Locomotion. [21-29] A distinct niche in this grouping is occupied by the work of McGhee and Tomovic. If an analogy may be drawn to aerospace applications, the work discussed thus far has been concerned with control, whereas McGhee has successfully split off a pure guidance problem from the complex phenomena involved in locomotion. In McGhee's work, the dynamic aspects of the problem are suppressed, and concern is centered on the entirely kinematic question of what configuration should be assumed by the extremeties as a function of time if walking, crawling, running, and other gaits are to result.

*Postural Control. [1, 2, 5] The work of Houk attempts to integrate the data on muscle force-velocity characteristics with data on the muscle spindle receptor to develop equations describing the behavior of an agonist-antagonist muscle pair acting against a pure inertia load. Houk's experimentation was carried out on the human wrist rotation system, and led to the block diagram shown here as Figure 2.

Muscular Coordination

If one wishes to understand human muscular coordination as
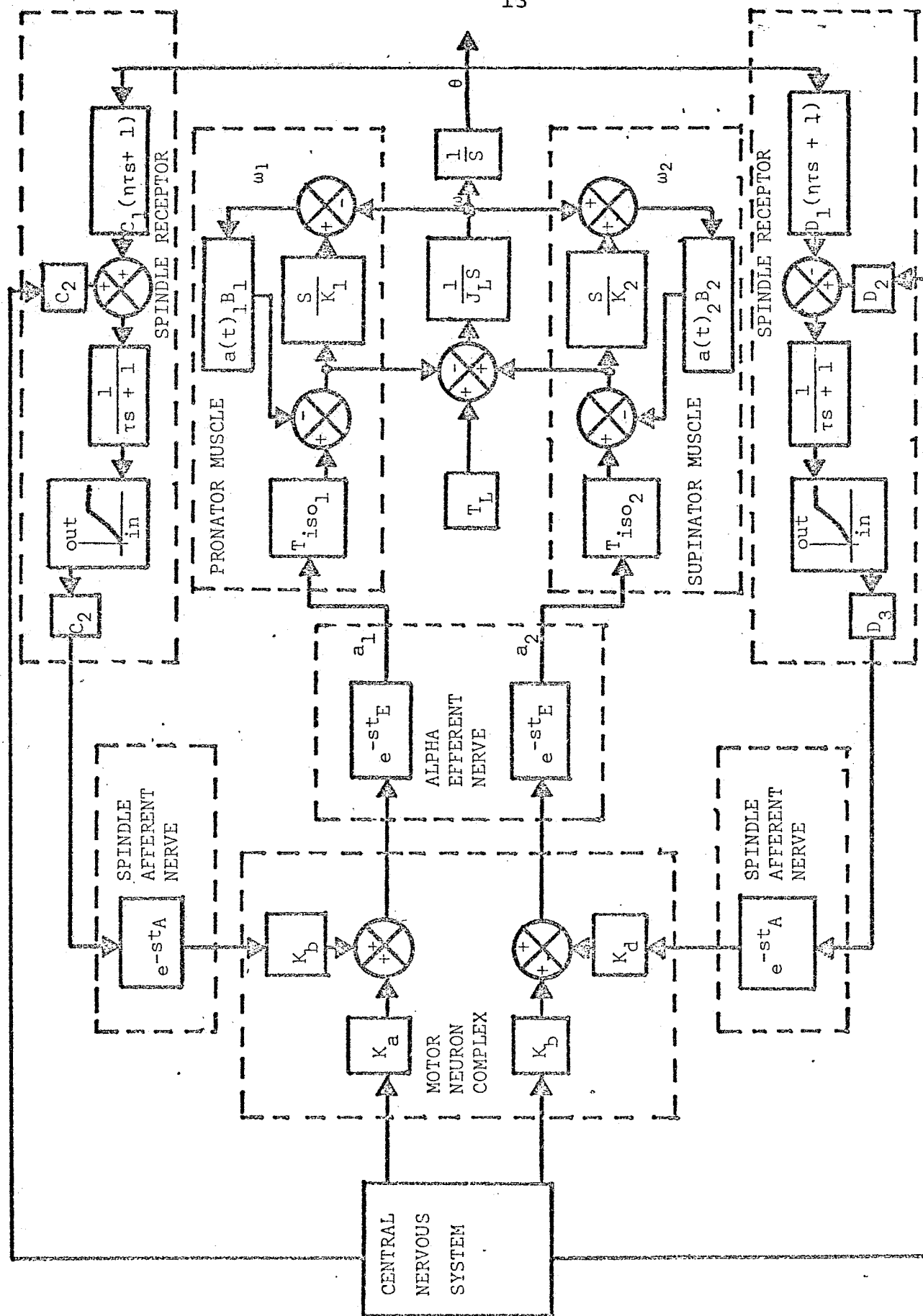
Figure 2. Block diagram of Postural Control System (Wrist Rotation, after Houk)

an example of an exacting multi-degree of freedom control system,
it seems improbable that much will be learned about it from a
study of Figure 2 and its underlying processes, for the coordina-
tion involved in the wrist rotation system is of a very rudimentary
sort. The rule might be stated as: Most of the time both the
agonist and the antagonist should not both be excited -- don't
push and pull at the same time. The coordination involved is
analogous to that required of the output transistors in a push-
pull audio amplifier. Because the muscles are basically
contractile force-producing elements, they must be arranged in
pairs in order to produce bipolar torques around a joint. Hence
a worthwhile degree of muscular coordination will occur only in
a system with more than one joint to be torqued.

The stick man we are studying has six joints to be torqued,
the wrist rotation system has only one; is there no middle
ground? Yes, there is, and the area is presently being researched
by Galiana, [6], who studies the dynamic aspects of legs in
biped locomotion. The model has two degrees of freedom, the
hip and the knee angles, and is forced by the hip and knee
torques. We felt that repetition of Galiana's work would be just
that, i.e., repetitive, and therefore chose a more complex model,
(which, however, we are attacking from a somewhat different
direction with different goals).

Thus Galiana's and our work may be characterized as an
attempt to generalize the work of Houk in two directions -- first,
increasing the number of joints, and second, extending the load

operated on by the joint musculature away from Houk's pure inertia assumption towards more realistic load dynamics -- in particular, to a manageable segment of the human frame, all in the hope that something can be learned about the principles of muscular coordination from analysis of the resulting models.

Dynamics of the Human Frame

The implicit assumption underlying the desire to study the complex model of the human frame proposed is that if insight is to be gained into Nature's principles of muscular coordination, some appreciation of the control problem she faces must be acquired, i.e., we must study the dynamics of the systems Nature controls so well. It seems unlikely that she would develop a sophisticated control principle that we would find useful in technological multi-degree of freedom systems in order to position a pure inertia load.

Tasks

In carrying out this study, we propose to follow a systems approach to the control of a complex dynamics system, which may be divided into the following three basic steps:

1. Derive the equations of motion, transfer functions, etc., of the basic system to be controlled;

2. Augment this model with a mathematical description of the sensors to be used to measure certain aspects of the state of the system (e.g., feedback pots, tachometers, inertial platforms, etc.)

3. Investigate ways to control the system utilizing the signals provided by the sensors.

Step 1:   Basic System Dynamics

It is instructive to examine what one has achieved after completion of each of the above steps.   Treating the joint angles and their derivatives as state variables x_i and the joint torques as yet to be specified inputs u_i, the equations of motion would be of the form

$$\dot{x} = f(x, u) \tag{1}$$

in standard state variable notation.   Given a time history of the muscle torques

$$u = u(t) \tag{2}$$

the motion of the system in response to those torques can be predicted from the solution of the highly nonlinear equation (1). However, the model of equation (1) cannot be experimentally compared with reality, for it is difficult to get a human subject to respond in a controlled torque manner, particularly in nine degrees of freedom.   In the human, the muscle torques are not prescribed or controlled as explicit functions of time as in equation (2), but are determined implicitly by the form of unknown control laws, whose nature it is the purpose of our study to determine.   The results of step 1 only do not appear directly verifiable experimentally without resort to drugs and/or surgery.

Step 2: Sensor Dynamics

Moving now to step 2, a great deal of information on the sensory mechanisms available to the human control system has been developed by other workers. Houk's work on the stretch reflex [2] and the work of Gottlieb, Agarwal, and Stark [11] on stretch receptor models provide a satisfactory indication of the basic properties of joint angle sensors; the basic conclusion is that (from Gottlieb, Agarwal, and Stark) the form of the rate of afferent nerve firing X is related to the muscle spindle receptor length X_M and force F_M by a transfer relation of the form

$$X = k_1 \frac{s + a}{(s + \frac{1}{T_1})(s + \frac{1}{T_2})} X_M + K_2 \frac{1}{(s + \frac{1}{T_1})(s + \frac{1}{T_2})} F_M \qquad (3)$$

From quick-stretch experimental data on cat muscle the parameters in equation (3) were reported as

$$X = \frac{83.4(s + 3.55)}{(s + 182)(s + 16.7)} X_M + \frac{3200}{(s + 182)(s + 16.7)} F_M \qquad (4)$$

The presence of the zero in the first term of (4) is of interest, for it indicates that at low frequencies the rate of nerve firing is proportional to a linear combination of muscle length and rate of change of muscle length; extrapolating to what would be expected as the net effect of an agonist-antagonist muscle pair, we would expect feedback signals proportional to joint angular rate. The muscle spindle receptor is a tachometer of sorts. We

make the assumption, based on its reasonableness from a control
systems point of view, that each joint in the human postural
control system is instrumented by a sensor whose equations are
of the form of equation (3); the gains and time constants may
vary from joint to joint, but the form is invariant. There
appears to be no direct physiological data supporting such a
gross generalization, nor is there likely to be in the reasonably
near future.

Turning now to sensors measuring dynamic variables of a
higher order, the work of Miery and Young [9, 10] on the human
vestibular system provide basic information on the primarily
inertial quantities measured by this apparatus and the transfer
functions from sensory input to sensory output. The result is
that the semicircular canals measure angular accelerations along
three mutually athogonal axes, and that the otolithic organs are
vectorial linear acceleration sensors.

Finally, the information provided by the visual sense must
be integrated into the control system; what little direct
knowledge (from the controls point of view) is known about this
subject is reported by Miery, with fringe benefits occurring
from scattered statements in the human operator literature.

The parallels between the types of sensors we have dis-
cussed here and their aerospace equivalents is striking; the
challenge now is to integrate their outputs into a control system
capable of mimicking some non-trivial aspect of human behavior.

Assuming now that step 2 has been completed, we are now in
possession of a mathematical model of the following form:

$$\dot{\underset{\sim}{x}} = \underset{\sim}{f}(\underset{\sim}{x}, \underset{\sim}{u}) \qquad\qquad (5)$$

$$\dot{\underset{\sim}{y}} = \underset{\sim}{g}(\underset{\sim}{x}, \dot{\underset{\sim}{x}}, \underset{\sim}{u}) \qquad\qquad (6)$$

Equation (5) describes the plant dynamics; equation (6) describes the sensory dynamics, and we therefore have a completely instrumented "human" at our disposal. The stick man dynamics has provided a framework within which the available sensory dynamic knowledge can be interpreted; the muscles torque the frame, the frame responds, and depending on its motion, the sensors provide outlets.

Step 3: The Control Law

What is now missing is step 3, the real object of our research: a <u>control law</u> that will make the muscle torques, u, dependent on the sensor outputs y and a statement (in some as yet unknown form) of what the system is to do. This last, a generalization of the command input in a conventional control system, appears to be a real conceptual difficulty at the present time. How does one instruct the simulation to stand, lift, walk, jump, sit, or do deep knee-bends without over-structuring its responses? It is proposed to attack this problem gradually, beginning by asking the system to recover its balance from an initially disturbed position, and progressing to more complex tasks as more is learned of the system's behavior from its performance on lower level tasks.

The basic point is that completion of steps 1 and 2 have provided a computer simulation that can predict the consequences of any hypothesized form of control law. Simulation of a proposed law will yield results that are directly comparable with experimental data taken on human subjects performing the same tasks, affording the opportunity to iterate the control law to improve agreement.

As long as the experiments performed may be directly compared with experimental data, our model will be "kept honest" in the most direct way possible: agreement with the system being modeled.

Control Principles

At the present stage of this research, it is impossible to state with any degree of certainty what control principles will result from the studies. However, a few possibilities appear probably enough to warrant further discussion:

*Load Relief: A basic property of the human postural control system is that on occasion it quits trying. If, in attempting to carry out the desired maneuvers, it is in danger of damaging the muscle and/or bone structures involved, sudden relaxation results. This "live to fight another day" strategy is not commonly encountered in technological control systems, whose performance is more usually limited by available power limitations rather than by structural strength limitations. Three exceptions, however, are modern high-performance aircraft, where g-limiting is used; large flexible launch vehicles, where

the control system may function in a bending stress alleviation mode during part of the boost phase; and remote manipulation and exploration machines, where single-minded performance of a specified task by brute force may be disastrous if unexpected obstacles are encountered. All three of these examples are clearly of interest to NASA. How, for example, can one design into a lunar exploration vehicle the ability to decide to <u>roll</u> down (tumbling) a ravine and then get up at the bottom as opposed to fighting desperately to remain upright at the cost of fracturing some critical element? Although rather far away in terms of present knowledge, understanding of this complex extrapolative decision process is a worthwhile eventual goal.

*<u>Anticipation</u>: Cursory examination of the simplest common examples of muscular coordination lead to the conclusion that <u>anticipation</u> is intimately related to load relief. A child jumping off of a chair learns that it must not hit the floor in the completely erect position -- unacceptably large stresses result if it does. Therefore, sometime prior to impact, the frame tends towards an "everywhere bent" configuration that the child has probably learned from experience minimizes something -- the index of performance may be "minimize energy expended subject to the constraint of survival", or some related criterion. At the instant of impact, the legs are already being drawn toward the trunk in an effort to control the peak loads exerted on the feet and toes; i.e., the forthcoming impact is <u>anticipated</u>, not purely <u>responded to</u>. The interesting question is through precisely

what senses this is carried out -- visual, tactile, or inertial,
or perhaps a nontrivial combination of the three -- clearly
interesting and informative experiments comparing simulation
results to real data could be carried out along these lines.

*Sensory Deprivation: In any given experiment, the
simulation may easily be deprived of one or more of its sensory
channels, and predictions of the effect of a corresponding loss
on the human (perhaps an astronaut) could be made. Certain of
these results could be easily verified experimentally. At
least the visual system may be easily inactivated in a human
subject.

*Incipient Tipping: A person, asked to remain erect at
a given location, is given a series of harder and harder pushes.
For weak pushes he is able to keep his balance without moving
his feet, but as the intensity of the pushes increase, a point
is eventually reached where he takes one or more hops forward
(assuming a feet together constraint is imposed), regains his
balance, and hops backwards to the desired spot. If obstacles
are present, great versatility in the length and trajectories
followed during each hop can result. This is an extremely
interesting behavior pattern; it could have great applicability
to off-road vehicles, in particular. Again, on what senses does
this capability depend? Can it be mimicked to a lower but still
technologically useful level?

All of the above-mentioned non-classical control problems
may be studied via the approach presently being followed. In

the next section, progress in carrying out the indicated program will be presented.

IV. Progress

As indicated in the First Quarterly Progress Report, expressions for the kinetic and potential energies of the stick man of Figure 1 become so complex that reliable hand calculation of these expressions becomes hopeless. Preliminary study of several computer programs indicated that the FORMAC pre-compiler for PL-1 could carry out the required symbolic manipulations. An IBM 360/65 with this pre-compiler as part of its program library was located at the General Motors Technical Center in Warren, Michigan. This computer was equipped with one million bytes of rapid access core storage, and surprisingly, it turned out that the present problem required it all. Symbolic algebraic processors apparently need fantastic amounts of core.

The FORMAC program we developed (see Appendix II) carried out all the operations needed to derive Lagrange's equations in the form

$$\frac{d}{dt}\left(\frac{\partial T}{\partial \dot{q}_i}\right) - \frac{\partial V}{\partial q_i} + \frac{\partial V}{\partial q_i} = Q_i \qquad i = 1,2,\ldots,9 \qquad (7)$$

including:

1. Generation of analytic expressions for T and V.

2. Analytic partial differentiation of these expressions to generate

$$\frac{\partial T}{\partial \dot{q}_i} \; , \; \frac{\partial T}{\partial q_i} \; , \; \text{and} \; \frac{\partial V}{\partial q_i} \; .$$

3. Analytic total differentiation of the expression $\frac{\partial T}{\partial \dot{q}_i}$ with respect to time, generating the term

$$\frac{d}{dt}\left(\frac{\partial T}{\partial \dot{q}_i}\right).$$

The generalized forces Q_i were derived by hand calculation.

The FORMAC source program (see Appendix II) was over 300 statements long and produced 200 pages of symbolic output; therefore, the output will not be included in this report, but will be provided upon request.

In order to communicate what this program does, a simpler example utilizing the same approach will be presented.

EXAMPLE: We desire the equations of motion of the double Figure 3 in terms of the generalized coordinates θ_1, θ_2 .

For this simple problem, the potential energy may be written as

$$V = (M_1 + M_2)\ell_1 g - (M_1 + M_2)\ell_1 g \, \cos \, \theta_1 + M_2\ell_2 g - M_2\ell_2 g \, \cos(\theta_1 + \theta_2)$$

$$(8)$$

The velocity of mass 1 is

$$\underset{\sim}{v}_1 = \ell_1 \dot{\theta}_1 \underset{\sim}{u}_{\theta_1}$$
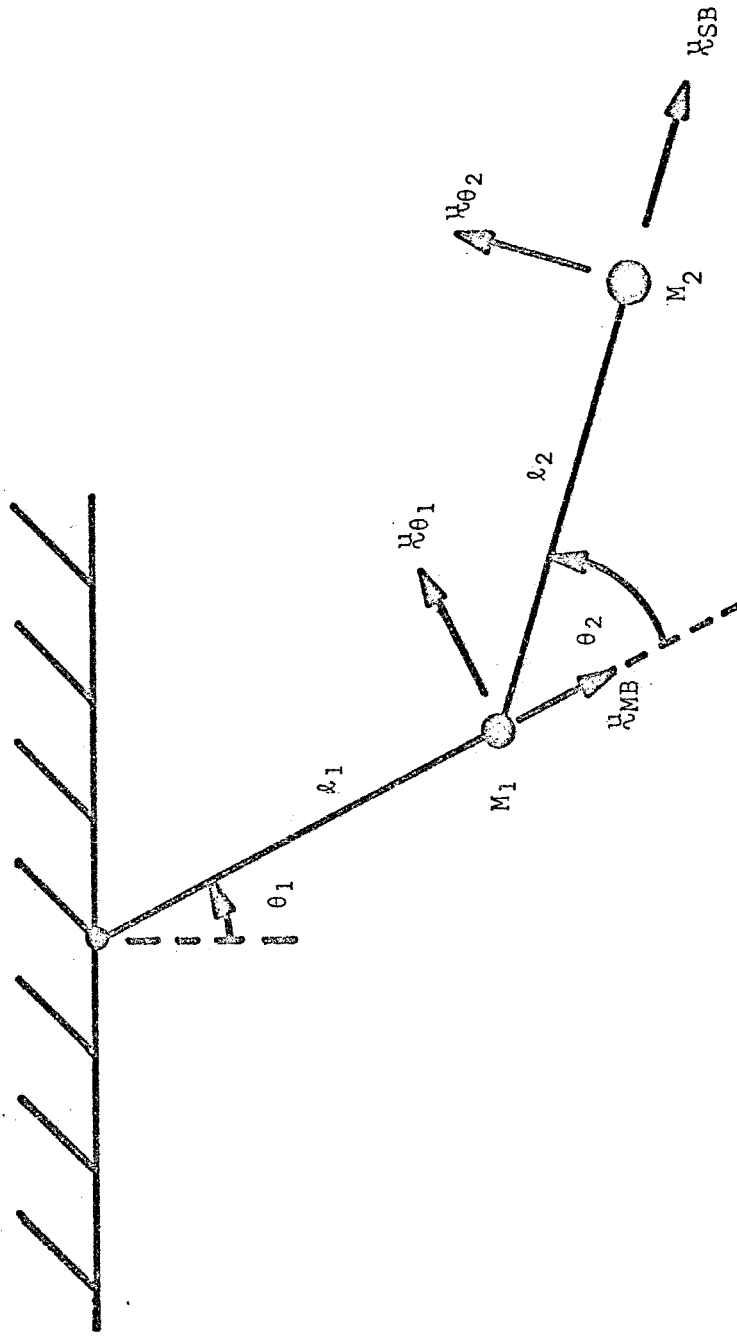
DOUBLE PENDULUM IN THE GENERALIZED COORDINATES θ_1, θ_2

Figure 3.

where $\underset{\sim}{u}_{\theta_1}$ is a unit vector in the increasing θ_1 direction.

The velocity of mass 2 can be expressed in terms of the velocity of mass 1 by use of the relative velocity theorem as

$$\underset{\sim}{v}_2 = \underset{\sim}{v}_1 + \ell_2 \dot{\theta}_2 \underset{\sim}{u}_{\theta_2} \tag{10}$$

where $\underset{\sim}{u}_{\theta_2}$ is a unit vector in the increasing θ_2 direction. The addition indicated in (10) is a vector sum; since $\underset{\sim}{v}_1$ as given by (1) and the second term in (10) are not expressed in the same coordinate system, the relation between the coordinate systems must be specified, viz:

$$\underset{\sim}{u}_{\theta_2} = \underset{\sim}{u}_{\theta_1} \cos \theta_2 - \underset{\sim}{u}_{MB} \sin \theta_2 \tag{11}$$

$$\underset{\sim}{u}_{SB} = \underset{\sim}{u}_{\theta_1} \sin \theta_2 + \underset{\sim}{u}_{MB} \cos \theta_2 \tag{12}$$

where $\underset{\sim}{u}_{MB}$ and $\underset{\sim}{U}_{SB}$ are unit vectors directed as shown in Figure 3.

The FORMAC program of Figure 4

1. Sets up V

2. Calculates $\underset{\sim}{v}_1$ (VELM1)

3. Enters the relation between the coordinate systems*

4. Evanuates $\underset{\sim}{v}_2$ (VELM2)

5. Computes $\frac{\partial V}{\partial \theta_1}$ and $\frac{\partial V}{\partial \theta_2}$ (DVT1 and DVT2)

---

*Note that besides working with symbols, FORMAC is also manipulating vector expressions, neither of which a computer is commonly considered able to do.

6. Evaluates T (KE)

7. Evaluates $\frac{\partial T}{\partial \theta_1}$ and $\frac{\partial T}{\partial \theta_2}$ (DTT1 and DTT2)

8. Evaluates $\frac{\partial T}{\partial \dot{\theta}_1}$ and $\frac{\partial T}{\partial \dot{\theta}_2}$ (DTDT1 and DTDT2)

9. Specifies θ_1, θ_2, $\dot{\theta}_1$, $\dot{\theta}_2$ as functions of time

10. Evaluates $\frac{d}{dt} (\frac{\partial T}{\partial \dot{\theta}_1})$ and $\frac{d}{dt} (\frac{\partial T}{\partial \dot{\theta}_2})$ (DTDT1T and DTDT2T)

11. Adds $\frac{d}{dt} (\frac{\partial T}{\partial \dot{q}_i})$, $\frac{\partial T}{\partial \dot{q}_i}$, and $\frac{\partial V}{\partial q_i}$ to get Q_i.

Output from this program is presented on next two pages.
All intermediate results have been dumped, and the final answers
appear as the last nine lines of symbolic output. We have

$$Q1 = \frac{\text{SIN (THETA1) G L1 M1 + DTHTA1}^{(1)}. (T) L1^2 \text{ M1 + SIN}}{\text{—}}$$

$$\frac{\text{(THETA1) G L1 M2 } - \text{THETA2}^{(1)}. (T) \text{ SIN (THETA2. (T)) DTHTA2.}}{}$$

$$\frac{\text{(T) L2 L1 M2 + DTHTA2}^{(1)}. (T) \text{ COS (THETA2. (T)) L2 L1 M2}}{}$$

$$\frac{\text{+ SIN (THETA1 + THETA2) L2 G M2 + DTHTA1}^{(1)}. (T) L1^2 \text{ M2}}{}$$

$$Q2 = \frac{\text{SIN (THETA2) DTHTA1 L2 L1 M2 DTHTA2 } - \text{THETA2}^{(1)}. (T)}{}$$

$$\frac{\text{SIN (THETA2. (T)) DTHTA1. (T) L2 L1 M2 + DTHTA1}^{(1)}. (T)}{}$$

$$\frac{\text{COS (THETA2. (T)) L2 L1 M2 + SIN (THETA1 + THETA2) L2 G M2}}{}$$

$$\frac{\text{+ DTHTA2}^{(1)}. (T) \text{ SIN}^2 (\text{THETA2. (T)) L2}^2 \text{ M2 + DTHTA2}^{(1)}.}{}$$

$$\frac{\text{(T) COS}^2 (\text{THETA2. (T)) L2}^2 \text{ M2}}{}$$

```
INPUT TO FORMAC PREPROCESSOR
PENDU: PROCEDURE OPTIONS(MAIN);
FORMAC_OPTIONS;
OPTSET(LINELENGTH=72); OPTSET(PRINT); OPTSET(EXPND);
/*                                                               */
      /*    ENTER POTENTIAL ENERGY                               */
/*                                                               */
LET(V=(M1+M2)*L1*G-(M1+M2)*L1*G*COS(THETA1));
LET(V=V+M2*L2*G-M2*L2*G*COS(THETA1+THETA2));
/*                                                               */
      /*    ENTER VELOCITY OF MASS 1                             */
/*                                                               */
LET(VELM1=DTHTA1     *L1*UTHTA1);
LET(UTHTA2=UTHTA1*COS(THETA2     )-UMB*SIN(THETA2     ));
LET(USB=UTHTA1*SIN(THETA2     )+UMB*COS(THETA2     ));
/*                                                               */
      /*    FIND VELOCITY OF MASS 2 USING RELATIVE VEL. THEORM   */
/*                                                               */
LET(VELM2=DTHTA2     *L2*UTHTA2+VELM1);
/*                                                               */
      /*    DV/QI                                                */
/*                                                               */
LET(DVT1=DERIV(V,THETA1     ));
LET(DVT2=DERIV(V,THETA2     ));
/*                                                               */
      /*    KINETIC ENERGY                                       */
/*                                                               */
LET(KE=1/2*M1*(COEFF(VELM1,UTHTA1)**2+COEFF(VELM1,UMB)**2));
LET(KE=KE+1/2*M2*(COEFF(VELM2,UTHTA1)**2+COEFF(VELM2,UMB)**2));
/*                                                               */
      /*    DT/QI                                                */
/*                                                               */
LET(DTT1=DERIV(KE,THETA1     ));
LET(DTT2=DERIV(KE,THETA2     ));
/*                                                               */
      /*    DT/QIDOT                                             */
/*                                                               */
LET(DTDT1     =DERIV(KE,DTHTA1     ));
LET(DTDT2     =DERIV(KE,DTHTA2     ));
      LET(DTDT1=REPLACE(DTDT1,DTHTA1,DTHTA1.(T),DTHTA2,DTHTA2.(T)));
      LET(DTDT1=REPLACE(DTDT1,THETA1,THETA1.(T),THETA2,THETA2.(T)));
      LET(DTDT2=REPLACE(DTDT2,DTHTA1,DTHTA1.(T),DTHTA2,DTHTA2.(T)));
      LET(DTDT2=REPLACE(DTDT2,THETA1,THETA1.(T),THETA2,THETA2.(T)));
/*                                                               */
      /*    D/DT OF DT/QIDOT                                     */
/*                                                               */
LET(DTDT1T=DERIV(DTDT1     ,T));
LET(DTDT2T=DERIV(DTDT2     ,T));
/*                                                               */
      /*    EQUATIONS OF MOTIONS                                 */
/*                                                               */
LET(Q1=DVT1-DTT1+DTDT1T);
LET(Q2=DVT2-DTT2+DTDT2T);
END PENDU;
```

Figure 4. FORMAC Program to Generate Equations
of Motion of Double Pendulum.

leading to the equations of motion

$$M_1 \ell_1{}^2 + M_2 \ell_1{}^2 \ddot{\theta}_1 + \ell_1 \ell_2 M_2 \quad \cos\theta_2 \ddot{\theta}_2 - \sin\theta_2 \dot{\theta}_2{}^2 \tag{13}$$

$$+ M_1 + M_2) \ell_1 g \sin\theta_1 + M_2 \ell_2 g \sin(\theta_1 + \theta_2) = Q_1$$

$$M_2 \ell_2{}^2 \ddot{\theta}_2 + M_2 \ell_1 \ell_2 \cos\theta_2 \ddot{\theta}_1 - M_2 \ell_1 \ell_2 \left[\dot{\theta}_1 \dot{\theta}_2 \sin\theta_2 - \dot{\theta}_1 \dot{\theta}_2 \right]$$

$$\sin\theta_2 + M_2 \ell_2 g \sin(\theta_1 + \theta_2) = Q_2 \tag{14}$$

Following this procedure on the seven element stick man leads to a complex set of equations. We have calculated these equations completely, but they do not appear amenable to straight forward machine solution at the present time (basically because they are prohibitively long.)

However, if small angle approximations are made and only terms in the first power in each state variable are kept, the resulting linearized equations may be put in the form

$$A\ddot{\underset{\sim}{x}} = B\dot{\underset{\sim}{x}} + C\underset{\sim}{x} + D\underset{\sim}{f} + E\underset{\sim}{T} + \underset{\sim}{V} \tag{15}$$

where

$$V = G\ L1\ M1 - COS\ (\ THETA1\ )\ G\ L1\ M1 + G\ L1\ M2 - COS\ (\ THETA1\ )\ G\ L1\ M2$$

$$V = G\ L1\ M1 - COS\ (\ THETA1\ )\ G\ L1\ M1 + G\ L1\ M2 - COS\ (\ THETA1\ )\ G\ L1\ M2$$

$$+ L2\ G\ M2 - COS\ (\ THETA1 + THETA2\ )\ L2\ G\ M2$$

$$VELM1 = DTHTA1\ L1\ UTHTA1$$

$$UTHTA2 = COS\ (\ THETA2\ )\ UTHTA1 - SIN\ (\ THETA2\ )\ UMB$$

$$USB = SIN\ (\ THETA2\ )\ UTHTA1 + COS\ (\ THETA2\ )\ UMB$$

$$VELM2 = COS\ (\ THETA2\ )\ L2\ DTHTA2\ UTHTA1 + DTHTA1\ L1\ UTHTA1 - SIN\ ($$

$$THETA2\ )\ L2\ DTHTA2\ UMB$$

$$DVT1 = SIN\ (\ THETA1\ )\ G\ L1\ M1 + SIN\ (\ THETA1\ )\ G\ L1\ M2 + SIN\ (\ THETA1 +$$

$$THETA2\ )\ L2\ G\ M2$$

$$DVT2 = SIN\ (\ THETA1 + THETA2\ )\ L2\ G\ M2$$

$$KE = 1/2\ DTHTA1^2\ \ L1^2\ \ M1$$

$$KE = COS\ (\ THETA2\ )\ DTHTA1\ L2\ L1\ M2\ DTHTA2 + 1/2\ DTHTA1^2\ \ L1^2\ \ M1 + 1/2$$

$$DTHTA1^2\ \ L1^2\ \ M2 + 1/2\ SIN^2\ (\ THETA2\ )\ L2^2\ \ M2\ DTHTA2^2 + 1/2\ COS^2\ ($$

$$THETA2\ )\ L2^2\ \ M2\ DTHTA2^2$$

$$DTT1 = 0$$

$$DTT2 = \ -\ SIN\ (\ THETA2\ )\ DTHTA1\ L2\ L1\ M2\ DTHTA2$$

$$DTDT1 = COS\ (\ THETA2\ )\ L2\ L1\ M2\ DTHTA2 + DTHTA1\ L1^2\ \ M1 + DTHTA1\ L1^2\ \ M2$$

$$DTDT2 = SIN^2\ (\ THETA2\ )\ L2^2\ \ M2\ DTHTA2 + COS^2\ (\ THETA2\ )\ L2^2\ \ M2\ DTHTA2$$

$$+ COS\ (\ THETA2\ )\ DTHTA1\ L2\ L1\ M2$$

$$DTDT1 = DTHTA1.(\ T\ )\ L1^2\ \ M1 + COS\ (\ THETA2\ )\ DTHTA2.(\ T\ )\ L2\ L1\ M2 +$$

$$DTHTA1.(\ T\ )\ L1^2\ \ M2$$

$$DTDT1 = DTHTA1.(\ T\ )\ L1^2\ \ M1 + COS\ (\ THETA2.(\ T\ )\ )\ DTHTA2.(\ T\ )\ L2\ L1$$

$$M2 + DTHTA1.(\ T\ )\ L1^2\ \ M2$$

$$DTDT2 = COS\ (\ THETA2\ )\ DTHTA1.(\ T\ )\ L2\ L1\ M2 + SIN^2\ (\ THETA2\ )\ DTHTA2.($$

$$T) \; L2^{2} \; M2 + COS^{2} (THETA2) \; DTHTA2.(T) \; L2^{2} \; M2$$

$$DTDT2 = COS (THETA2.(T)) \; DTHTA1.(T) \; L2 \; L1 \; M2 + SIN^{2} (THETA2.(T)$$

$$) \; DTHTA2.(T) \; L2^{2} \; M2 + COS^{2} (THETA2.(T)) \; DTHTA2.(T) \; L2^{2} \; M2$$

$$DTDT1T = DTHTA1^{(1)}.(T) \; L1^{2} \; M1 - THETA2^{(1)}.(T) \; SIN (THETA2.(T)$$

$$) \; DTHTA2.(T) \; L2 \; L1 \; M2 + DTHTA2^{(1)}.(T) \; COS (THETA2.(T)) \; L2 \; L1$$

$$M2 + DTHTA1^{(1)}.(T) \; L1^{2} \; M2$$

$$DTDT2T = - THETA2^{(1)}.(T) \; SIN (THETA2.(T)) \; DTHTA1.(T) \; L2 \; L1 \; M2$$

$$+ DTHTA1^{(1)}.(T) \; COS (THETA2.(T)) \; L2 \; L1 \; M2 + DTHTA2^{(1)}.(T) \; SIN$$

$$^{2} (THETA2.(T)) \; L2^{2} \; M2 + DTHTA2^{(1)}.(T) \; COS^{2} (THETA2.(T)) \; L2^{2}$$

$$M2$$

$$Q1 = SIN (THETA1) \; G \; L1 \; M1 + DTHTA1^{(1)}.(T) \; L1^{2} \; M1 + SIN (THETA1)$$

$$G \; L1 \; M2 - THETA2^{(1)}.(T) \; SIN (THETA2.(T)) \; DTHTA2.(T) \; L2 \; L1 \; M2 +$$

$$DTHTA2^{(1)}.(T) \; COS (THETA2.(T)) \; L2 \; L1 \; M2 + SIN (THETA1 + THETA2)$$

$$L2 \; G \; M2 + DTHTA1^{(1)}.(T) \; L1^{2} \; M2$$

$$Q2 = SIN (THETA2) \; DTHTA1 \; L2 \; L1 \; M2 \; DTHTA2 - THETA2^{(1)}.(T) \; SIN ($$

$$THETA2.(T)) \; DTHTA1.(T) \; L2 \; L1 \; M2 + DTHTA1^{(1)}.(T) \; COS (THETA2.(T$$

$$)) \; L2 \; L1 \; M2 + SIN (THETA1 + THETA2) \; L2 \; G \; M2 + DTHTA2^{(1)}.(T) \; SIN$$

$$^{2} (THETA2.(T)) \; L2^{2} \; M2 + DTHTA2^{(1)}.(T) \; COS^{2} (THETA2.(T)) \; L2^{2}$$

$$M2$$

$$
\underset{\sim}{x} = \left\{ \begin{array}{c} x \\ y \\ \theta \\ \alpha \\ \beta \\ \gamma \\ \delta \\ \varepsilon \\ \zeta \end{array} \right\}, \quad
\underset{\sim}{\dot{x}} = \left\{ \begin{array}{c} x \\ y \\ \dot{\theta} \\ \dot{\alpha} \\ \dot{\beta} \\ \dot{\gamma} \\ \dot{\delta} \\ \dot{\varepsilon} \\ \dot{\zeta} \end{array} \right\}, \quad
\underset{\sim}{\ddot{x}} = \left\{ \begin{array}{c} \ddot{x} \\ \ddot{y} \\ \ddot{\theta} \\ \ddot{\alpha} \\ \ddot{\beta} \\ \ddot{\gamma} \\ \ddot{\delta} \\ \ddot{\varepsilon} \\ \ddot{\zeta} \end{array} \right\}, \quad
\underset{\sim}{f} = \left\{ \begin{array}{c} F_{Hx} \\ F_{Tx} \\ F_{Hy} \\ F_{Ty} \\ F_{Tx}\theta \\ F_{Hy}\theta \\ F_{Ty}\theta \\ F_{Tx}\gamma \\ F_{Hy}\gamma \\ F_{Ty}\gamma \\ F_{Tx}\beta \\ F_{Hy}\beta \\ F_{Ty}\beta \\ F_{Tx}\alpha \end{array} \right\}, \quad
\underset{\sim}{T} = \left\{ \begin{array}{c} T_{\gamma} \\ T_{\beta} \\ T_{\alpha} \\ T_{\delta} \\ T_{\varepsilon} \\ T_{\zeta} \end{array} \right\}, \quad
\underset{\sim}{V} = \left\{ \begin{array}{c} V_{x} \\ V_{y} \\ V_{\theta} \\ V_{\alpha} \\ V_{\beta} \\ V_{\gamma} \\ V_{\delta} \\ V_{\varepsilon} \\ V_{\zeta} \end{array} \right\} \quad (16)
$$

and A, B, C, D, and E are matrices of appropriate size to be con-
formable with the indicated vectors. In equation (16), T_{γ}, T_{β},
etc., are the torques about the joints whose angles are γ, β, etc.;
F_{Hx}, f_{Hy} are the x, y components of the ground reaction force on
the heel, and F_{Tx}, F_{TY} are the x, y components of the ground
reaction force on the toe (see Figure Ia).

The A matrix is given in equation (17).

$$A = \begin{bmatrix} 4.800 & 0.000 & -1.879 & 1.589 & -0.569 & 0.000 & 0.079 & 0.039 & 0.239 \\ 0.000 & 4.800 & 0.000 & 0.000 & 0.000 & -0.019 & 0.000 & 0.000 & 0.000 \\ 0.839 & 0.000 & 4.141 & -3.041 & 0.763 & 0.005 & 0.030 & 0.023 & 0.204 \\ 1.589 & 0.000 & -2.117 & 2.117 & -0.820 & -0.005 & 0.000 & 0.000 & 0.000 \\ -0.569 & 0.000 & 0.763 & -0.763 & 0.763 & 0.005 & 0.000 & 0.000 & 0.000 \\ 0.000 & -0.019 & 0.005 & -0.005 & 0.005 & 0.008 & 0.000 & 0.000 & 0.000 \\ 0.180 & 0.000 & 0.030 & 0.000 & 0.000 & 0.000 & 0.065 & 0.048 & 0.000 \\ 0.039 & 0.000 & -0.009 & 0.000 & 0.000 & 0.000 & 0.009 & 0.024 & 0.000 \\ 0.239 & 0.000 & 0.203 & 0.000 & 0.000 & 0.000 & 0.000 & 0.000 & 0.203 \end{bmatrix} \quad (17)$$

Since A is _not_ sparse, nearly every acceleration couples into nearly every other one, and we have a bad algebraic loop problem. Analog simulation is indicated, but every nonzero co-efficient in A requires an analog pot, as is also true for B, C, D, and E; the number of pots required is more than we have at our disposal.

However, premultiplication of (15) by A^{-1} yields

$$\ddot{\underset{\sim}{x}} = (A^{-1}C)\underset{\sim}{x} + (A^{-1}D)\underset{\sim}{f} + (A^{-1}E)\underset{\sim}{T} + (A^{-1}V) \qquad (18)$$

and in this form there is no algebriac loop problem.

It turns out that $C \equiv 0$; the rest of the matrices in (18) are as follows:

34

$$
\begin{Bmatrix} x \\ y \\ \theta \\ \gamma \\ \beta \\ \alpha \\ \delta \\ \omega \\ \xi \end{Bmatrix} \tag{19}
$$

x	y	θ	γ	β	α	δ	ω	ξ
1.023	-0.170	3.295	0.000	-0.730	2.253	-8.343	0.000	0.000
-0.001	0.000	-0.005	0.000	0.057	0.052	-0.041	0.000	0.000
5.503	-0.917	1.160	0.000	-31.860	-85.201	41.914	0.000	0.000
4.732	-0.788	-1.322	0.000	-60.671	-155.735	117.037	0.000	0.000
-0.004	0.000	-0.015	0.000	-53.470	-92.958	92.987	0.000	0.000
-0.429	0.071	-1.383	0.000	13.827	12.574	-10.017	0.000	0.000
-7.571	1.261	-154.551	0.000	32.921	79.197	-116.980	0.000	0.000
3.069	-0.511	50.783	0.000	-22.151	-62.789	70.551	0.000	0.000
-6.706	1.117	-5.037	0.000	32.720	82.549	-32.099	0.000	0.000

$$A^{-1}C\tilde{x} =$$

Columns (left to right): F_{Hx}, F_{Tx}, F_{Hy}, F_{Ty}, F_{Tx}^{θ}, F_{Hy}^{θ}, F_{Ty}^{θ}, F_{Tx}^{γ}, F_{Hy}^{γ}, F_{Ty}^{γ}, F_{Tx}^{β}, F_{Hy}^{β}, F_{Ty}^{β}, F_{Tx}^{α}

$$
A^{-1}_{Df} =
\begin{bmatrix}
-0.267 & -0.267 & -0.000 & -0.041 & -0.146 & -0.589 & 0.691 & 0.146 & 0.431 & -0.310 & -0.146 & -0.162 & 0.234 & -0.146 \\
0.005 & 0.005 & 0.210 & -0.069 & 0.283 & -0.005 & -0.005 & -0.283 & 0.003 & 0.005 & 0.283 & -0.004 & -0.005 & 0.283 \\
0.381 & 0.381 & 0.000 & 0.092 & 0.325 & -6.718 & 4.240 & -0.325 & 5.863 & 1.876 & 0.325 & -2.658 & -0.521 & 0.325 \\
1.499 & 1.499 & 0.000 & 0.108 & 0.382 & -7.189 & 5.116 & -0.382 & 6.454 & 3.025 & 0.382 & -2.448 & -0.611 & 0.382 \\
-1.053 & -1.053 & -0.003 & -0.364 & -1.283 & 1.057 & 3.364 & 1.283 & -1.056 & -1.053 & -1.283 & 2.057 & 2.056 & -1.283 \\
1.217 & 1.217 & 0.469 & -66.609 & 68.041 & -0.857 & -1.395 & -68.041 & 0.923 & 1.235 & 68.041 & -1.036 & -1.203 & 68.041 \\
0.186 & 0.186 & -0.000 & -0.003 & -0.013 & 7.857 & -5.630 & 0.013 & -6.682 & -1.196 & -0.013 & 2.960 & 0.021 & -0.013 \\
0.498 & 0.498 & 0.000 & 0.101 & 0.356 & -4.303 & 2.446 & -0.356 & 3.826 & 1.602 & 0.356 & -1.762 & -0.570 & 0.356 \\
-0.066 & -0.066 & -0.000 & -0.043 & -0.153 & 7.412 & -5.053 & 0.153 & -6.371 & -1.510 & -0.153 & 2.849 & 0.245 & -0.153
\end{bmatrix}
$$

(20)

$$A^{-1}_{ET} = \begin{bmatrix} 0.2065 & 0.3046 & 0.2169 & -0.3327 & -0.1247 & -0.3694 \\ -0.0003 & -0.0036 & 0.4655 & 0.0005 & 0.0002 & 0.0006 \\ 2.4660 & 3.1600 & 3.3551 & 0.5482 & -0.1575 & 0.0407 \\ 3.0814 & 4.5302 & 4.7590 & 0.7989 & -0.0635 & 0.3191 \\ 0.7700 & 2.9120 & 2.1434 & 0.0015 & 0.0005 & 0.0017 \\ -0.0867 & -0.8645 & 111.7349 & 0.1397 & 0.0523 & 0.1551 \\ -0.8632 & -3.7530 & -3.7609 & 20.8373 & -19.4339 & 0.7360 \\ 1.5881 & 2.0013 & 2.2146 & -6.7716 & 47.1390 & 0.3408 \\ -2.7090 & -3.5184 & -3.6103 & -0.1567 & 0.3042 & 5.2958 \end{bmatrix} \begin{Bmatrix} T_\gamma \\ T_\beta \\ T_\alpha \\ T_\delta \\ T_\varepsilon \\ T_\xi \end{Bmatrix} \qquad (21)$$

$$A^{-1}V = \begin{Bmatrix} -3.0199 \\ -33.5509 \\ 0.9946 \\ 3.3083 \\ 0.9180 \\ -2.2267 \\ 57.5667 \\ -67.0540 \\ 40.4406 \end{Bmatrix} \qquad (22)$$

For convenience in debugging the simulation, a simple control law relating the joint torques to the joint angles and angular rates of the following form was used:

$$T_\alpha = K_\alpha(\alpha) + K_{\dot\alpha}(\dot\alpha)$$

$$T_\beta = K_\beta(\beta) + K_{\dot\beta}(\dot\beta)$$

$$T_\gamma = K_\gamma(\gamma) + K_{\dot\gamma}(\dot\gamma)$$

$$T_\delta = K_\delta(\delta) + K_{\dot\delta}(\dot\delta)$$

$$T_\varepsilon = K_\varepsilon(\varepsilon) + K_{\dot\varepsilon}(\dot\varepsilon)$$

$$T_\zeta = K_\zeta(\zeta) + K_{\dot\zeta}(\dot\zeta)$$

(23)
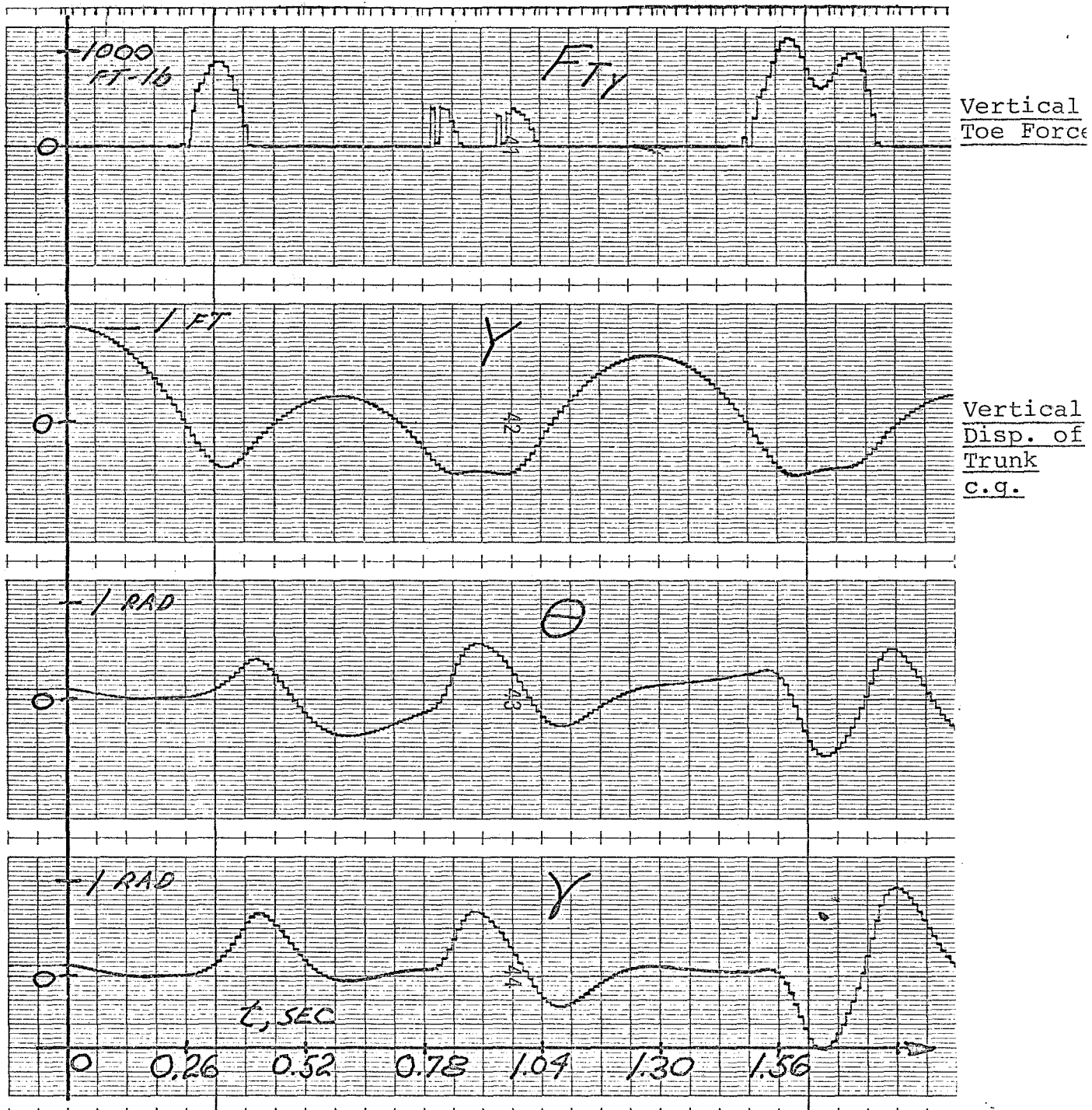
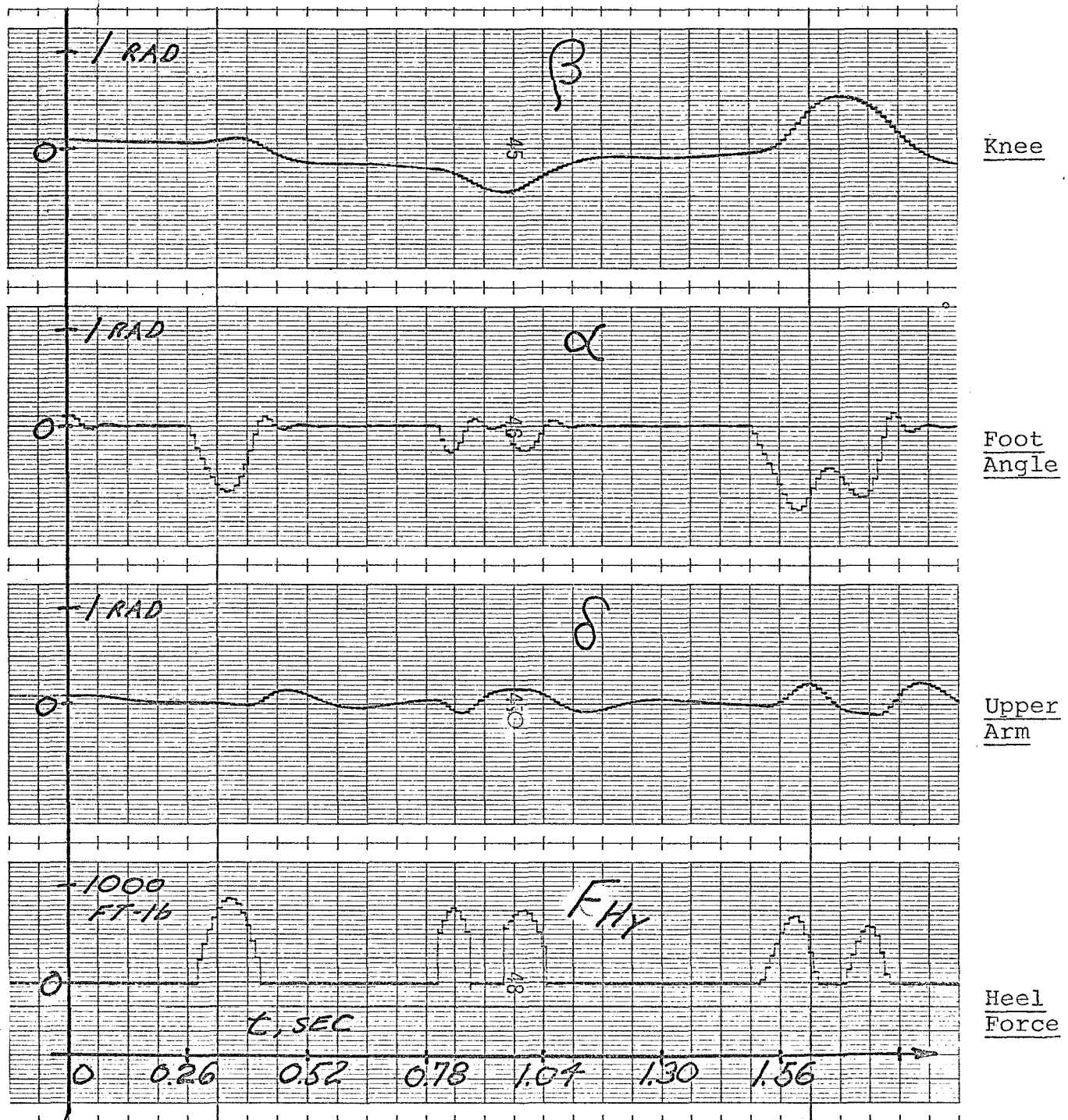Figure 5.   Joint Angles for a One Foot Drop.

Figure 5 (Cont'd). Joint Angles for a One Foot Drop.

i.e., each joint was torqued proportional to a linear combination of joint angle and joint angular rate. Numerically,

$$K_{q_i} \cong -100 \ \frac{ft-lb}{rad} \qquad\qquad (24)$$

$$K_{\dot{q}_i} \cong -5 \ \frac{ft-lb}{rad} \qquad\qquad (25)$$

Figure 5 presents tenative time histories of the joint angles resulting when the above simulation is dropped from an initial altitude of one foot using the above form of control law.

Channel 2 is y, the vertical displacement of the trunk c.g. Released one foot above its equilibrium position, y decreases parabolically under gravity until the toe strikes the ground (see F_{Ty}) (Channel 8 shows the heel strike (F_{Hy}) occurring slightly later in time. The vertical heel and toe forces cause y to decelerate and begin to move up (y, Channel 2), the trunk pitches forward (θ, Channel 3), the thigh moves up (γ, Channel 4), the knee bends back (β, Channel 5), the foot angle goes negative (α, Channel 6), and the upper arm pitches forward slightly (δ, Channel 7).

Conclusions

Based on the work we have completed so far, the research program we have outlined still appears feasible; no major alterations appear necessary at the present time.

V. Future Work

1. The simulation results of the preceeding sections
   are based on equations derived primarily by
   hand, and therefore are likely to contain a number
   of analytic and numerical errors. The FORMAC
   results are now being used to verify and correct
   these equations.

2. Certain constraints, such as the physiological
   facts that knees, ankles, and elbows don't bend
   backwards, have thus far been neglected in the
   model. They will be included.

3. The control law of equations (23) - (25) will be
   investigated more thoroughly and modified and
   refined, in the hope of beginning an investigation
   of load relief properties in the near future.

References

1. Milhorn, H. T., Jr., "The Application of Control Theory to
   Physiological Systems", W. B. Saunders Company, Chapter 17:
   "The Stretch Reflex in Human Muscle Systems", pp. 283-316.

2. Houk, J. C., "A Mathematical Model of the Stretch Reflex
   in Human Muscle Systems," M. A. Thesis, Massachusetts
   Institute of Technology, Cambridge, 1963.

3. Fenn, W. O., and Marsh, B. S., "Muscular Force at Different
   Speeds of Shortening", Journal of Physiology (London),
   Vol. 85, pp. 277ff, 1935.

4. Bahler, A. S., "Modeling of Mammalian Skeletal Muscle",
   I.E.E.E. Transactions on Bio-Medical Engineering, Vol. BME-15,
   No. 4, pp. 249-257, October, 1968.

5. Vickers, W. H., and Sheridan, T. B., "A Dynamic Model of an
   Agonist-Antagonist Muscle Pair", I.E.E.E. Transactions on
   Man-Machine Systems, March, 1968.

6. Galiana, H. L., "Modeling the Human Leg in Walking", Master
   of Engineering Thesis, Department of Electrical Engineering,
   McGill University, Montreal, Canada, August, 1968.

7. Magdaleno, R. E., and McRuer, D. T., "A Closed-Loop
   Neuromuscular System Explanation of Force Disturbance
   Regulation and Tremor Data", Fourth Annual NASA-University
   of Michigan, Ann Arbor, March 21-23, 1968.

8. DeWhurst, D. J., "Neuromuscular Control System", I.E.E.E.
   Transactions on Bio-Medical Engineering, Vol. BME-14,
   No. 3, pp. 167-171, July, 1967.

9. Miery, J. L., "The Vestibular System and Human Dynamic Space
   Orientation", Doctor of Science Thesis, M.I.T., June, 1965.

10. Young, L. R., "A Control Model of the Vestibular System",
    I.F.A.C. Symposium on Technical and Biological Problems in
    Cybernetics, Yerivan, Armenia, U.S.S.R., September, 1968.

11. Gottlieb, G. L., Agarwal, G. C., and Stark, L., "Stretch
    Receptor Models, I-Single-Efferent Single Affevent Innovation",
    I.E.E.E. Transactions on Man-Machine Systems, Vol. MMS-10,
    No. 1, pp. 17-27, March, 1969.

12. McRuer, D. T., and Magdaleno, R. E., "Human Pilot Dynamics
    with Various Manipulators", Technical Report No. AFFDL-TR-
    66-138, Air Force Flight Dynamics Laboratory, Research and
    Technology Division, Air Force Systems Command, Wright-
    Patterson AFB, Ohio; December, 1966.

13. Wasicko, R. J., McRuer, D. T., and Magdaleno, R. E., "Human Pilot Dynamic Response in Single-loop Systems with Compensatory and Pursuit Displays", Technical Report AFFDL-TR-66-137, Air Force Flight Dynamics Laboratory, Research and Technology Division, Air Force Systems Command, Wright-Patterson AFB, Ohio; December, 1966.

14. Magdaleno, R. E. and McRuer, D. T., "Effects of Manipulator Restraints on Human Operator Performance", Technical Report AFFDL-TR-66-72, Air Force Flight Dynamics Laboratory, Research and Technology Division, Air Force Systems Command, Wright-Patterson AFB, Ohio; December, 1966.

15. McRuer, D. T., Graham, D., Kvendal, E., and Reisener, W., Jr., "Human Pilot Dynamics in Compensatory Systems: Theory, Models, and Experiments with Controlled Element and Forcing Function Variations", Technical Report No. AFFDL-TR-65-15, Air Force Flight Dynamics Laboratory, Research and Technology Division, Air Force Systems Command, Wright-Patterson AFB, Ohio; December, 1966.

16. Shirley, R. S., and Young, L. R., "Motion Cues in Man-Vehicle Control", Fourth Annual NASA-University Conference on Manual Control, University of Michigan, Ann Arbor, March 21-23, 1968.

17. Adams, J. J., "Synthesis of Human Response in Closed-Loop Control Tasks", Fourth Annual NASA-University Conference on Manual Control, University of Michigan, Ann Arbor, March 21-23, 1968.

18. Wier, D. H., and McRuer, D. T., "Models for Steering Control of Motor Vehicles", Fourth Annual NASA-University of Michigan, Ann Arbor, March 21-23, 1968.

19. Crossman, E. R. F. W., "Man-Machine Models for Car Steering", Fourth Annual NASA-University Conference on Manual Control, University of Michigan, Ann Arbor, March 21-23, 1968.

20. Agarwal, G. C., Berman, G., Hogins, M. T., Lohnberg, P., and Stark, L., "Effect of External Loading on Human Motor Reflexes", Fourth Annual NASA-University Conference on Manual Control, University of Michigan, Ann Arbor, March 21-23, 1968.

21. McGhee, R. B., "Some Finite State Aspects of Legged Locomotion", Mathematical Biosciences, Vol. 2, No. 2, pp. 67-84, 1968.

22. McGhee, R. B., "Finite State Control of Quadruple Locomotion", Simulation, Vol. 9, No. 3, pp. 135-140, September, 1967.

23. McGhee, R. B., and Frank, A. A., "On the Stability Properties of Quadruped Creeping Gaits", Mathematical Biosciences, December, 1968.

24. Frank, A. A., and McGhee, R. B., "Some Considerations Relating to the Design of Autopilots for Legged Vehicles", Symposium on Aids to Human Motion, January 21, 22, 1968, sponsored by the General Electric Company, and the U. S. Army Tank and Automotive Command, Warren, Michigan.

25. Tomovic, R., and McGhee, R. B., "A Finite State Approach to the Synthesis of Bioengineering Control Systems", I.E.E.E. Transactions on Human Factors in Electronics, Vol. HFE-7, No. 2, June, 1966, pp. 65-69.

26. Gibson, J. E., di Tada, E. G., Hill, J. C. and Ibrahim, E. S., "Describing Function Inversion: Theory and Computational Techniques", Technical Report TR-EE62-10, Purdue University School of Electrical Engineering, December, 1962.

27. Mosher, Ralph S., "Exploring the Potential of a Quadruped", S.A.E. Paper No. 690191, International Automotive Engineering Conference, Detroit, Michigan, January 13-17, 1969.

28. Blackmer, R. H., Interian, A., and Clodfelter, R. G., "The Role of Space Manipulator Systems for Extravehicular Tasks", Second National Conference on Space Maintenance and Extravehicular Activities, Las Vegas, Nevada, August 6-8, 1968.

29. Whitney, Daniel E., "Resolved Motion Rate Control of Manipulators and Human Prostheses", I.E.E.E. Transactions on Man-Machine Systems, Vol. MMS-10, No. 2, June, 1969, pp. 47-53.

NASA BIOSYSTEMS - BIO-OPTICS

This is a report on the work on bio-optics since the initial progress report. The first section of this chapter will deal with questions as to the application of liquid crystals to control problems. A later section will be concerned with the theoretical results for ellipsoidal particles representing long molecules in a simple shear field.

Applications

The application of liquid crystals proposed in the first report was centered around the control of the index of refraction of "eye glasses" to allow continuous focusing as substitute for bifocal or trifocal lenses now used for vision correction. The next extension would be to the augmentation of visual accommodation in dynamic tracking problems. Most tracking models of visual response have dealt with the motor control of the eye in following objects in a plane or essentially "far away". (i.e., the up-down and sidewise motion of the eye.) If one examines the reaction times of the important control processes in vision, however, the limiting response time is that of accommodation or focus control. The response time for eye movement is approximately 120 milliseconds, for pupil reaction 250 miliseconds, but for accommodation 400 milliseconds. The ability to maintain focus on an

object which is in motion toward and away from the observer
appears to be the limiting function in eye control. (The 400
milliseconds response time is that recorded for a 2 diopter
change in focus.[1])

The question remains as to what this effect has on our
ability to track rapidly-approaching or receding objects.
Possible consequences on man's ability to respond to rapidly
changing visual events have not been explored.

As an example of the situations where control of accommodation may be important let us consider the response of the
eye in tracking or observing an object which is viewed through
a screen. The eye has great difficulty in focusing on the
screen from a focus on a distant object. If the object is to
be fixed in position on the grid, this is an oscillatory
tracking maneuver difficult to maintain. It is known that in
the adjustment in focus required to follow receding objects
the eye may lose focus and instead of continuing to track may
fluctuate about an intermediate focus. Another response is an
oscillatory focus with with lens of the eye moving in the
opposite direction from the object being tracked. All these
effects or combinations may occur in the processes of visually
observing a sequence of near and distant objects. If the human
physiological focus control is not adequate for these type
tasks an augmentation using a rapid focus technique will be
required. Liquid crystal devices are a possible mechanism
which could be used to augment this visual accommodation. It

remains then to consider whether a fast controlled focus is compatible with the physiological control system of the eye and could be used in rapid observation changes.

The theory of eye tracking or saccadic motion is well established and understood as noted in the work of Young and Stark.[2] The problem of importance in obtaining information from moving objects is certainly more involved than this theory. Eye tracking theory is based on obtaining information on only the spatial position of an object in a two-dimensional space. No information is asked about the size, shape or configuration of the object. To include this information, an understanding of the accommodation response of the eye needs to be included. "Tracking for information" could be attacked in several ways:

1. Experiments with an optometer to change the object distance rapidly in order to quantify the physiological response and test an augmentation system.

2. Build a focusing system which has a manually controllable focus for use in tracking an object in space. Then use this to examine the feedback response requirements needed.

3. Provide a system whereby eye lens motion is sensed to control the focus of an augmentated system.

The control questions which must be answered in an automatic focus system or zoom lens control are: (1) What will be the physiological reaction to the automatic control? (2) What conscious response feedback control is present in the focus feedback loop? (3) If a focus system is built with a step-response behavior will this operate more adequately than a continuous focus system?

The use of liquid crystals as a focus control mechanism has an advantage over pressure or lens movement systems because their response time can be much faster since the inertial elements are smaller.

Present research in liquid crystals has been based on observation of effects. The results are in terms of full orientation of molecular groups rather than continuous control of this orientation. The study of the shear-field orientation effect is in part motivated by its potential for continuous control.

The more general applications of the analysis of the action of particles or molecules in flow or in energy fields include the continuous control of liquid slurries in an electrostatic or magnetic clutch or control of the flow of fluids by alternating or direct fields. The applications as field sensors are also numerous and will not be discussed here. (The application to blood flow measurement is discussed in a paper which is in preparation.[3]) The general observation should be made here, however, that emphasis is being

placed on nematic liquid crystals (i.e., those which are vector field sensitive rather than energy or intensity sensitive.)

In the First Progress Report, rough estimates of the change in index of refraction of a lens required to produce an accommodation assist were outlined. A change in focal power of 9 diopters was shown to be adequate for this application. This accommodation could be obtained by altering the radius of curvature or the index of refraction of a lens. The technique of altering the index of refraction was chosen to take advantage of the rapid response possibilities of liquid crystals and their recent availability of room-temperature nematic (shear type) crystals.

Analysis

The index of refraction variation is analyzed by utilizing the relation between index of refraction and dielectric constant

$$n = (K \frac{\mu}{\mu_o})^{1/2} \qquad (1)$$

where n is the index of refraction, K the dielectric constant and $\frac{\mu}{\mu_o}$ the relative magnetic permeability. For this analysis the relative permeability is assumed fixed and the dielectric constant effect examined.

The first method of focus control has been the application of a shear field to a nematic type liquid crystal. In order to analyze the index of refraction change possible in

these materials, an analytical model of a liquid crystal as
consisting long symmetrical ellipsoids approximating long
molecules is assumed. The hydrodynamic effect of a simple
shear field on these ellipsoids is then examined. From the
motion of the ellipsoids the change in index of refraction is
predicted in this section of the report.

As a first approximation, then, long molecules in a
fluid will be assumed as ellipsoids with different properties
than the fluid in which they are contained. These ellipsoids
will be assumed randomly dispersed in a media and free to
rotate and translate under the influence of electrical or
mechanical forces. The flow geometry of Figure (1) will be
assumed with the properties of the fluid designated with
subscript "s" and that of the ellipsoids with a subscript "p".

For a random dispersion of ellipsoids (a suspension at
rest in the absence of a disturbance) the dielectric constant
has been shown[4] to be approximated by the equations

$$K = K_s + \frac{\rho}{3}(K_p - K_s) \sum_{\alpha=a,b,c} \left[\frac{1 + x_\alpha}{x_\alpha + K_p/K_s} \right] \qquad (2)$$

where

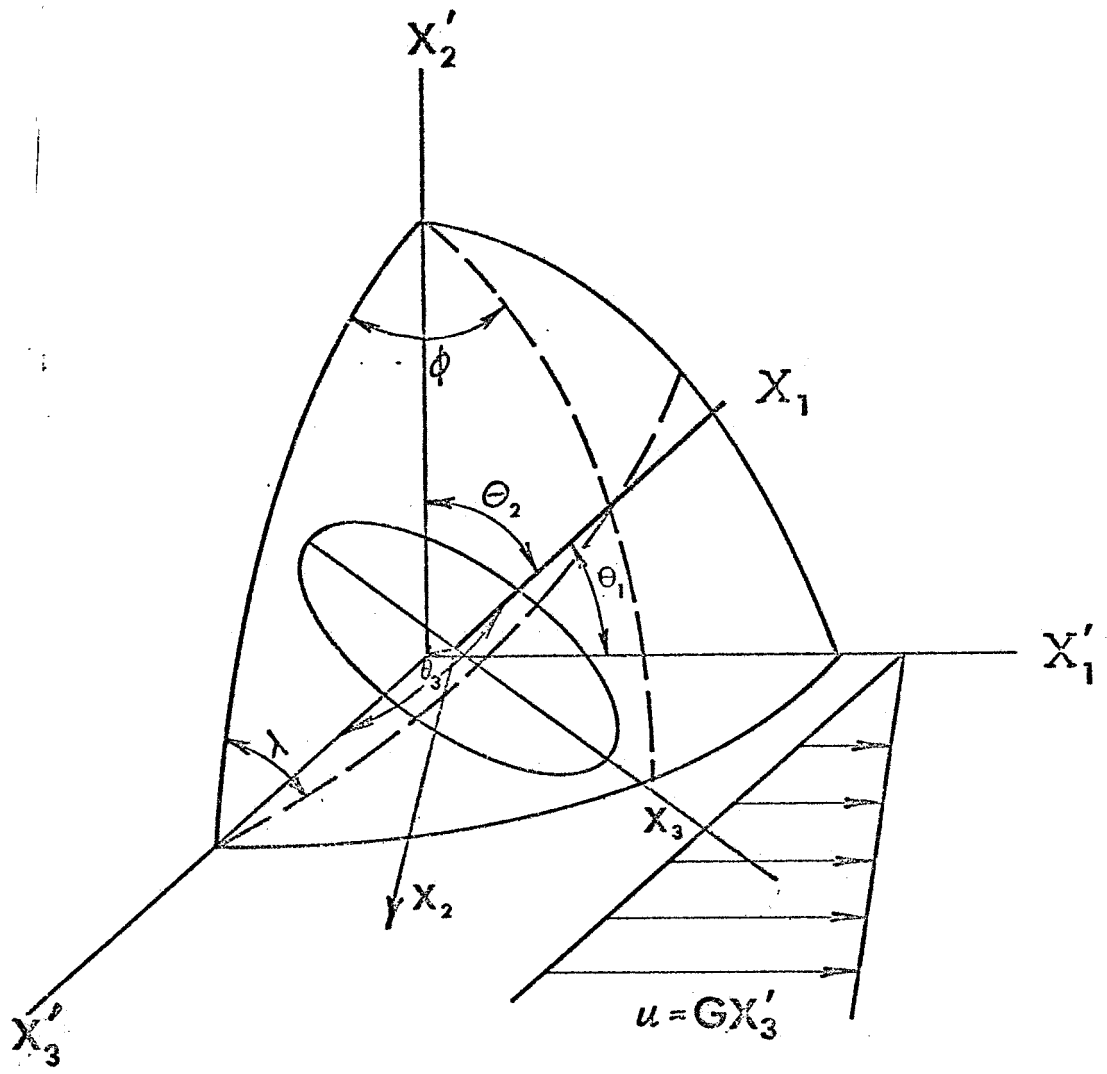$$x_\alpha = \frac{2 - abc\ L_\alpha}{abc\ L_\alpha} \qquad (3)$$

and

Fig. 1 Coordinate Geometry for an Ellipsoid of Revolution in a Shear Flow

52

$$L_\alpha = \int_0^\infty \frac{d\lambda}{(\alpha^2+\lambda)\ \sqrt{a^2+\lambda)\ (b^2+\lambda)\ (c^2+\lambda)}} \quad . \qquad (4)$$

((a,b,c,) are the axes of the ellipsoid.)

These equations can be reduced to the dielectric

constant for an aligned suspension by replacing $\frac{\rho}{3}$ by ρ and

removing the summation sign. For example, to obtain the

conductivity of a suspension aligned with the a axes in the

direction of the applied field

$$K_a = K_s + (K_p - K_s)\ \rho \left[\frac{1 - x_a}{x_a + K_p/K_s}\right] . \qquad (5)$$

We are concerned in this report with the dielectric

constant of a suspension in which the ellipsoids are in motion

produced by a field (in particular a simple mechanical shear

field).

Similar equations with a replaced by b or c represent

the dielectric constant of a solution with the axes b or c

aligned with the field. These quantities designated K_a, K_b, and

K_c give the principle dielectric constant of a suspension of

uniform ellipsoids. The variation of the principle dielectric

constants K_a and K_b if the dielectric constant of the particle

(K_p) is assumed to be zero is shown in Figure (2) for a particle

density of 0.5 as a function of the axis ratio $r = \frac{a}{b}$. To find

the dielectric constant at any angle to the principle axes the

dielectric constant is assumed to be a second order tensor

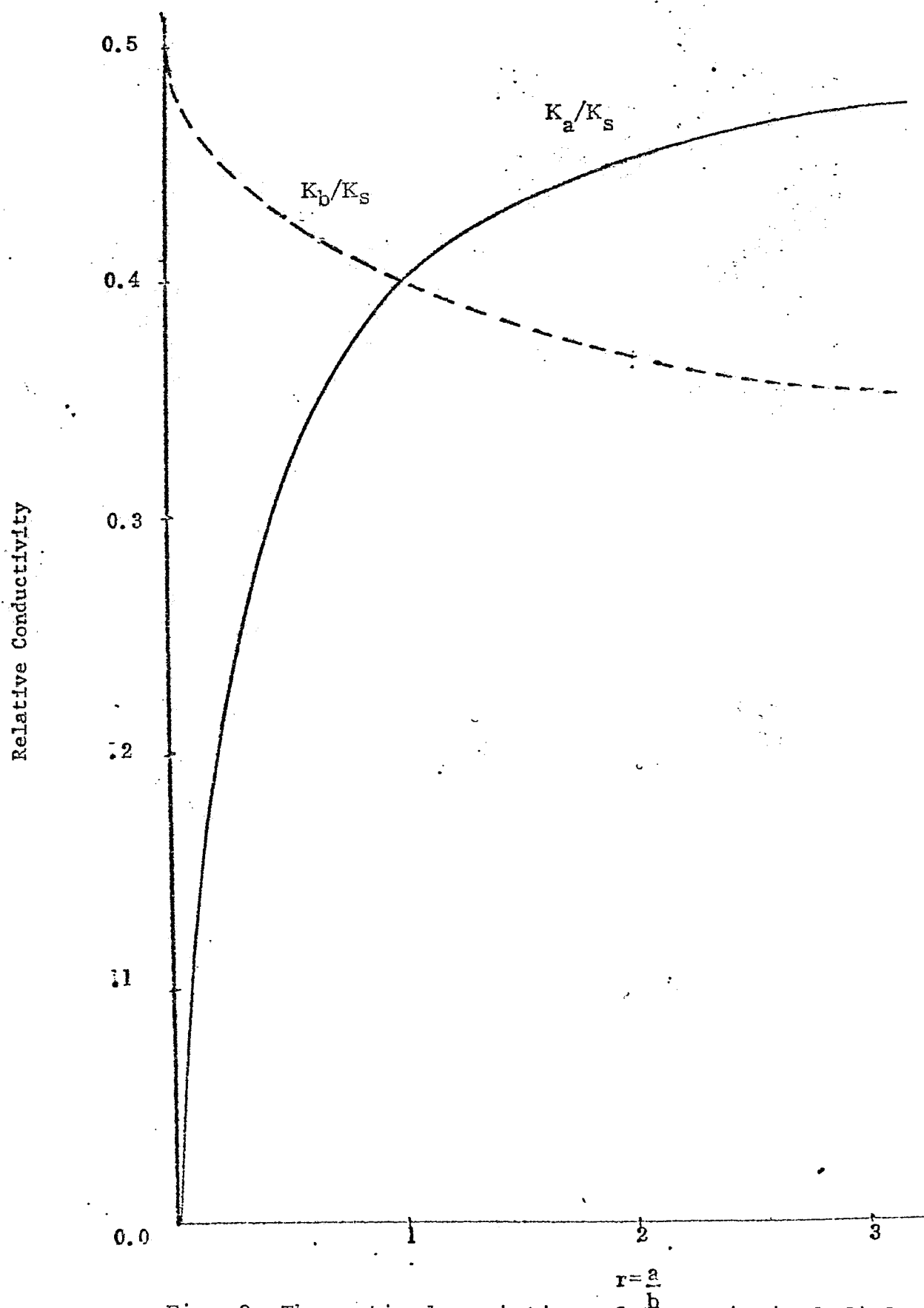quality, which transforms according to the tensor relation

Fig. 2   Theoretical variation of the principal dielectric
         constant of symmetrical ellipsoids in suspension
         as a function of the axis ratio r = a/b.   The
         volume density shown is ζ = 0.5.

$$K_{ij}' = a_{ik} \, a_{j\ell} \, K_{k\ell} \, . \qquad\qquad (6)$$

$a_{j\ell}$ represent the cosines of the angles between the original axes and the new axes. In this case $a_{j\ell}$ represent the cosines of the angles between the axes of the ellipsoid and the applied field.

Using the tensor property of the conductivity, the conductivity in the direction of the x_3^1 axis is

$$K_{33}^1 = a_{31}a_{31}K_{11} + a_{32}a_{32}K_{22} + a_{33}a_{33}K_{33} \, .$$

Setting $K_{22} = K_{33}$ and using the geometrical relations

$$a_{31}{}^2 + a_{32}{}^2 + a_{33}{}^2 = 1 \, , \qquad\qquad (7)$$

and

$$a_{31} = \cos\,\theta_3$$

then

$$a_{32}{}^2 + a_{33}{}^2 = 1 - \cos^2\,\theta_3 \, ,$$

and

$$K_{33}^1 = K_a \cos^2\,\theta_3 + K_b(1 - \cos^2\,\theta_3) \, . \qquad (8,a)$$

Similarly

$$K_{22}{}^1 = K_a \cos^2 \theta_2 + K_b(1 - \cos^2 \theta_2) \qquad (8,b)$$

and

$$K_{11}{}^1 = K_a \cos^2 \theta_1 + K_b(1 - \cos^2 \theta_1) \; . \qquad (8,c)$$

These three equations define the dielectric constant of a
suspension in which the electric field is in the direction of
one of the prime axes in terms of the principle dielectric con-
stants and the cosine of the angle between the axis of symmetry
and the direction of the field.

The dielectric constant is then obtained by proper
averaging as a function of angle of the ellipsoids to the
applied electric field. (See Appendix III.)

The results of this analysis may be summarized by the
following discussion and equations.

The dielectric constant of a sheared suspension in the
three directions x_1', x_2', x_3' may be represented by the
equations

$$\overline{K_{11}'} = K_b + (K_a - K_b) \; \overline{F_1} \qquad (9,a)$$

$$\overline{K_{22}'} = K_b + (K_a - K_b) \; \overline{F_2} \qquad (9,b)$$

$$\overline{K_{33}'} = K_b + (K_a - K_b) \; \overline{F_3} \qquad (9,c)$$

The variation which can be produced by a shear field is summarized in Figure (3) where the shear factors F_1, F_2 and F_3 are shown as a function of the ellipsoidal axis ratio, r.

Since the factor F is 0.5 (Equation A5, Appendix A) when the suspension is randomly orientated (i.e., when the suspension is dispersed due to Brownian motion), the variation from this value with shear represents the magnitude of the effect. If we are concerned with long molecules (prolate ellipsoids) where $r \gg 1$ it is clear that slight variation with shear occurs in the direction perpendicular to shear planes ($\overline{F_3}$). The maximum variation occurs along the shear planes in the direction of the shear (F_1). For control of properties by a shear field the maximum response can be obtained (for $r \gg 1$) by motion in the x_1^1 direction and observation in the same direction. If the control is provided by a sandwich the plates should be moved parallel to each other and the observation made as shown in Figure (4,a). The other alternative is to vibrate a plane perpendicular to the sandwich and observe as whown in Figure (4,b). If we are concerned with a fluid with oblate particles [(or discs with ($r \ll 1$)], then the response will depend upon the direction of observation. The effect is much greater for observation in the x_3 and x_2 directions than for prolate spheroids. If a choice of form of the particles is possible then oblate spheroids have a clear advantage from the control or detection point of view. For liquid crystals we do not have this choice, the molecules are approximated by long prolate
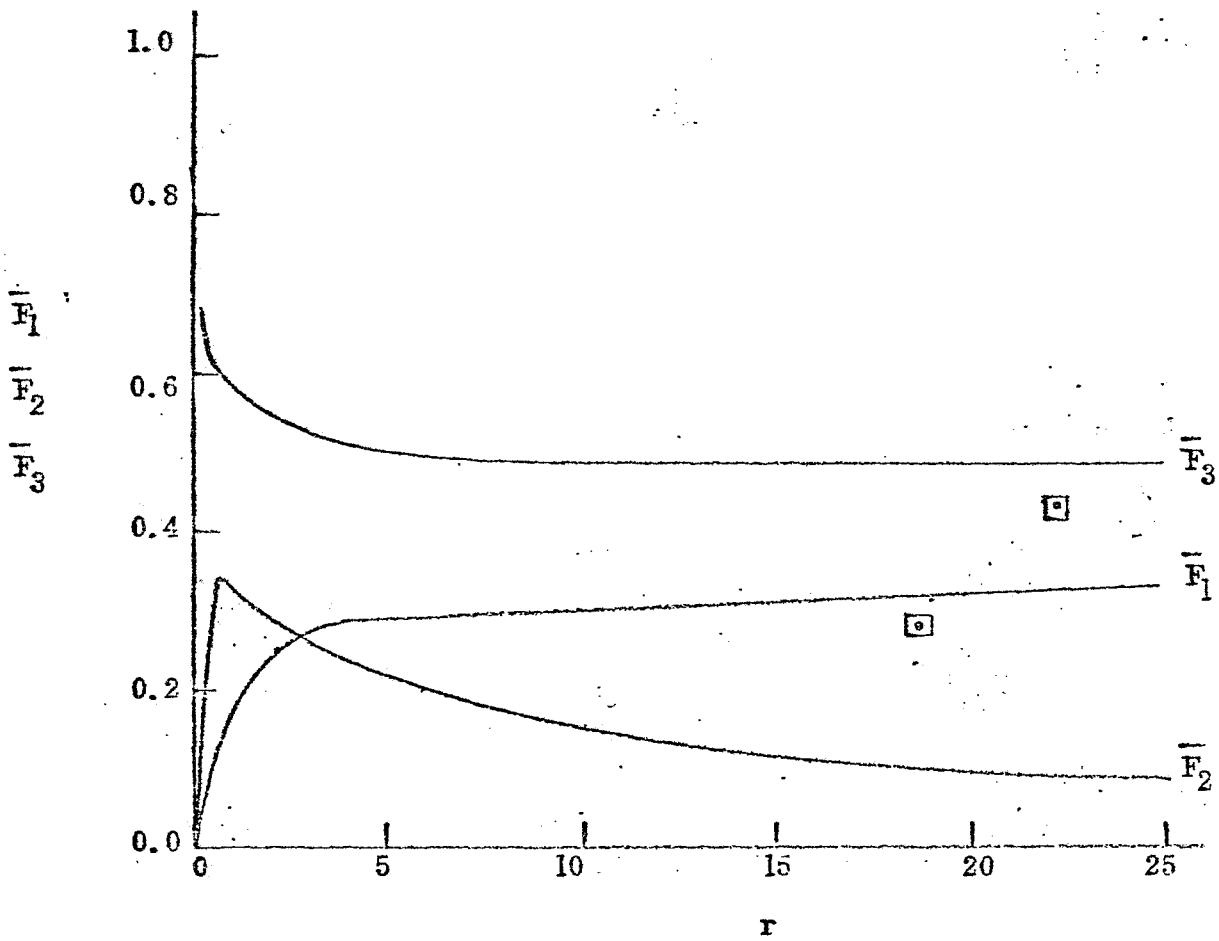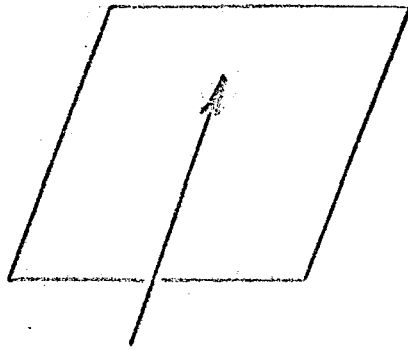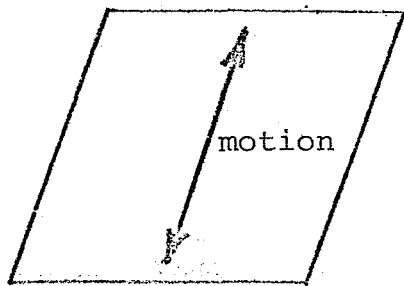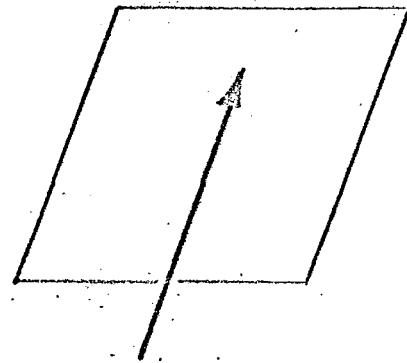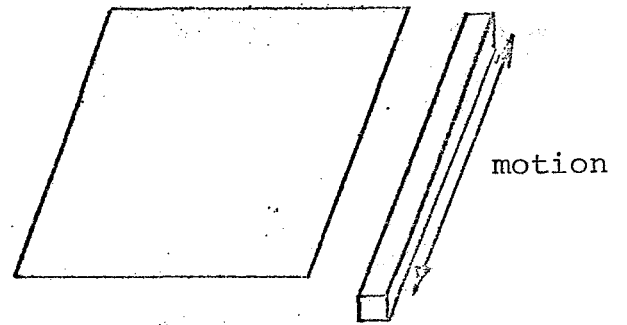
Fig. 3   Computed theoretical conductivity factors for
conductivity as a function of the ellipsoid
axis ratio r = a/b.

Figure 4a

Figure 4b

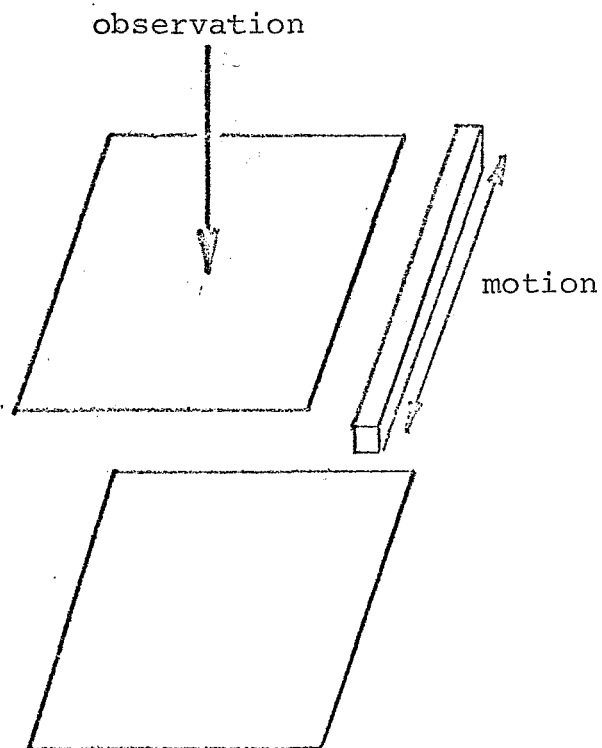Figure 5

ellipsoids. In this case the best alternative at present is the system shown in Figure (5).

Experiments-Observations on Corneal Transparency

The incidental problem of corneal transparency which is important in the context of fibrous material transparency has been examined further with some physiological exploratory experiments.

Excised rabbit cornea have been examined in the laboratory for determination of their scattering properties. From observations with polarized laser light, it is observed that scattering from particles greater than the size of the fibrils involved is appreciable (using techniques of crossed polarizer transmission). The scattering has been difficult to quantitate because of the rapid deterioration of these cornea in saline solution. By the use of crossed polarizers, it has been estimated in preliminary experiments that the ratio of the intensity transmitted to scattered light by the cornea is approximately 10 to 1. These are preliminary data and improvement in experimental technique will be required to describe this more accurately.

These experiments are directed toward the understanding of the transparency of the cornea and its relation to the transparency of orientated fiber type materials. The relation of this work to liquid crystals was discussed briefly in the First Progress Report.

Summary

The theoretical analysis of the effect of a shear field on a suspension of long ellipsoids (representing a nematic liquid crystal) has been completed. The dielectric constant and index of refraction changes to be expected have been estimated. The other two steps outlined in the First Progress Report are now to be attempted.

1. Experimental demonstration of control of index of refraction by a shear field including flat and cylindrical configurations.

2. Further work on corneal transparency is in progress including scattering from corneal fibrils. In addition, an extension to focus or accommodation control is expected as explained briefly in the beginning of this section.

PATTERN RECOGNITION OF RANDOM SPATIAL SIGNALS
USING COHERENT OPTICAL TECHNIQUES

In Progress Report 1 (PR1) it was shown how biological photomicrographs could be considered to be random diffracting screens when illuminated with coherent light. This is a particular example of the general problem of pattern recognition of random spatial signals. The main purpose of current research is to determine to what extent statistical analysis and identification of random spatial signals can be carried out by optical techniques. The development of such techniques would be important for a wide variety of possible applications. As described in PR1 application of these techniques to biological photomicrographs would permit the direct determination of such statistical quantities as mean cell size and distribution.

Another area of application of these techniques is to provide a quantitative measure of "randomness" to be used as an error signal in automatic control systems. For example, the total light scattered off-axis in the transform plane provides a direct measure of the variance of the random process. Such measurements could provide an index of smoothness of reflecting surfaces. Based on such an index, for example, a spacecraft might be landed automatically on the smoothest terrain of a moon or planet. Another spatially random control signal might

be the distribution of stars in the sky. If different regions

of the sky have different statistical distributions of stars,

then direct optical measurements of these properties might be

used in the automatic control and navigation of spacecraft.

In PRl it was shown how an optical processing system could

be used for power spectrum and autocorrelation measurements.

The standard optical processing system contains a collimating

lens, a transforming lens, and an imaging (or second transforming)

lens. By appropriately locating the input plane, the same lens

can be used for both transforming and imaging the input signal.

As will be shown below, the incident wave need not be a plane

wave so that the collimating lens can also be eliminated. An

analysis of this system will allow one to determine the relation-

ship between the spatial frequency in the power spectrum measure-

ments and the geometry of the system.

A schematic of the optical processing system is shown in

Figure 1 where $g(x,y)$ is the complex transmittance of the photo-

micrograph or other random spatial signal. The single lens in

this system could be replaced by a spherical mirror resulting

in the lensless optical processor discussed in PRl. Such a

system could be designed to accept photomicrographs of large

spatial extent thus justifying the ergodic hypothesis when making

power spectrum measurements of random signals. The analysis below

applies to either a single lens system or a lensless system using
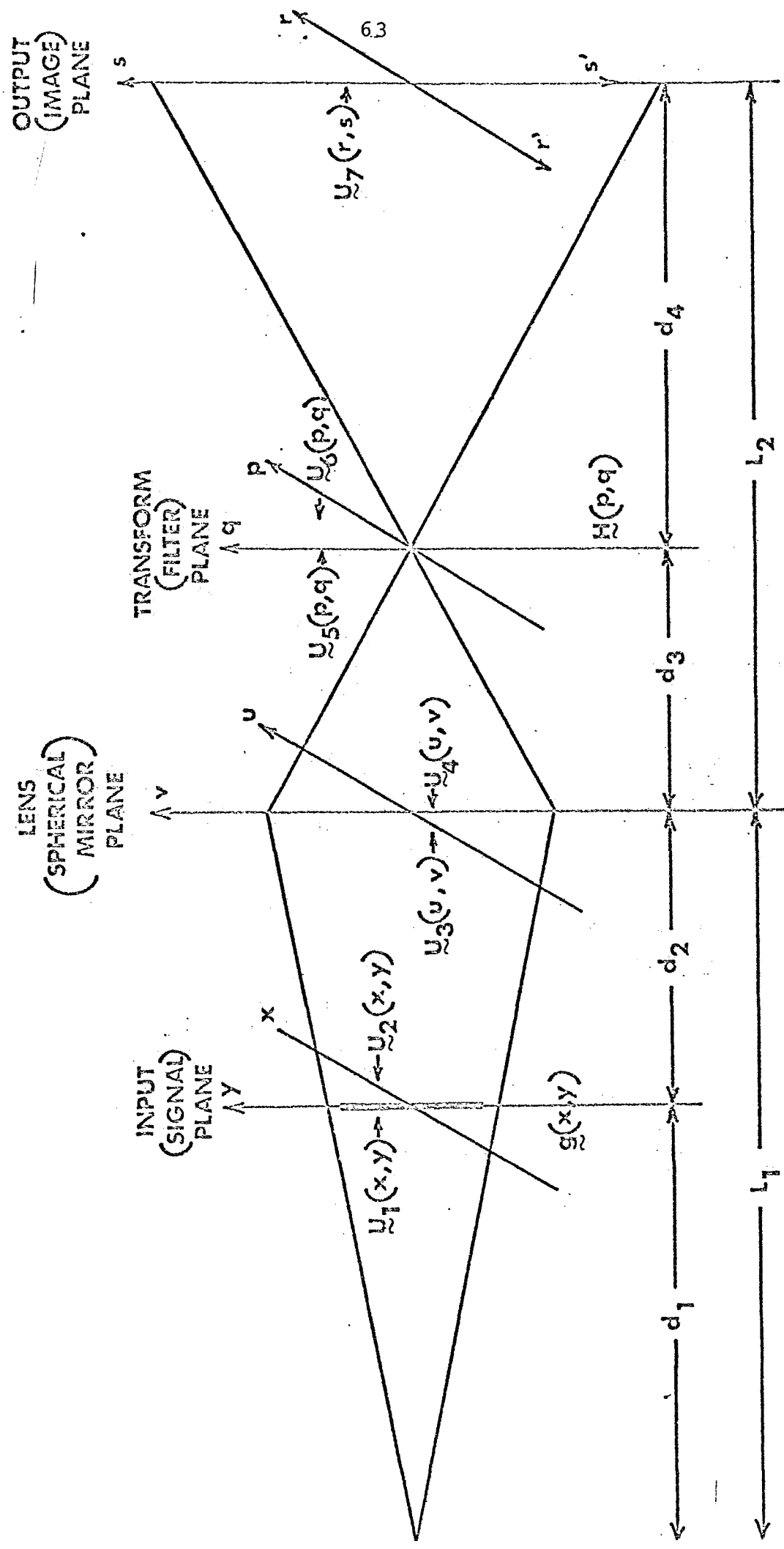
a spherical mirror.

Fig. 1 Geometry of Single Lens Optical Processor

Analysis of the Optical Processing System

A wave analysis of the optical system in Figure 1 can be carried out by determining the complex amplitude of the wave $\underset{\sim}{U}(x,y)$ at any plane perpendicular to the optical axis. If $\underset{\sim}{U}'(x_1,y_1)$ is the complex amplitude of the wave at plane $z = 0$, then the complex amplitude $\underset{\sim}{U}(x_o,y_o)$ at a parallel plane a distance z away is given by the Huygen-Fresnel principle[1,2] as shown in Figure 2. Referring to Figure 2 one sees that the effect of traveling a distance d in free space is to change $\underset{\sim}{U}'(x_1,y_1)$ to $\underset{\sim}{U}(x_o,y_o)$ through the relation

$$\underset{\sim}{U}(x_o,y_o) = \underset{\sim}{K} \iint\limits_{-\infty}^{\infty} \underset{\sim}{U}'(x_1,y_1) e^{j\frac{k}{2d}[(x_o-x_1)^2 + (y_o-y_1)^2]} dx_1 dy_1 \qquad (1)$$

where $\underset{\sim}{K}$ is a complex constant and $\underset{\sim}{U}'(x_1,y_1)$ is assumed to be zero outside the aperture. The result for light from a point source on the axis traveling a distance d is found by letting $\underset{\sim}{U}'(x_1,y_1) = \delta(x_1,y_1)$ in (1) from which

$$\underset{\sim}{U}_d(x_o,y_o) = \underset{\sim}{K} e^{j\frac{k}{2d}(x_o^2 + y_o^2)} \qquad (2)$$

The effect of the lens (or spherical mirror) is to multiply the incident amplitude function $\underset{\sim}{U}(x,y)$ by some complex amplitude $\underset{\sim}{\psi}(x,y)$. To determine $\underset{\sim}{\psi}(x,y)$ recognize that light from a point source which is incident on the lens (or mirror) after traveling a distance f equal to the focal length will be transmitted (or reflected) as a plane wave. That is

Fig. 2 Geometry of Huygen-Fresnel principle
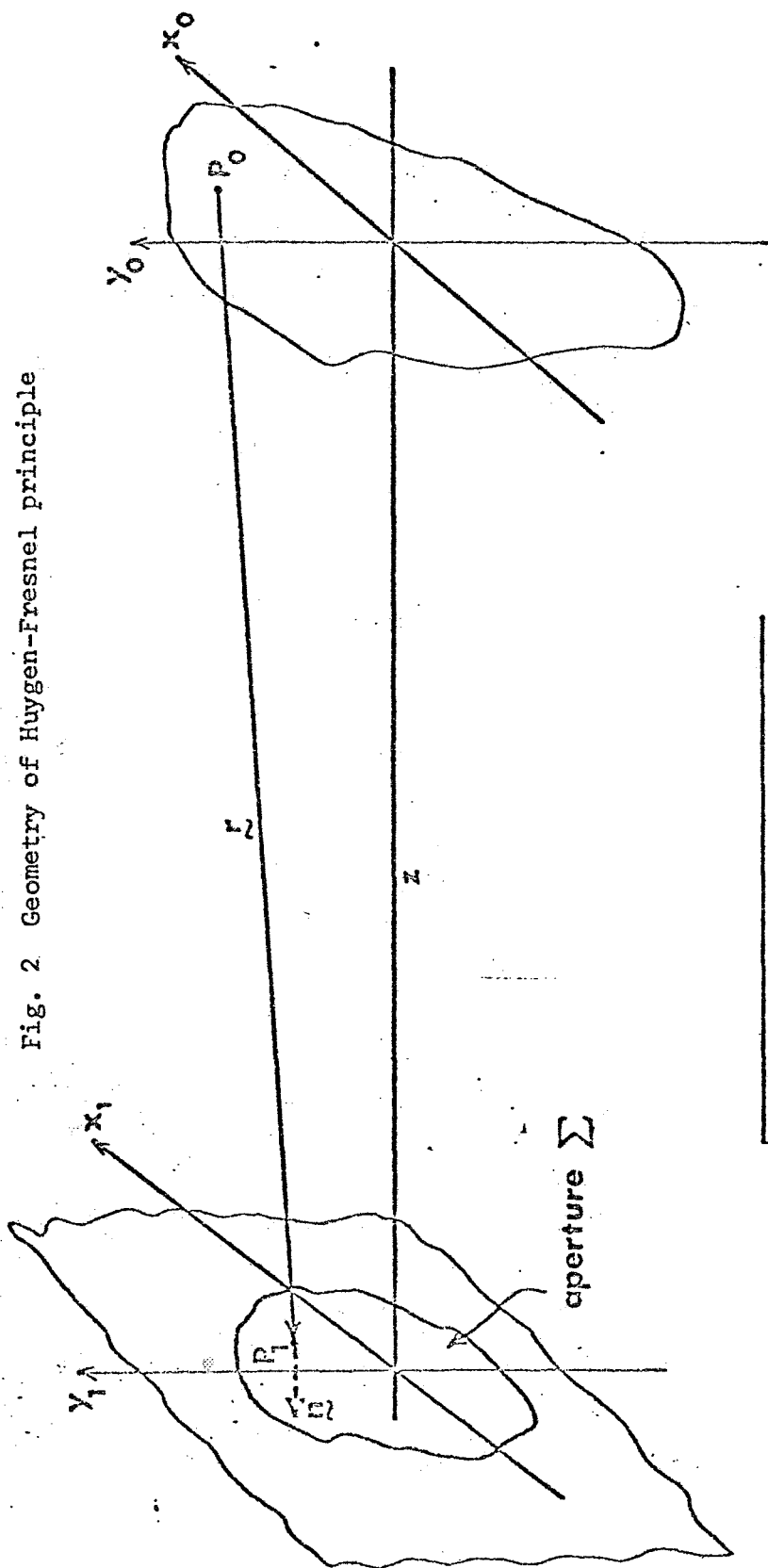
$$r = \sqrt{z^2 + (x_0 - x_1)^2 + (y_0 - y_1)^2}$$

$$\approx z \left[1 + \frac{1}{2} \left(\frac{x_0 - x_1}{z} \right)^2 + \frac{1}{2} \left(\frac{y_0 - y_1}{z} \right)^2 \right]$$

(Paraxial Approximation)

$$U(x_0, y_0) = \frac{1}{i\lambda} \iint_\Sigma U'(x_1, y_1) \cdot \frac{e^{ikr}}{r} \cos(n, r) \, dx_1 \, dy_1$$

$$\approx \frac{e^{ikz}}{i\lambda z} \int\!\!\!\int_{-\infty}^{\infty} U'(x_1, y_1) \, e^{i\frac{k}{2z} \left[(x_0 - x_1)^2 + (y_0 - y_1)^2 \right]} \, dx_1 \, dy_1$$

$$\underset{\sim f}{U}(x,y) \; \underset{\sim}{\psi}(x,y) \;\; = \;\; \text{constant}$$

and thus from (2) it follows that

$$\underset{\sim}{\psi}(x,y) \; = \; e^{-j\frac{k}{2f}(x^2 + y^2)} \tag{3}$$

represents the effect of the lens (or spherical mirror) where

f is the focal length of the lens (or mirror).

Refer now to Figure 1 where $\underset{\sim 1}{U}(x,y)$ is the light amplitude

just to the left of the signal plane. From (2) $\underset{\sim 1}{U}(x,y)$ is given

by

$$\underset{\sim 1}{U}(x,y) \; = \; \underset{\sim 1}{K} \; e^{j\frac{k}{2d_1}(x^2 + y^2)} \tag{4}$$

To the right of the input plane $\underset{\sim 2}{U}(x,y)$ is given by

$$\underset{\sim 2}{U}(x,y) \; = \; \underset{\sim 1}{U}(x,y) \; \underset{\sim}{g}(x,y) \tag{5}$$

Equation (1) can be used to find $\underset{\sim 3}{U}(u,v)$ in terms of $\underset{\sim 2}{U}(x,y)$.

Thus

$$\underset{\sim 3}{U}(u,v) \; = \; \underset{\sim 2}{K} \iint_{-\infty}^{\infty} \underset{\sim 2}{U}(x,y) e^{j\frac{k}{2d_2}[(u-x)^2 + (v-y)^2]} \, dxdy \tag{6}$$

The effect of the lens (or mirror) is to multiply $\underset{\sim 3}{U}(u,v)$ by

$\psi(u,v)$ given by (3). Thus

$$\underset{\sim 4}{U}(u,v) \; = \; \underset{\sim 3}{U}(u,v) \; e^{-j\frac{k}{2f}(u^2 + v^2)} \tag{7}$$

Using (1) again $\underset{\sim 5}{U}(p,q)$ can be written as

$$U_5(p,q) = K_3 \iint_{-\infty}^{\infty} U_4(u,v) \; e^{\,j\frac{k}{2d_3}\,[(p-u)^2 + (q-v)^2]} \; dudv \qquad (8)$$

If a filter with a complex transmittance $H(p,q)$ is inserted in the p-q plane, then $U_6(p,q)$ is given by

$$U_6(p,q) = U_5(p,q) \; H(p,q) \qquad (9)$$

Finally the light amplitude in the output plane $U_7(r,s)$ is given by

$$U_7(r,s) = K_4 \iint_{-\infty}^{\infty} U_6(p,q) \; e^{\,j\frac{k}{2d_4}\,[(r-p)^2 + (s-q)^2]} \qquad (10)$$

It is convenient to first evaluate $U_5(p,q)$. Combining Equations (4) through (8) one can write

$$U_5(p,q) = K_5 \iiiint_{-\infty}^{\infty} g(x,y) \; e^{\,j\frac{k}{2}\rho} \; dudv \; dxdy \qquad (11)$$

where

$$\rho = \frac{x^2 + y^2}{d_1} + \frac{u^2 + v^2 + x^2 + y^2 - 2ux - 2vy}{d_2} - \frac{u^2 + v^2}{f}$$

$$+ \frac{p^2 + q^2 + u^2 + v^2 - 2pu - 2qv}{d_3} \qquad (12)$$

It is first necessary to do the integration over u and v. To this end let the parts of ρ containing u and v be represented by ρ_u and ρ_v respectively. Thus

$$\rho_u = u^2 \left(\frac{1}{d_2} - \frac{1}{f} + \frac{1}{d_3} \right) - 2u \left(\frac{x}{d_2} + \frac{p}{d_3} \right)$$

$$\rho_v = v^2 \left(\frac{1}{d_2} - \frac{1}{f} + \frac{1}{d_3} \right) - 2v \left(\frac{y}{d_2} + \frac{q}{d_3} \right) \tag{13}$$

Since

$$\int_{-\infty}^{\infty} e^{jC_1 (u-C_2)^2} \, du = C_3 \int_{-\infty}^{\infty} e^{j\frac{\pi}{2} \xi^2} \, d\xi = \text{constant}$$

it is desirable to complete the squares in (13) and write

$$\rho_u = \rho_u{}' - \frac{d_2 L_1}{d_1} \left(\frac{x}{d_2} + \frac{p}{d_3} \right)^2$$

$$\rho_v = \rho_v{}' - \frac{d_2 L_1}{d_1} \left(\frac{y}{d_2} + \frac{q}{d_3} \right)^2 \tag{14}$$

where

$$\rho_u{}' = \frac{d_1}{d_2 L_1} \left[u - \frac{d_2 L_1}{d_1} \left(\frac{x}{d_2} + \frac{p}{d_3} \right) \right]^2$$

$$\rho_v{}' = \frac{d_1}{d_2 L_1} \left[u - \frac{d_2 L_1}{d_1} \left(\frac{y}{d_2} + \frac{q}{d_3} \right) \right]^2 \tag{15}$$

and the lens formula $1/f = 1/L_1 + 1/d_3$ has been used. Combining (14) with the remaining terms in (12) one can write ρ in the form

$$\rho = \rho_u{}' + \rho_v{}' + \left(\frac{1}{d_1} + \frac{1}{d_2} - \frac{L_1}{d_1 d_2} \right) \left(x^2 + y^2 \right)$$

$$+ \left(\frac{1}{d_3} - \frac{d_2 L_1}{d_1 d_3{}^2} \right) \left(p^2 + q^2 \right) - \frac{2L_1}{d_1 d_3} (xp + yq) \tag{16}$$

The terms ρ_u' and ρ_v' give a constant when integrated over u and v. The coefficient of $(x^2 + y^2)$ in (16) is identically zero. Thus (11) can be written as

$$\underset{\sim}{U}_5(p,q) = \underset{\sim}{K}_6 \ e^{j\frac{k}{2d_3}\left(1 - \frac{d_2L_1}{d_1d_3}\right)\left(p^2 + q^2\right)}\iint\limits_{-\infty}^{\infty} \underset{\sim}{g}(x,y) \ e^{-j\frac{2\pi L_1}{\lambda d_1 d_3}(xp + yq)} dxdy$$

$$= \underset{\sim}{K}_6 \ e^{j\frac{k}{2d_3}\left(1 - \frac{d_2L_1}{d_1d_3}\right)\left(p^2 + q^2\right)} \underset{\sim}{G}\left(\frac{L_1 p}{\lambda d_1 d_3} \ , \ \frac{L_1 q}{\lambda d_1 d_3}\right) \qquad (17)$$

where $\underset{\sim}{G}(f_x, f_y)$ is the two-dimensional·Fourier transform of $\underset{\sim}{g}(x,y)$ with spatial frequencies $f_x = L_1 p/\lambda d_1 d_3$ and $f_y = L_1 q/\lambda d_1 d_3$.

A filter with an impulse response $\underset{\sim}{h}(x,y)$ and a transfer function $\underset{\sim}{H}(f_x, f_y)$ is to be inserted in the p-q plane. Then from (17), (9) and (10), $\underset{\sim}{U}_7(r,s)$ can be written as

$$\underset{\sim}{U}_7(r,s) = \underset{\sim}{K}_7 \iint\limits_{-\infty}^{\infty} \underset{\sim}{G}\left(\frac{L_1 p}{\lambda d_1 d_3} \ , \ \frac{L_1 q}{\lambda d_1 d_3}\right) \underset{\sim}{H}\left(\frac{L_1 p}{\lambda d_1 d_3} \ , \ \frac{L_1 q}{\lambda d_1 d_3}\right) e^{j\frac{k}{2}u} \ dpdq$$

$$\tag{18}$$

where

$$u = \frac{1}{d_3}\left(1 - \frac{d_2 L_1}{d_1 d_3}\right)\left(p^2 + q^2\right) + \frac{1}{d_4}\left(r^2 + s^2 + p^2 + q^2 - 2rp - 2sq\right)$$

$$\tag{19}$$

The coefficient of $(p^2 + q^2)$ in (19) is

$$\frac{1}{d_3} + \frac{1}{d_4} - \frac{d_2 L_1}{d_1 d_3^2} \qquad (20)$$

Applying the lens formula to Figure 1 one can write

$$\frac{1}{f} = \frac{1}{L_1} + \frac{1}{d_3} = \frac{1}{d_2} + \frac{1}{L_2} \qquad (21)$$

By cross-multiplying and combining terms in (21) one can show that

$$\frac{L_1}{d_1 d_3} = \frac{L_2}{d_2 d_4} \qquad (22)$$

Substituting (22) into (20) one obtains

$$\frac{1}{d_3} + \frac{1}{d_4} - \frac{L_2}{d_3 d_4} = 0$$

so that the coefficient of $(p^2 + q^2)$ in (19) vanishes. Thus, (18) reduces to

$$\underset{\sim}{U}_7 (r,s) = \underset{\sim}{K}_7 \, e^{j\frac{k}{2d_4} (r^2 + s^2)} \int\!\!\!\int_{-\infty}^{\infty} \underset{\sim}{G} \left(\frac{L_1 p}{\lambda d_1 d_3} , \frac{L_1 q}{\lambda d_1 d_3} \right) \underset{\sim}{H} \left(\frac{L_1 p}{\lambda d_1 d_3} , \frac{L_1 q}{\lambda d_1 d_3} \right)$$

$$e^{-j\frac{2\pi}{\lambda d_4} (rp + sq)} \, dp dq \qquad (23)$$

In terms of the spatial frequencies $f_x = L_1 p/\lambda d_1 d_3$, $f_y = L_1 q/\lambda d_1 d_3$ and the reduced coordinates $r' = -(d_2/L_2) r$, $s' = -(d_2/L_2) s$ Equation (23) can be written as

$$U_7(r', s') = K_8 \, e^{j\dfrac{kL_2^2}{2d_4 d_2^2}(r'^2 + s'^2)} \int\!\!\!\int_{-\infty}^{\infty} G(f_x, f_y) \, H(f_x, f_y)$$

$$e^{j2\pi(f_x r' + f_y s')} \, df_x df_y \tag{24}$$

where (22) has been used. Thus to within a quadratic phase factor $U_7(r', s')$ is proportional to the inverse Fourier transform of the product $G(f_x, f_y) \, H(f_x, f_y)$. The light intensity in the output plane will therefore be proportional to the magnitude squared of this inverse Fourier transform or alternatively to the magnitude squared of the convolution of the input signal $g(x,y)$ with the impulse response $h(x,y)$. In particular, if no filter is used $H(p,q) = 1$, $h(x,y) = \delta(x,y)$ and the output intensity reduces to

$$I(r,s) = \left| K_8 \, g\left(-\frac{d_2}{L_2} r, \; -\frac{d_2}{L_2} s \right) \right|^2 \tag{25}$$

which as expected is an inverted image of $g(x,y)$ that has been magnified by an amount L_2/d_2.

Design Criteria for the Optical Processor

In designing the lensless processor for a particular application a compromise is often required between the magnification $M = L_2/d_2$, the actual size of the diffraction pattern in the transform (filter) plane, and the maximum spatial frequency that can be faithfully transmitted by the system in the

absence of any filtering in the transform plane. This

maximum spatial frequency can be determined from the coherent

transfer function which is equal to the pupil function of the

spherical mirror $P(\lambda L_2 f_x', \lambda L_2 f_y')^{1,2}$. This coherent transfer

function is defined as the ratio of the frequency spectrum of

the image to the frequency spectrum of the image predicted by

geometrical optics. The spatial frequencies f_x' and f_y' are

associated with the image coordinates. However, the spatial

frequencies f_x and f_y related to the Fourier transform in (17)

are associated with the input signal. These two sets of spatial

frequencies are related by the magnification through the

expression $f_{x,y} = M f_{x,y}'$. Thus, in terms of the input spatial

frequencies the coherent transfer function is given by

$P(\lambda L_2 f_x/M, \lambda L_2 f_y/M) = P(\lambda d_2 f_x, \lambda d_2 f_y)$. For a lens (or spherical

mirror) of diameter D the cut-off frequency f_o is thus given

by

$$f_o = \frac{D}{2\lambda d_2} \qquad (26)$$

This cut-off frequency f_o corresponds to the spatial

frequency of an on-axis object whose diffracted light just makes

it through the aperture of the lens (or spherical mirror). This

is illustrated in Figure 3 where the solid line passing through

the center of an object of width a belongs to the bundle of

rays which converge to a point in the transfer plane at a

distance p_o from the axis. This distance corresponds to the
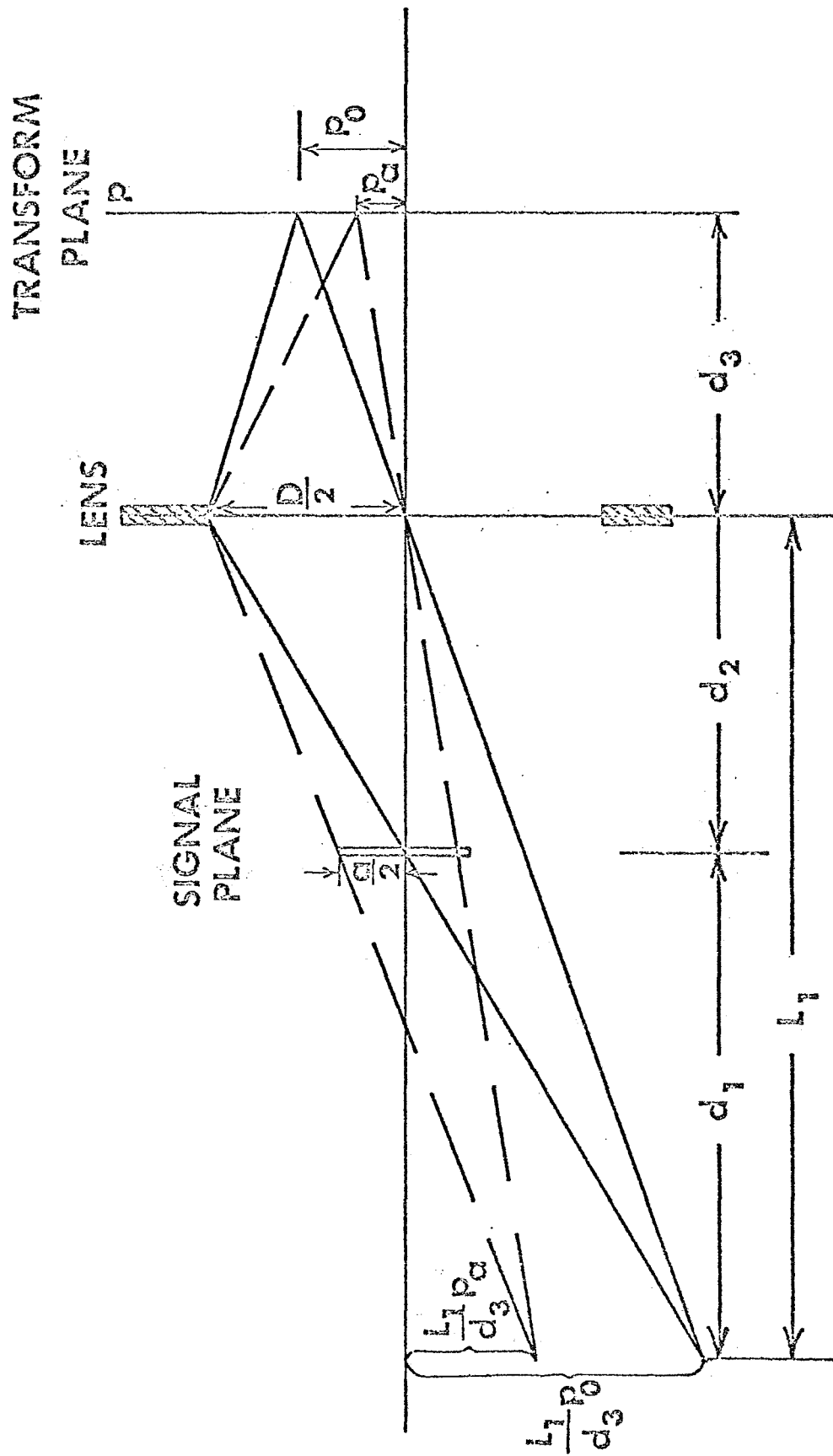
maximum spatial frequency

Fig. 3 Effect of lens aperture on maximum spatial frequency

$$f_o = \frac{L_1 p_o}{\lambda d_1 d_3} \tag{27}$$

which will be passed by an aperture of diameter D. From the geometry of Figure 3 one can readily show that

$$p_o = \frac{D \, d_1 d_3}{2 \, d_2 L_1} \tag{28}$$

so that one can obtain (26) by substituting (28) into (27). Equation (26) is derived by considering the optical system to be space-invariant (isoplanatic). One would then expect this cut-off frequency f_o to apply to all points in the image. In fact, it does not as shown by the bundle of dashed rays in Figure 3. Light that is diffracted in the signal plane at a distance a/2 from the axis will only pass through the aperture of diameter D if the spatial frequency is less·than $f_a = L_1 p_a / \lambda d_1 d_3$ as shown in Figure 3. From the geometry of this figure one can show that f_a is related to the cut-off frequency f_o given by (26) by the equation

$$f_a = f_o \left(1 - \frac{L_1}{d_1} \frac{a}{D} \right) \tag{29}$$

Thus the effect of the finite aperture is to reduce the maximum spatial frequency that can be faithfully transmitted by the system proportionately to the ratio a/D.

Optical Processing of Random Spatial Signals

A general computer technique has been developed for generating random spatial patterns with known statistical characteristics. The technique consists of locating a random point in a two dimensional space by means of an appropriate random function generator on a digital computer. Using a digital to analog converter voltages are obtained which automatically locate the random point as a spot on an oscilloscope face. A large number of random points can therefore be plotted rapidly and photographed by standard techniques. These techniques can be used, for example, to simulate the distribution of stars in different regions of the sky. Optical identification techniques can then be used to recognize the different random patterns.

One such pattern produced in this manner is shown in Figure 4. This pattern actually consists of a large number of two-spot patterns. The distance between the two spots in each case is a constant d. The orientation line joining the two spots is a random variable that is uniformly distributed from 0 to 2π radians. Thus this random pattern is a collection of the two-hole patterns described in PR 1.

The optical processing system described above was used to measure the power spectrum of this random dot pattern. The result as measured in the transform plane of Figure 2 is shown in Figure 5. The envelope of this power spectrum varies as
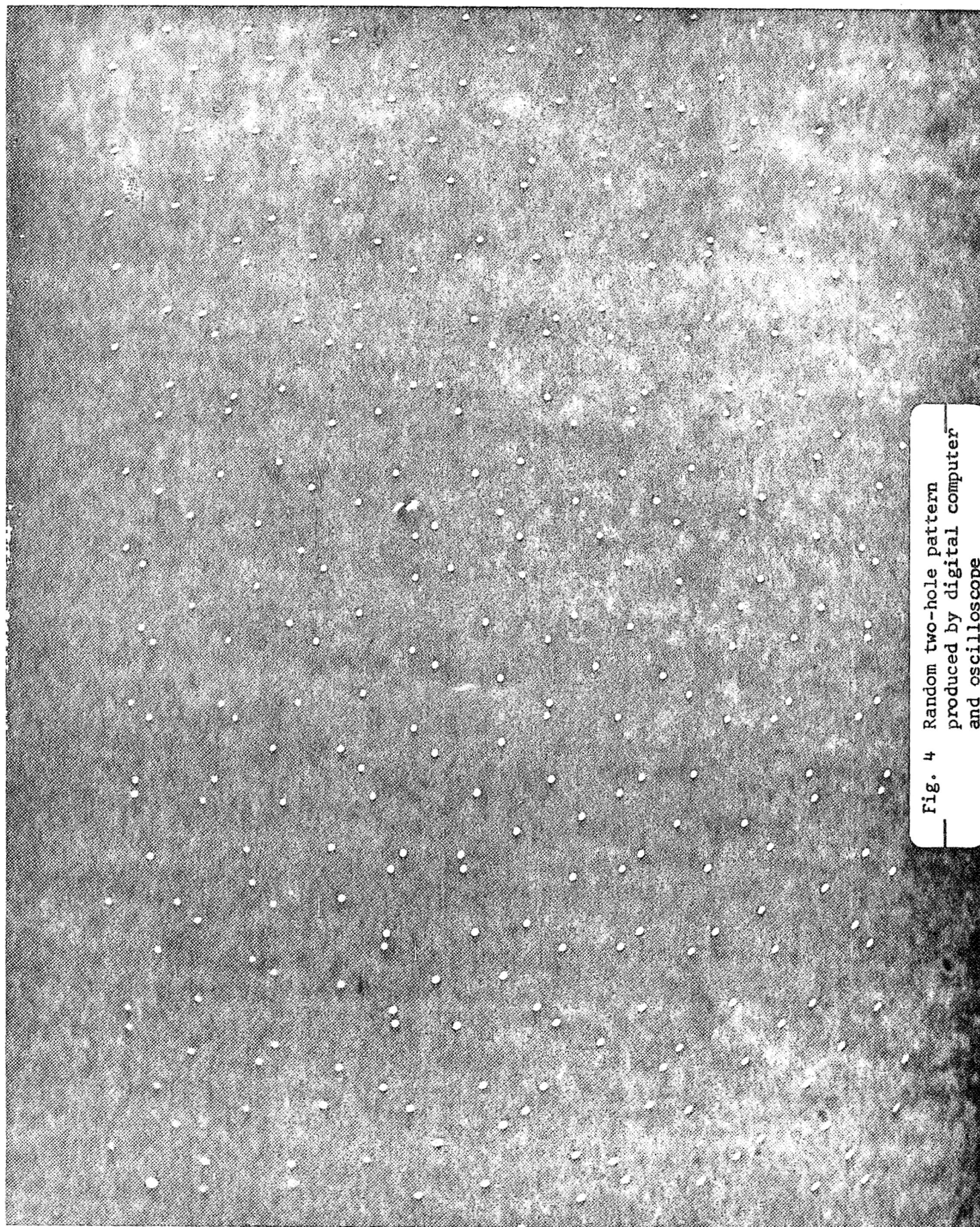
Fig. 4   Random two-hole pattern
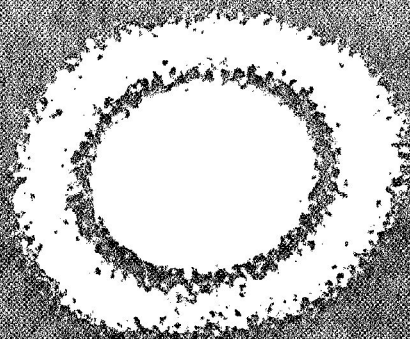produced by digital computer
and oscilloscope

Fig. 5 Power spectrum measurement of random two-hole pattern

$[J_1(\pi a f_o)/\pi a f_o]^2$ as described in PR1. This variation is clearly evident in Figure 5 and contains information about the spot diameter a.

As pointed out in PR1, the power spectrum should also contain information about the separation distance d. This information is contained in a higher frequency modulation of the single hole transform. To see if this information is actually contained in Figure 5 a contact print of this power spectrum measurement was made and used as a signal in the optical processor. As shown in PR1 the transform of this power spectrum is proportional to the autocorrelation function of the original random pattern in Figure 4. Figure 6 shows the resulting autocorrelation function as measured in the transform plane of the optical processor. The circle surrounding the central peak has a radius proportional to d. This circle is a direct result of light being diffracted by the predicted modulations of the single hole pattern. A larger periodic pattern is also observed in the autocorrelation measurement. This results from the fact that the random two-hole patterns were actually arranged periodically on the scope when constructing Figure 4. This inherent periodicity while not obvious in Figure 4 due to the random orientation of each individual two-hole pattern becomes quite evident in the autocorrelation measurement.

This example shows that optical measurements of the power spectrum and autocorrelation function of a random spatial
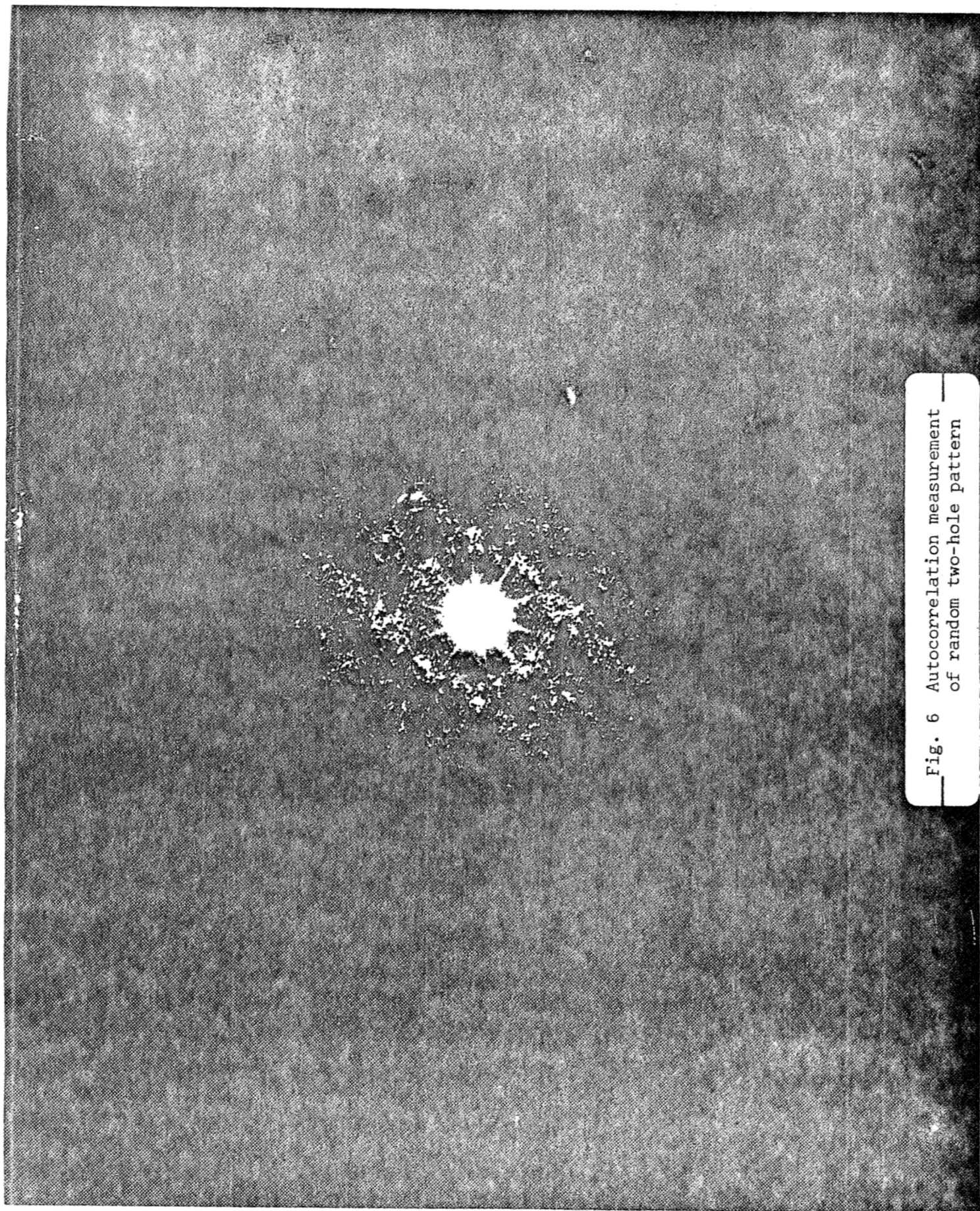
Fig. 6 Autocorrelation measurement
        of random two-hole pattern

pattern contain important information about the statistical nature of the random signal. This information can be used to recognize random patterns with certain prescribed statistical properties. The example also shows that often the autocorrelation (or in general a corss-correlation) measurement provides the most useful information for pattern recognition applications.

The two-step procedure used above for measuring the autocorrelation function is somewhat awkward and would be unsuitable in a real-time automatic control system application. What is needed for this case is a spatial filter in the transform plane proportional to $G^*(f)$ so that the autocorrelation function will appear instantaneously in the output plane. Such a filter can be made holographically which will then permit direct measurement of either the autocorrelation function or the cross-correlation with a known type of random pattern. Techniques are now being developed for making these types of spatial filters and using them for autocorrelation and cross-correlation meausrements.

References

1. Goodman, J. W., Introduction to Fourier Optics, McGraw-
        Hill: New York, 1968.

2. Born, M. and E. Wolf, Principles of Optics, 2nd Ed.,
        Macmillan, New York, 1964.

MANUAL CONTROL SYSTEMS RESEARCH

I. Introduction

Since Oakland University submitted its original proposal
to NASA/ERC, several things have occurred at the University
which have directly affected the course of manual control systems
research at the institution. Briefly these changes are:

(1) The School of Engineering has installed a Hybrid

computing facility consisting of an IBM 1130 digital

computer and an EAI 680 analog computer with the

EAI 693 interface package. Due to the new dimensions

this equipment adds to the area of system identifica-

tion, it is felt that all future research in this

area should be designed to make optimum use of the

Hybrid facility. The wide range of computational

techniques made possible by the Hybrid computer

includes all state-of-the-art analog and digital

techniques, such as: continuous parameter tracking,

regression analysis, orthogonal filtering and

describing functions. Additionally, the IBM 1130's

core memory interfaced with the high speed analog capa-

bility of the EAI 680 enables the repetitive analysis of

large amounts of data in very short periods of time.

This iterative property can be used to obtain

faster parameter identification than is possible

by any one-pass analog scheme. It will be shown
later in this chapter how the Hybrid computer is
being used to greatly improve the continuous
parameter tracking method of parameter identifica-
tion.

(2)   Robert White, a last-semester engineering student at
Oakland University, has designed and built an arm
movement control stick. This unit, which is now
operational, is interfaced with the Hybrid facility
and enables the on-line testing of subjects using
analog, digital and/or Hybrid techniques. Through
the disc storage unit on the IBM 1130, off-line
data analysis is also possible if this form of
analysis proves desirable. Figure 1 is a photograph
of Oakland University's Hybrid facility with the arm
movement control stick in the foreground.

(3)   Glenn A. Jackson recently completed a preliminary
study into one aspect of the optimal properties of
the human operator. This research was conducted
under a National Science Foundation Grant [1] and a
copy of the terminal report is attached, since it is
undoubtedly of interest to NASA/ERC. The main
conclusion of this study was that all human operators
appear to adjust their mode of operation to minimize
the same control cost functional, while they are
controlling low order compensatory systems. There

Figure 1: The Oakland University Hybrid Computer Facility with Arm Movement Control Stick.

are several interesting extensions to this work, to

be discussed later, which can be studied in conjunc-

tion with other aspects of the present research

project.

II. Manual Control Research Activities

Several avenues of research are actively being pursued in

the manual control area at the present time. This work builds

directly on the work of Jackson on the above mentioned NSF

project. We feel that this NSF report is an important factor

in the excellent cost effectiveness achieved on this NASA/ERC

contract. For the past month and for the remainder of this

contract it is expected that Jackson will devote his full

efforts on the NASA/ERC tasks.

The two projects discussed below deal with fast parameter

identification methods. Fast parameter identification is of

great interest to people working with systems containing a

human operator, since the human is highly adaptive and is known

to modify his mode of operation when any system characteristic

is changed. In systems where any change in the operator's

characteristics could have drastic consequences, such as those

changes which occur in a pilot when his aircraft handling

properties change, fast parameter identification could be the

difference between life and death. Also, for basic research

purposes, it is of interest to determine how the human operator

adapts when he is confronted with sudden changes in the system

he is controlling.

The projects being investigated represent different
approaches to the development of high speed identification
techniques which can be used to monitor the changes which occur
in the human operator while he is controlling low order systems.
These methods have potential applications in such manual control
systems as attitude control of aircraft, attitude control of
spacecraft during re-entry, and automobile steering in the face
of wind gusts.

Project 1:

White, under the direction of Jackson, is developing
an identification technique which is essentially a Hybrid
modification of the continuous parameter tracking method
previously developed by Jackson [2]. Two variations of
this method are to be investigated, both variations using
the crossover model [3] as the basic compensatory system
model. The object in each case is the on-line identification
of the crossover model parameters K and τ. This identifi-
cation will be possible over short intervals of time, so
that any sudden changes in human operator characteristics
will be detected a few seconds after they occur.

A. Continuous Parameter Tracking Variation 1:

In this method the compensatory system input and
output, $\theta_i(t)$ and $\theta_o(t)$, are sampled for a short period
of time (5 - 10 seconds) with the samples being stored
in the IBM 1130. During the next time interval (<1
second) the stored values will be fed into a fast-time,

analog, continuous parameter tracking model of the
compensatory system (i.e., a crossover model). However,
since 5 - 10 seconds worth of data are not sufficient
for a parameter tracking system to converge in the
face of noise [2], the fast-time system will iterate
through the same data several times. The initial
values of K and τ for the $(n + 1)^{st}$ iteration will be
the average values of $K(t)$ and $\tau(t)$ determinated during
the nth iteration:

$$K_{n+1}(0) = \frac{1}{T} \int_{0}^{T} K_n(t)\,dt = \overline{K}_n$$

$$\tau_{n+1}(0) = \frac{1}{T} \int_{0}^{T} \tau_n(t)\,dt = \overline{\tau}_n$$

Additionally, the gradient gains used in the parameter
adjusting networks for $K(t)$ and $\tau(t)$ will be systema-
tically reduced after each iteration to insure smooth
convergence even if a considerable amount of noise is
present. It is felt that only 5 or 6 iterations will
be required to give satisfactory convergence. Figure 2
shows postulated plots of what the parameter $K(t)$ will
look like for three iterations on the fast-time model.
($\tau(t)$ will have comparable plots.) The reduction in the
amount of fluctuation in the successive plots is a
direct result of the parameter adjustment loop gain
reduction.

a) $K_i(t)$ = parameter tracking value of K during i^{th} iteration.

b) T and t are time-scaled variables here.

c) The estimated value of K is $\overline{K}_n$ from the last iteration.
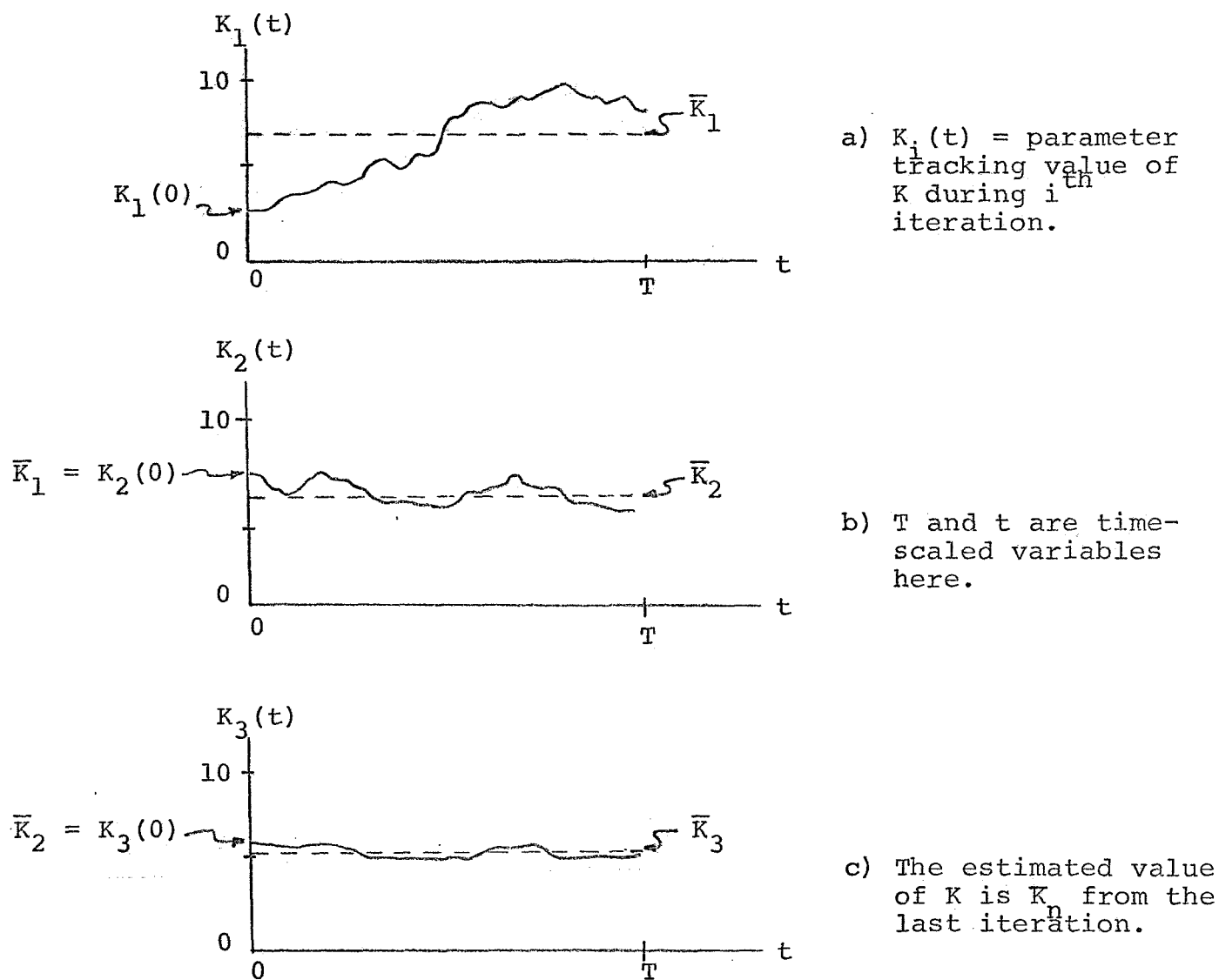
Figure 2:   Convergence of Parameter K(t)
            for Three Iterations of the
            Tracking Data.

Utilizing this method the average value of a parameter existing over the interval $[t_1, t_1 + T]$ will be known at $t = t_1 + T + T_I$, where T_I is the total iteration time required by the fast-time tracking system. The real-time sampling followed by the fast-time iteration will be repeated over and over during each subject's tracking task. A time-sequence plot of the basic method is given in Figure 3. Again, only the K estimate is shown for simplicity.

B. Continuous Parameter Tracking Variation 2:

In this method the real-time sampling of the compensatory system and the fast-time iterations into the continuous parameter tracking model will be done simultaneously. The compensatory system under test will have its input and output sampled at a fixed rate. Call these samples $\theta_i(n\Delta t)$ and $\theta_o(n\Delta t)$, respectively. If it is assumed that N samples are used during each fast-time iteration, then the input and output signals to the fast-time parameter tracking system during the first iteration will be

$$\sum_{n=1}^{N} \theta_i(n\Delta t)\ \delta(t_o - n\Delta t) \quad \text{and} \quad \sum_{n=1}^{N} \theta_o(n\Delta t)\ \delta(t_o - n\Delta t)$$

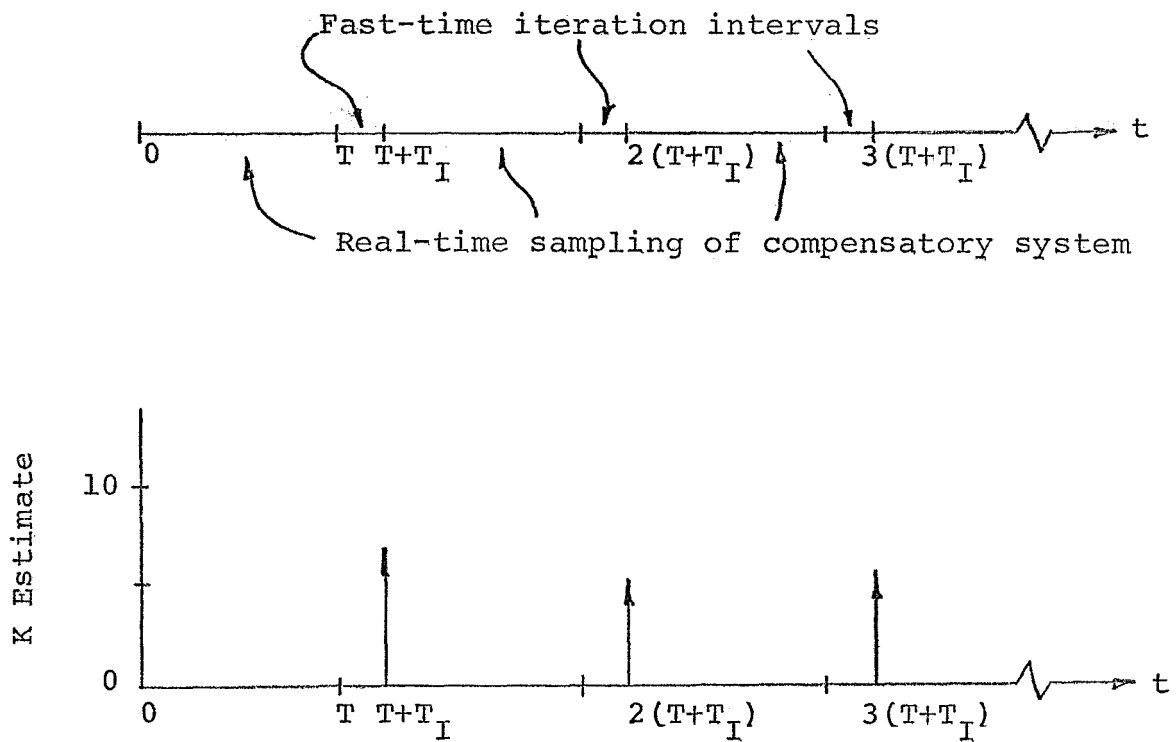respectively. (t_o is the time-scaled time variable,

Figure 3: A Time-Sequence Plot Indicating When Parameter Estimates are Determined.

and $\delta(t_o - n\Delta t)$ is a delta function located at $t_o = n\Delta t$.)
While this first fast-time iteration is being made, d
new samples of $\theta_i(t)$ and $\theta_o(t)$ from the real-time system
will have been taken. Thus, the second iteration of
the fast-time model can use input and output signals
of

$$\sum_{n=k+d}^{N+d} \theta_i(n\Delta t)\ \delta(t_o - n\Delta t) \quad \text{and} \quad \sum_{n=k+d}^{N+d} \theta_o(n\Delta t)\ \delta(t_o - n\Delta t).$$

Each iteration will therefore use d new data points while
discarding an equal number of the oldest data points
stored. The gradient gains in the tracking system will
again be cycled up and down in order to obtain good
convergence. This particular Hybrid version of con-
tinuous parameter tracking will not be investigated
until version 1 has been fully tested, since some type
of time-sharing technique will have to be developed
before it can be implemented.

Project 2

Jackson is developing an iterative Hybrid identifica-
tion technique utilizing estimates by stochastic approxi-
mation [4]. In particular, parameter adjustments will be
made using the Keifer-Wolfowitz algorithm discussed by
Bekey and Neal at the 5th Annual Manual Control Conference
[5].

This is also an on-line Hybrid identification method
which will operate on short lengths of sampled data from
the input and output signals of the compensatory system.
The fast-time implementation will use three different
crossover models operating simultaneously on the same
stored input and output data taken from the compensatory
system. The model parameters will be fixed over each
fast-time iteration with the parameters stepwise adjusted
after each iteration via the Keifer-Wolfowitz algorithm.
During the nth iteration using one set of compensatory
system input-output sampled data, Model 1 will have
parameters K_n, τ_n; Model 2 parameters $K_n + c_n$, τ_n; and
Model 3 parameters K_n, $\tau_n + d_n$. During this n^{th} iteration,
three performance indices will be measured:

$$J_{n1} = \int_{t_1}^{t_1+T} ||e_1(t_o, K_n, \tau_n, \theta_i(t_o)|| dt_o$$

$$J_{n2} = \int_{t_1}^{t_1+T} ||e_2(t_o, K_n + c_n, \tau_n, \theta_i(t_o)|| dt_o$$

$$J_{n3} = \int_{t_1}^{t_1+T} ||e_3(t_o, K_n, \tau_n + d_n, \theta_i(t_o)|| dt_o$$

where $||e_i||$ is a norm of the error existing between the
recorded compensatory system output and the output of the

i^{th} crossover model. The adjustment, as dictated by the Keifer-Wolfowitz algorithm, is

$$K_{n+1} = K_n + a_n(J_{n1} - J_{n2})/c_n$$

$$\tau_{n+1} = \tau_n + b_n(J_{n1} - J_{n3})/d_n$$

where

$$\lim_{n\to\infty} a_n = \lim_{n\to\infty} b_n = \lim_{n\to\infty} c_n = \lim_{n\to\infty} d_n = 0$$

$$\sum_{n=1}^{\infty} \left(\frac{a_n}{c_n}\right)^2 < \infty \text{ and } \sum_{n=1}^{\infty} \left(\frac{b_n}{d_n}\right)^2 < \infty$$

$$a_n = \frac{A}{n} \text{ , } b_n = \frac{B}{n}$$

$$c_n = \frac{C}{n^{1/6}} \text{ , } d_n = \frac{D}{n^{1/6}}$$

with A, B, C and D positive constants.

The system will iterate on one set of stored data until convergence of the parameters K and τ is achieved. At this time new data will again be sampled from the compensatory system and the process will start again. This will give a time plot similar to that in Figure 3 above. A general block diagram of the method is given in Figure 4.
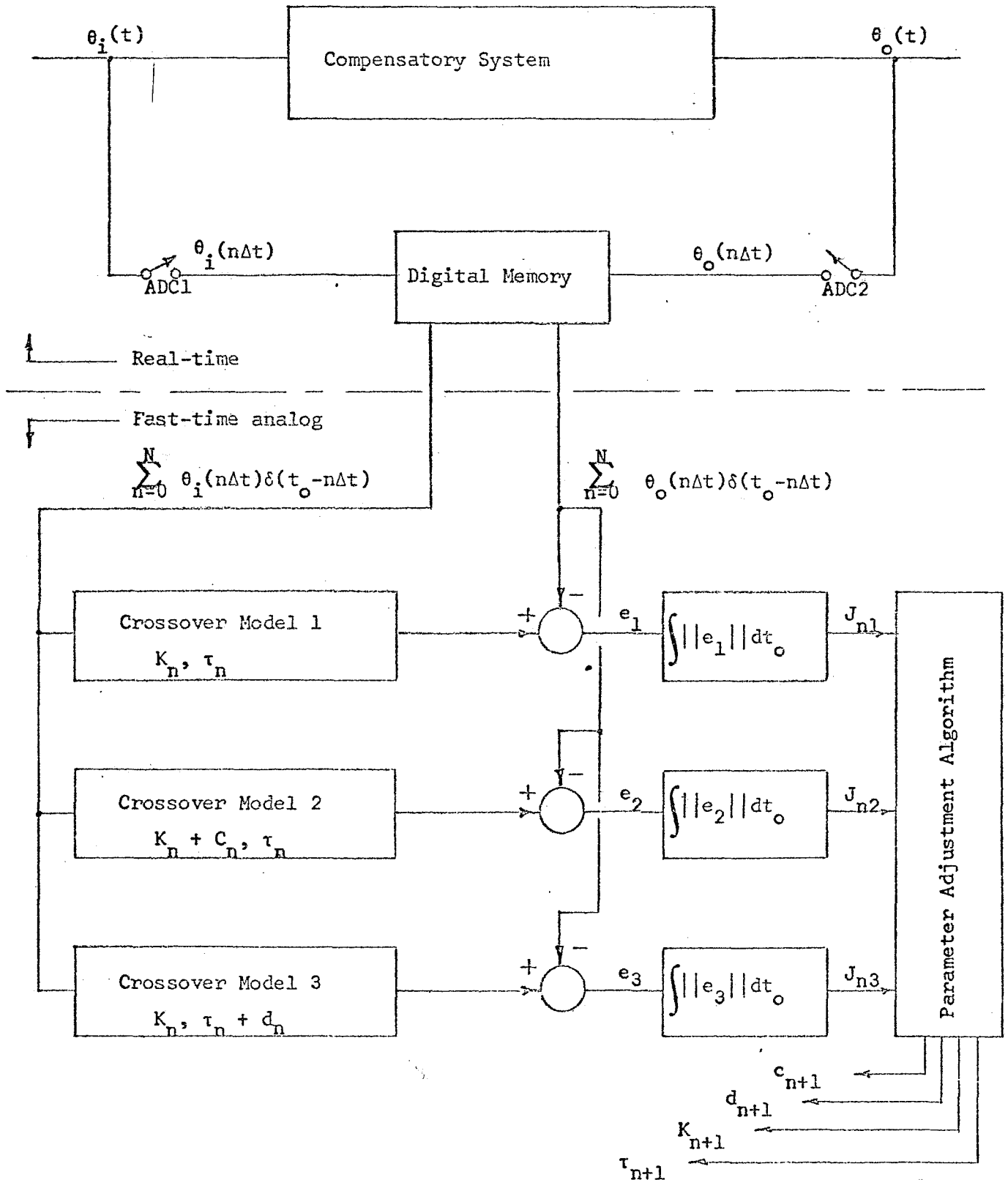
Figure 4: Block Diagram of a Stockastic
Approximation Method of Parameter
Identification

III. <u>Further Studies</u>

Once the basic identification techniques discussed above have been completely implemented, they will be used as vehicles for several other studies.

First, the basic techniques themselves will be analyzed and, hopefully, improved.

Second, the basic techniques will be used to evaluate the manual control research originally proposed to NASA/ERC with regard to continuous parameter tracking. Namely, can some form of state variable error be used to improve the speed of parameter convergence (rather than using simply output error), and can knowledge of the remnant spectrum [6] be used to filter out those portions of the remnant which cause parameter tracking problems?

Third, the basic techniques will be used to determine average K and τ values for new subjects in order to substantiate, or disprove, Jackson's hypotheses on the optimality of the human operator discussed in his NSF report [1]. In particular, can the changes which are known to occur in the average K and τ values, due to variations in the input signal spectrum, be accounted for by the optimal policy developed in Jackson's report? Jackson's optimal policy fits his original data [2,7], but needs further testing and analysis. These tests can be run at the same time evaluations of the parameter identification techniques are being conducted, and thus double use of the tests can be made.

References

1. G. A. Jackson, "Determination of the Error Cost Functional
   Used by Human Operators While Controlling Certain Compensa-
   tory Systems," Terminal Report for NSF Grant GK-3490,
   September 30, 1969.

2. G. A. Jackson, "Measuring Human Performance with a Parameter
   Tracking Version of a Crossover Model," NASA CR-910,
   October, 1967.

3. D. T. McRuer, D. Graham, E. S. Krendel, and W. Reisner, Jr.,
   "Human Pilot Dynamics in Compensatory Systems,"
   AFFDL-TR-65-15, July, 1965.

4. C. B. Neal, "Estimation of the Parameters of Sampled-data
   Systems by Stochastic Approximation," University of Southern
   California Technical Report USCEE-333, January, 1969.

5. C. B. Neal and G. A. Bekey, "Identification of Human Operators
   by Stochastic Approximation," Paper presented at 5th Annual
   Manual Control Conference, MIT, March 27-29, 1969.

6. W. H. Levison, S. Baron, and D. L. Kleinman, "A Model for
   Human Controller Remnant," Paper presented at 5th Annual
   Manual Control Conference, MIT, March 27-29, 1969.

7. G. A. Jackson, "A Method for the Direct Measurement of
   Crossover Model Parameters," IEEE Transactions on Man-
   Machine Systems, Vol. MMS-10, No. 1, March, 1969, pp. 27-33.

APPENDIX I

A MODEL OF THE HUMAN POSTURAL CONTROL SYSTEM

J. C. Hill

Presented at the

1969 I.E.E.E. Systems Science and Cybernetics Conference

October 22-24, 1969

Philadelphia, Pennsylvania

A MODEL OF THE HUMAN POSTURAL CONTROL SYSTEM

J.C. Hill
Professor of Engineering
Oakland University
Rochester, Michigan

Abstract

A nine degree of freedom pitch axis model of the human postural control system is proposed. Expressions for the kinetic and potential energies of the system are derived. The trunk, thigh, shank, foot, upper arm, forearm, and head are each modeled by a lumped mass at the element center of mass and an associated rotational inertia.

Background

Analysis related to an understanding of the human postural control system appears to be proceeding on five fronts. An excellent introduction to the first area, analytic representation of the force-velocity characteristics of human muscle tissue as an actuator, is provided in Milhorn's account [1] of the work on Houk [2]. This account is representative of a long preoccupation with muscle characteristics in reptiles, small vertebrates, and people dating back to 1935 [3]. Extensive references to more modern work are contained in Bahler [4], Vickers and Sheridan [5], Galiana [6], and Magdalena and McRuer [7]. The paper by Dewhurst [8] is also of interest in this area.

A second concentration of effort has occurred in the development of models for the physiological sensors involved in the postural control system; see, for example, the work on the vestibular system by Miery [9] and Young [10], and the work on the muscle spindle receptor by Houk [1,2] and by Gottlieb, Agarwal, and Stark [11], and Agarwal, et al. [20].

A third area, stimulated by a long-term Air Force interest in the capabilities of human pilots, is the view of certain elements of the postural control system seen in the context of human operator studies. An entree to this area of research is provided by the work of McRuer, Graham, Magdeleno, et al. [12-15], Shirley and Young [16], and Adams [17]; it is characteristic of this work that the human is seen from a black box viewpoint. The results and techniques developed in these studies are beginning to find application in analysis of the more prosaic automobile handling and control task; see Wier and McRuer [18] and Crossman [19].

A fourth area, quite distinct in viewpoint and methodology, is provided by the work of McGhee and Tomovic [25] in the theory of quadruped locomotion [21-24].

A representative mechanistic view of the postural control system for which there is some physiological support is provided by the block diagram developed by Houk [1,2] and redrawn here as Figure 1, which although developed with reference to the wrist-rotation reflex system, could in its essentials refer to the biceps-triceps pair or to any other distinct agonist-antagonist combination. The areas of research mentioned above concern themselves with different aspects of this block diagram. Results from the muscle force-velocity experimental studies have led to the form of the block diagram depicted in the pronator muscle and supinator muscle blocks; results from the sensor studies lead to the form given for the spindle receptor blocks, and human operator studies, together with some physiological support, lead to the form presented for the motor neuron complex, the spindle afferent nerves, and the alpha efferent nerves.

Such block diagrams usually have two general characteristics. First, the diagram "dead-ends" on the central nervous system block; apparently, this is where science ends and mysticism begins at our present state of knowledge. Secondly, this complex diagram relates to the control of a single joint angle -- a one degree of freedom system, hardly representative of the degree of muscular coordination commonly exhibited by Kittens and Kids.

The work of McGhee [21-25] and McRuer [12-15] attempts to meet these objections in two different ways.

In the majority of McGhee's work, the dynamic aspects of the system are suppressed, and concern is centered entirely on the question of what command inputs should be issued to the autopilot consisting of the proprioceptive loops if it is assumed that these loops function properly, or even better, ideally. Whether the leg motions that make walking possible are produced by the central nervous system in a purely voluntary mode of operation or whether a more autonomous type of reflex arc is involved is, of course, a question of long standing; McGhee provides convincing evidence for

the latter, and shows that useful quadruped gaits may be generated either by open loop (synchonous) or closed loop (asynchronous) digital networks. An open loop controller would consist of a clock-pulse driven shift register that issues leg commands at certain instants in time, independent of the actual state of the leg system at those times, whereas changes in the state of a closed loop controller would be triggered by satisfactory transfer of the leg system to the previously commanded state.

From the point of view of this paper, the importance of McGhee's work is that it begins to ask and provide technologically useful answers to questions about how the heretofore unassailable central nervous system might work, although it appears unlikely that we will soon have direct physiological evidence that this is the way it does work.

In McRuer's work, the known system dynamics are taken into account, and everything left over is lumped into a single black-box representation of the human operator performance, usually obtained in the form of a describing function for the box. A particularly good example of this approach is contained in Reference 14. Although this approach allows characterization of the human operator in a way that has extrapolative power to basically similar tasks, it has little synthetic power from the point of view of this paper -- it tells how the central nervous system works in certain tasks, but not why it works that way in circuitry terms. This difficulty is possibly due to the lack of any well-established describing function inversion techniques for describing functions that are both amplitude and frequency dependent [26].

Finally, the work of the General Electric corporation in the development of walking machines and remote manipulators should be mentioned [27,28]. Rather than to attempt the construction of a self-sufficient automaton, the GE approach is to imbed a human operator in a walking machine in such a way that through the use of force reflecting servos, the coordination capabilities of the operator are used to direct the machine's activities at a much higher force level. The concept is now being used in the development of off-road vehicles, machines for increasing the strength of an individual in lifting, and a variety of other applications. The basic difference between the GE research and that cited previously is that GE intends to utilize and extend the human muscular coordination capabilities, whereas the other approaches are directed towards an eventual replacement of the human, or toward purely scientific ends.

It is the purpose of this paper to pursue the behavior of the postural control system in a different direction than those outlined above. We would like to progress toward an understanding, from a systems point of view, of how some of the simpler common examples of large-scale human muscular coordination (for example, deep knee-bends) might be carried out, with the hope that someone might eventually develop an understanding of some

of the more spectacular examples (like playing basketball).

To this end, it would be justifiable to gloss over some of the fine points other investigators have developed in the hope that taking such liberties will result in a systems model more appropriate to the large-scale phenomena we want to study; for example, only the gross features of muscle force-velocity characteristics will be retained on the grounds that from the point of view of understanding coordination, everything else known about muscle is irrelevant detail.

In more abstract language, we would like to develop an understanding of the goal-oriented integration of a number of proprioceptive loops into a more complete organism. We would accept simplified models of the individual loops to the extent necessary to achieve adequate complexity at the overall system level, with the goal of eventually achieving the development of a six degree-of-freedom simulation capable of predicting human capabilities and limitations in untested situations.

It is proposed to study this problem by means of simulation. A simplified, "pitch axis only" computer model of a human involving arms, legs, feet, head, and an (initially) rigid torso will be developed which can be dropped from various initial orientations, with the objective being to survive impact with a ground plane and return to an erect position. The work will follow the familiar pattern of simulation of a complex aerospace system: continuing development of the simulation will interact with continuing gathering of experimental data as critical questions are posed and understanding of the system progresses.

Our thesis is that the control algorithms necessary to provide command inputs to the proprioceptive loops would be more or less obvious from a consideration of the dynamic requirements of the specific task to be performed, depending on the complexity of the task. Obviously, an easy task should be selected first.

Kinetic and Potential Energies for the Model

In carrying out the derivation of the equations of motion of the postural control system model by use of Lagrange's equations, expressions for the potential and kinetic energies of the system are needed. A derivation of these expressions follows.

In terms of the generalized coordinates indicated in Figure 2, the total system kinetic energy may be expressed as the sum of the point mass kinetic energy and the kinetic energy due to the distributed nature of the arms, legs, etc.,

$$T = T_{DIST} + T_{POINT} \tag{1}$$

The distributed kinetic energy is due only

to rotation of the various elements, and is easily obtained as

$$T_{DIST} = 1/2J_{TR}\dot{\theta}^2 + 1/2J_{HD}(\dot{\theta} + \dot{\zeta})^2$$

$$+ 1/2J_{UA}(\dot{\theta} - \dot{\delta})^2 + 1/2J_{FA}(\dot{\theta} - \dot{\delta} - \dot{\epsilon})^2$$

$$+ 1/2J_{TH}(\dot{\theta} - \dot{\gamma})^2 + 1/2J_{SH}(\dot{\theta} - \dot{\gamma} + \dot{\beta})^2$$

$$+ 1/2J_{FT}(\dot{\theta} - \dot{\gamma} + \dot{\beta} + \dot{\alpha})^2 \qquad (2)$$

The kinetic energy due to the point masses is more difficult to obtain, as it involves repetitive application of the relative velocity theorem together with a long chain of coordinate resolutions to enable expression of the kinetic energy of each point mass in the form

$$T = 1/2M(V_a^2 + V_b^2)$$

where V_a and V_b are velocity components along any set of perpendicular axes, usually a set chosen to provide as much analytical simplicity as possible. A derivation of the V_a, V_b components for each of the masses follows. The absolute velocity of, say, the c.g. of the trunk is denoted by $\underset{\sim}{V}_{TR/0}$, while the relative velocity of, say, the hip with respect to the c.g. of the trunk is denoted by $\underset{\sim}{V}_{H/TR}$.

Unit vectors in a variety of directions are indicated on the diagram, and are denoted by, for example, $\underset{\sim}{u}_x$ and $\underset{\sim}{u}_y$. (See list of symbols).

The velocity components of each mass point must now be obtained along any convenient set of orthogonal axes, the choice of which varies during the analysis.

We have

$$\underset{\sim}{V}_{TR/0} = \dot{x}\underset{\sim}{u}_x + \dot{y}\underset{\sim}{u}_y \qquad (3)$$

$$\underset{\sim}{V}_{H/TR} = \ell_{TRM}\dot{\theta}\underset{\sim}{u}_\theta \qquad (4)$$

Using the relative velocity theorem, the absolute velocity of the hip can be expressed as the relative velocity of the hip with respect to the c.g. of the trunk plus the absolute velocity of the trunk:

$$\underset{\sim}{V}_{H/0} = \underset{\sim}{V}_{H/TR} + \underset{\sim}{V}_{TR/0}$$

$$= \ell_{TRM}\dot{\theta}\underset{\sim}{u}_\theta + \dot{x}\underset{\sim}{u}_x + \dot{y}\underset{\sim}{u}_y \qquad (5)$$

Resolving into $\underset{\sim}{u}_\theta$, $\underset{\sim}{u}_{TR}$ coordinates so that the vector addition can be performed,

$$\underset{\sim}{V}_{H/0} = \ell_{TRM}\dot{\theta}\underset{\sim}{u}_\theta + [-\dot{x}\cos\theta + \dot{y}\sin\theta]\underset{\sim}{u}_\theta$$

$$+ [\dot{x}\sin\theta + \dot{y}\cos\theta]\underset{\sim}{u}_{TR}$$

$$= [\ell_{TRM}\dot{\theta} - \dot{x}\cos\theta + \dot{y}\sin\theta]\underset{\sim}{u}_\theta$$

$$+ [\dot{x}\sin\theta + \dot{y}\cos\theta]\underset{\sim}{u}_{TR}$$

$$= v_{H\theta}\underset{\sim}{u}_\theta + v_{HTR}\underset{\sim}{u}_{TR} \qquad (6)$$

The absolute velocity of the CG of the thigh is then

$$\underset{\sim}{V}_{TH/0} = \underset{\sim}{V}_{TH/H} + \underset{\sim}{V}_{H/0}$$

$$= \ell_{THM}\dot{\gamma}\underset{\sim}{u}_\gamma + \underset{\sim}{V}_{H/0}$$

$$= \ell_{THM}\dot{\gamma}\underset{\sim}{u}_\gamma + v_{H\theta}\underset{\sim}{u}_\theta + v_{HTR}\underset{\sim}{u}_{TR}$$

$$= \ell_{THM}\dot{\gamma}\underset{\sim}{u}_\gamma + [\ell_{TRM}\dot{\theta} - \dot{x}\cos\theta + \dot{y}\sin\theta]\underset{\sim}{u}_\theta$$

$$+ [\dot{x}\sin\theta + \dot{y}\cos\theta]\underset{\sim}{u}_{TR} \qquad (7)$$

Resolving into $\underset{\sim}{u}_\gamma$, $\underset{\sim}{u}_{TH}$ coordinates,

$$\underset{\sim}{V}_{TH/0} = [\ell_{THM}\dot{\gamma} - (\ell_{TRM}\dot{\theta} - \dot{x}\cos\theta$$

$$+ \dot{y}\sin\theta)\cos\gamma + (\dot{x}\sin\theta$$

$$+ \dot{y}\cos\theta)\sin\gamma]\underset{\sim}{u}_\gamma + [-(\dot{x}\sin\theta$$

$$+ \dot{y}\cos\theta)\cos\gamma - (\ell_{TRM}\dot{\theta} - \dot{x}\cos\theta$$

$$+ \dot{y}\sin\theta)\sin\gamma]\underset{\sim}{u}_{TH} \qquad (8)$$

Similarly, the absolute velocity of the knee is given by

$$\underset{\sim}{V}_{K/0} = \underset{\sim}{V}_{K/H} + \underset{\sim}{V}_{H/0}$$

$$= [\ell_{TH}\dot{\gamma} - (\ell_{TRM}\dot{\theta} - \dot{x}\cos\theta + \dot{y}\sin\theta)\cos\gamma$$

$$+ (\dot{x}\sin\theta + \dot{y}\cos\theta)\sin\gamma]\underset{\sim}{u}_\gamma$$

$$+ [-(\dot{x}\sin\theta + \dot{y}\cos\theta)\cos\gamma$$

$$- (\ell_{TRM}\dot{\theta} - \dot{x}\cos\theta + \dot{y}\sin\theta)\sin\gamma]\underset{\sim}{u}_{TH}$$

$$\qquad (9)$$

The absolute velocity of the center of the mass of the shank is given by

$$\underset{\sim}{V}_{SH/0} = \underset{\sim}{V}_{SH/K} + \underset{\sim}{V}_{K/0}$$

$$= \ell_{SHM}\dot{\beta}\underset{\sim}{u}_\beta + \underset{\sim}{V}_{K/0}$$

$$= \{\ell_{SHM}\dot{\beta} + [\ell_{TH}\dot{\gamma} - (\ell_{TRM}\dot{\theta}$$

$$- \dot{x}\cos\theta + \dot{y}\sin\theta)\cos\gamma]\cos\beta$$

$$- [-(\dot{x}\sin\theta + \dot{y}\cos\theta)\cos\gamma$$

$$- (\ell_{TRM}\dot{\theta} - \dot{x}\cos\theta + \dot{y}\sin\theta)]\sin\beta\}\underset{\sim}{u}_\beta$$

$$+ \{[-(\dot{x}\sin\theta + \dot{y}\cos\theta)\cos\gamma - (\ell_{TRM}\dot{\theta}$$

$$- \dot{x}\cos\theta + \dot{y}\sin\theta)\sin\gamma]\cos\beta - [\ell_{TH}\dot{\gamma}$$

$$- (\ell_{TRM}\dot{\theta} - \dot{x}\cos\theta + \dot{y}\sin\theta)\cos\gamma + (\dot{x}\sin\theta$$

$$+ \dot{y}\cos\theta)\sin\gamma]\sin\beta\}u_{SH} \qquad (10)$$

The absolute velocity of the ankle is obtained by substituting ℓ_{SH} for ℓ_{SHM} in equation (10), giving

$$X_{A/0} = \{\ell_{SH}\dot{\beta} + [\ell_{TH}\dot{\gamma} - (\ell_{TRM}\dot{\theta} - \dot{x}\cos\theta$$

$$+ \dot{y}\sin\theta)\cos\gamma]\cos\beta - [-(\dot{x}\sin\theta$$

$$+ \dot{y}\cos\theta)\cos\gamma - (\ell_{TRM}\dot{\theta} - \dot{x}\cos\theta$$

$$+ \dot{y}\sin\theta)\sin\beta\}u_\beta + \{[-(\dot{x}\sin\theta$$

$$+ \dot{y}\cos\theta)\cos\gamma - (\ell_{TRM}\dot{\theta} - \dot{x}\cos\theta$$

$$+ \dot{y}\sin\theta)\sin\gamma]\cos\beta - [\ell_{TH}\dot{\gamma} - (\ell_{TRM}\dot{\theta}$$

$$- \dot{x}\cos\theta + \dot{y}\sin\theta)\cos\gamma + (\dot{x}\sin\theta$$

$$+ \dot{y}\cos\theta)\sin\gamma]\sin\beta\}u_{SH} \qquad (11)$$

$$X_{FT/0} = X_{FT/A} + X_{A/0}$$

$$= \ell_{FTM}\dot{\alpha}u_\alpha + X_{A/0}$$

Resolving equation (11) into u_α, u_{SH} coordinates, the absolute velocity of the c.g. of the foot is

$$X_{FT/0} = [\ell_{FTM}\dot{\alpha} + \{[-(\dot{x}\sin\theta + \dot{y}\cos\theta)\cos\gamma$$

$$- (\ell_{TRM}\dot{\theta} - \dot{x}\cos\theta + \dot{y}\sin\theta)\sin\gamma]\cos\beta$$

$$- [\ell_{TH}\dot{\gamma} - (\ell_{TRM}\dot{\theta} - \dot{x}\cos\theta + y\sin\theta)\cos\gamma$$

$$+ (\dot{x}\sin\theta + \dot{y}\cos\theta)\sin\gamma]\sin\beta\}\cos\alpha$$

$$+ \{\ell_{SH}\dot{\beta} + [\ell_{TH}\dot{\gamma} - (\ell_{TRM}\dot{\theta} - \dot{x}\cos\theta$$

$$+ \dot{y}\sin\theta)\cos\gamma]\cos\beta - [-(\dot{x}\sin\theta$$

$$+ \dot{y}\cos\theta)\cos\gamma - (\ell_{TRM}\dot{\theta} - \dot{x}\cos\theta$$

$$+ \dot{y}\sin\theta)\sin\beta\}\sin\alpha]u_\alpha + [-\{\ell_{SH}\dot{\beta}$$

$$+ [\ell_{TH}\dot{\gamma} - (\ell_{TRM}\dot{\theta} - \dot{x}\cos\theta$$

$$+ \dot{y}\sin\theta)\cos\gamma]\cos\beta - [-(\dot{x}\sin\theta$$

$$+ \dot{y}\cos\theta)\cos\gamma - (\ell_{TRM}\dot{\theta} - \dot{x}\cos\theta$$

$$+ \dot{y}\sin\theta)\sin\beta\}\cos\alpha + [-(\dot{x}\sin\theta$$

$$+ \dot{y}\cos\theta)\cos\gamma - (\ell_{TRM}\dot{\theta} - \dot{x}\cos\theta$$

$$+ \dot{y}\sin\theta)\sin\gamma]\cos\beta - [\ell_{TH}\dot{\gamma} - (\ell_{TRM}\dot{\theta}$$

$$- \dot{x}\cos\theta + \dot{y}\sin\theta)\cos\gamma + (\dot{x}\sin\theta$$

$$+ \dot{y}\cos\theta)\sin\gamma]\sin\beta\}\sin\alpha]u_{SH} \qquad (12)$$

Expressions for the absolute velocities of the shoulder, upperarm, and forearm are obtained in similar fashion:

$$X_{S/0} = X_{S/TR} + X_{TR/0}$$

$$= - (\ell_{TR} - \ell_{TRM})\dot{\theta}u_\theta + \dot{x}u_x + \dot{y}u_y \qquad (13)$$

Resolving into u_θ, u_{TR} coordinates, the absolute velocity of the shoulder is obtained as

$$X_{S/0} = - (\ell_{TR} - \ell_{TRM})\dot{\theta}u_\theta + [-\dot{x}\cos\theta$$

$$+ \dot{y}\sin\theta]u_\theta + [\dot{x}\sin\theta + \dot{y}\cos\theta]u_{TR}$$

$$= [-(\ell_{TR} - \ell_{TRM})\dot{\theta} - \dot{x}\cos\theta + \dot{y}\sin\theta]u_\theta$$

$$+ [\dot{x}\sin\theta + \dot{y}\cos\theta]u_{TR} \qquad (14)$$

The velocity of the c.g. of the upper arm is then given by equation (15):

$$X_{UA/0} = X_{UA/S} + X_{S/0}$$

$$= \ell_{UAM}\dot{\delta}u_\delta + X_{S/0}$$

$$= \ell_{UAM}\dot{\delta}u_\delta + [-(\ell_{TR} - \ell_{TRM})\dot{\theta} - \dot{x}\cos\theta$$

$$+ \dot{y}\sin\theta]u_\theta + [\dot{x}\sin\theta + \dot{y}\cos\theta]u_{TR}$$

$$\qquad (15)$$

Resolving into u_δ, u_{UA} coordinates gives

$$X_{UA/0} = \{\ell_{UAM}\dot{\delta} + [-(\ell_{TR} - \ell_{TRM})\dot{\theta} - \dot{x}\cos\theta$$

$$+ \dot{y}\sin\theta]\sin\delta - [\dot{x}\sin\theta$$

$$+ \dot{y}\cos\theta]\cos\delta\}u_\delta + \{[[(\ell_{TR} - \ell_{TRM})\dot{\theta}$$

$$- \dot{x}\cos\theta + \dot{y}\sin\theta]\cos\delta + [\dot{x}\sin\theta$$

$$+ \dot{y}\cos\theta]\sin\delta\}u_{UA} \qquad (16)$$

The elbow velocity is obtained by replacing ℓ_{UAM} in equation (16) by ℓ_{UA}:

$$X_{E/0} = \{\ell_{UA}\dot{\delta} + [-(\ell_{TR} - \ell_{TRM})\dot{\theta} - \dot{x}\cos\theta$$

$$+ \dot{y}\sin\theta]\sin\delta - [\dot{x}\sin\theta + \dot{y}\cos\theta]\cos\delta\}u_\delta$$

$$+ \{[[(\ell_{TR} - \ell_{TRM})\dot{\theta} - \dot{x}\cos\theta + \dot{y}\sin\theta]\cos\delta$$

$$+ [\dot{x}\sin\theta + \dot{y}\cos\theta]\sin\delta\}u_{UA} \qquad (17)$$

The velocity of the forearm c.g. is obtained by the relative velocity theorem as

$$\dot{X}_{FA/0} = \dot{X}_{FA/E} + \dot{X}_{E/0}$$
$$= \ell_{FAM}\dot{\epsilon}\,\mathfrak{U}_\epsilon + \dot{X}_{E/0} \tag{18}$$

Resolving into $\mathfrak{U}_\epsilon$, $\mathfrak{U}_{FA}$ coordinates yields

$$\dot{X}_{FA/0} = \{\ell_{FAM}\dot{\epsilon} + [\ell_{UA}\dot{\delta} + [-(\ell_{TR} - \ell_{TRM})\dot{\theta}$$
$$- \dot{x}\cos\theta + \dot{y}\sin\theta]\sin\delta - [\dot{x}\sin\theta$$
$$+ \dot{y}\cos\theta]\cos\delta]\cos\epsilon - [(\ell_{TR} - \ell_{TRM})\dot{\theta}$$
$$- \dot{x}\cos\theta + \dot{y}\sin\theta]\cos\delta + [\dot{x}\sin\theta$$
$$+ \dot{y}\cos\theta]\sin\delta]\sin\epsilon\}\mathfrak{U}_\epsilon + [\ell_{UA}\dot{\delta} + [-(\ell_{TR}$$
$$- \ell_{TRM})\dot{\theta} - \dot{x}\cos\theta + \dot{y}\sin\theta]\sin\delta$$
$$- [\dot{x}\sin\theta + \dot{y}\cos\theta]\cos\delta]\sin\epsilon + [[(\ell_{TR}$$
$$- \ell_{TRM})\dot{\theta} - \dot{x}\cos\theta + \dot{y}\sin\theta]\cos\delta$$
$$+ [\dot{x}\sin\theta + \dot{y}\cos\theta]\sin\delta]\cos\epsilon\}\mathfrak{U}_{FA} \tag{19}$$

Finally, the absolute velocity of the head c.g. is given by

$$\dot{X}_{HD/0} = \dot{X}_{HD/S} + \dot{X}_{S/0}$$
$$= \ell_{HDM}\dot{\zeta}\,\mathfrak{U}_\delta + \dot{X}_{S/0} \tag{20}$$

Resolving into $\mathfrak{U}_\delta$, $\mathfrak{U}_{HD}$ coordinates,

$$\dot{X}_{HD/0} = \{\ell_{HDM}\dot{\zeta} - [-(\ell_{TR} - \ell_{TRM})\dot{\theta} - \dot{x}\cos\theta$$
$$+ \dot{y}\sin\theta]\cos\zeta - [\dot{x}\sin\theta + \dot{y}\cos\theta]\sin\zeta\}\mathfrak{U}_\zeta$$
$$+ \{-[-(\ell_{TR} - \ell_{TRM})\dot{\theta} - \dot{x}\cos\theta$$
$$+ \dot{y}\sin\theta]\sin\zeta + [\dot{x}\sin\theta$$
$$+ \dot{y}\cos\theta]\cos\zeta\}\mathfrak{U}_{HD} \tag{21}$$

Equations (3), (8), (10), (12), (16), (19), and (21) give the velocity components of the trunk, thigh, shank, foot, upper arm, forearm, and head respectively; these components are obtained in several different coordinate systems.

By combining equations (1) and (12), the kinetic energy of the trunk is

$$T_{TR} = 1/2J_{TR}\dot{\theta}^2 + 1/2M_{TR}\{\dot{x}^2 + \dot{y}^2\} \tag{22}$$

From (1) and (8), the kinetic energy of the thigh is

$$T_{TH} = 1/2J_{TH}(\dot{\theta} - \dot{\gamma})^2 + 1/2M_{TH}\{[\ell_{THM}\dot{\gamma}$$
$$- (\ell_{TRM}\dot{\theta} - \dot{x}\cos\theta + \dot{y}\sin\theta)\cos\gamma$$
$$+ (\dot{x}\sin\theta + \dot{y}\cos\theta)\sin\gamma]^2 + [-(\dot{x}\sin\theta$$
$$+ \dot{y}\cos\theta)\cos\gamma - (\ell_{TRM}\dot{\theta} - \dot{x}\cos\theta$$
$$+ \dot{y}\sin\theta)\sin\gamma]^2\} \tag{23}$$

From (1) and (10), the kinetic energy of the shank is

$$T_{SH} = 1/2J_{SH}(\dot{\theta} - \dot{\gamma} + \dot{\beta})^2 + 1/2M_{SH}[\{\ell_{SHM}\dot{\beta}$$
$$+ [\ell_{TH}\dot{\gamma} - \ell_{TRM}\dot{\theta} - \dot{x}\cos\theta$$
$$+ \dot{y}\sin\theta)\cos\gamma]\cos\beta - [-(\dot{x}\sin\theta$$
$$+ \dot{y}\cos\theta)\cos\gamma - (\ell_{TRM}\dot{\theta} - \dot{x}\cos\theta$$
$$+ \dot{y}\sin\theta)]\sin\beta\}^2 + \{[-(\dot{x}\sin\theta$$
$$+ \dot{y}\cos\theta)\cos\gamma - (\ell_{TRM}\dot{\theta} - \dot{x}\cos\theta$$
$$+ \dot{y}\sin\theta)\sin\gamma]\cos\beta - [\ell_{TH}\dot{\gamma} - (\ell_{TRM}\dot{\theta}$$
$$- \dot{x}\cos\theta + \dot{y}\sin\theta)\cos\gamma + (\dot{x}\sin\theta$$
$$+ \dot{y}\cos\theta)\sin\gamma]\sin\beta\}^2] \tag{24}$$

From (1) and (12), the kinetic energy of the foot is

$$T_{FT} = 1/2J_{FT}(\dot{\theta} - \dot{\gamma} + \dot{\beta} + \dot{\alpha})^2 + 1/2M_{FT}\{[\ell_{FTM}\dot{\alpha}$$
$$+ \{[-(\dot{x}\sin\theta + \dot{y}\cos\theta)\cos\gamma - (\ell_{TRM}\dot{\theta}$$
$$- \dot{x}\cos\theta + \dot{y}\sin\theta)\sin\gamma]\cos\beta - [\ell_{TH}\dot{\gamma}$$
$$- (\ell_{TRM}\dot{\theta} - \dot{x}\cos\theta + \dot{y}\sin\theta)\cos\gamma + \dot{x}\sin\theta$$
$$+ \dot{y}\cos\theta)\sin\gamma]\sin\beta\}\cos\alpha + \{\ell_{SH}\dot{\beta} + [\ell_{TH}\dot{\gamma}$$
$$- (\ell_{TRM}\dot{\theta} - \dot{x}\cos\theta + \dot{y}\sin\theta)\cos\gamma]\cos\beta$$
$$- [-(\dot{x}\sin\theta + \dot{y}\cos\theta)\cos\gamma - (\ell_{TRM}\dot{\theta}$$
$$- \dot{x}\cos\theta + \dot{y}\sin\theta)\sin\beta]\sin\alpha\}^2 + [-\{\ell_{SH}\dot{\beta}$$
$$+ [\ell_{TH}\dot{\gamma} - (\ell_{TRM}\dot{\theta} - \dot{x}\cos\theta$$
$$+ \dot{y}\sin\theta)\cos\gamma]\cos\beta - [-(\dot{x}\sin\theta$$
$$+ \dot{y}\cos\theta)\cos\gamma - (\ell_{TRM}\dot{\theta} - \dot{x}\cos\theta$$
$$+ \dot{y}\sin\theta)\sin\beta]\cos\alpha + [-(\dot{x}\sin\theta$$
$$+ \dot{y}\cos\theta)\cos\gamma - (\ell_{TRM}\dot{\theta} - \dot{x}\cos\theta$$

$+ \dot{y} \sin\theta)\sin\gamma]\cos\beta - [\ell_{TH}\dot{\gamma} - (\ell_{TRM}\dot{\theta}$

$- \dot{x} \cos\theta + \dot{y} \sin\theta)\cos\gamma + (\dot{x} \sin\theta$

$+ \dot{y} \cos\theta)\sin\gamma]\sin\beta\}\sin\alpha\Big]\Big\}$ (25)

which clearly makes one wonder if it is worth the effort.

From (1) and (16), the kinetic energy of the upper arm is

$$T_{UA} = 1/2J_{UA}(\dot{\theta} - \dot{\delta})^2 + 1/2M_{UA}\Big[\{\ell_{UAM}\dot{\delta}$$

$$+ [-(\ell_{TR} - \ell_{TRM})\dot{\theta} - \dot{x} \cos\theta + \dot{y} \sin\theta]\sin\delta$$

$$- [\dot{x} \sin\theta + \dot{y} \cos\theta]\cos\delta\}^2 + \{[(\ell_{TR}$$

$$- \ell_{TRM})\dot{\theta} - \dot{x} \cos\theta + \dot{y} \sin\theta]\cos\delta + [\dot{x} \sin\theta$$

$$+ \dot{y} \cos\theta]\sin\delta\}^2\Big]$$ (26)

From (1) and (19), the kinetic energy of the forearm is

$$T_{FA} = 1/2J_{FA}(\dot{\theta} - \dot{\delta} - \dot{\epsilon})^2 + 1/2M_{FA}\Big[\{\ell_{FAM}\dot{\epsilon}$$

$$+ [\ell_{UA}\dot{\delta} + [-(\ell_{TR} - \ell_{TRM})\dot{\theta} - \dot{x} \cos\theta$$

$$+ \dot{y} \sin\theta]\sin\delta - [\dot{x} \sin\theta$$

$$+ \dot{y} \cos\theta]\cos\delta]\cos\epsilon - [(\ell_{TR} - \ell_{TRM})\dot{\theta}$$

$$- \dot{x} \cos\theta + \dot{y} \sin\theta]\cos\delta + [\dot{x} \sin\theta$$

$$+ \dot{y} \cos\theta]\sin\delta]\sin\epsilon\}^2 + \{[\ell_{UA}\dot{\delta} + [-(\ell_{TR}$$

$$- \ell_{TRM})\dot{\theta} - \dot{x} \cos\theta + \dot{y} \sin\theta]\sin\delta$$

$$- [\dot{x} \sin\theta + \dot{y} \cos\theta]\cos\delta]\sin\epsilon + [[(\ell_{TR}$$

$$- \ell_{TRM})\dot{\theta} - \dot{x} \cos\theta + \dot{y} \sin\theta]\cos\delta + [\dot{x} \sin\theta$$

$$+ \dot{y} \cos\theta]\sin\delta]\cos\epsilon\}^2\Big]$$ (27)

and, finally, the kinetic energy of the head is obtained from (1) and (21) as

$$T_{HD} = 1/2J_{HD}(\dot{\theta} + \dot{\zeta})^2 + 1/2M_{HD}\Big[\{\ell_{HDM}\dot{\delta}$$

$$- [-(\ell_{TR} - \ell_{TRM})\dot{\theta} - \dot{x} \cos\theta + \dot{y} \sin\theta]\cos\zeta$$

$$- [\dot{x}\sin\theta + \dot{y} \cos\theta]\sin\zeta\}^2 + \{- [-(\ell_{TR}$$

$$- \ell_{TRM})\dot{\theta} - \dot{x} \cos\theta + \dot{y} \sin\theta]\sin\zeta + [\dot{x} \sin\theta$$

$$+ \dot{y} \cos\theta]\cos\zeta\}^2\Big]$$ (28)

The total system kinetic energy is then given by

$$T = T_{TR} + T_{TH} + T_{SH} + T_{FT} + T_{UA} + T_{FA} + T_{HD}$$
    (29)

The potential energy of the system is more easily obtained. By element, the potential energies of the trunk, thigh, shank, foot, upper arm, forearm, and head are given by (30)-(36),

$$V_{TR} = M_{TR}gy$$ (30)

$$V_{TH} = M_{TH}g[y - \ell_{TRM} \cos\theta - \ell_{THM} \cos(\gamma - \theta)]$$
    (31)

$$V_{SH} = M_{SH}g[y - \ell_{TRM} \cos\theta - \ell_{TH} \cos(\gamma - \theta)$$

$$- \ell_{SHM} \cos(\gamma - \theta - \beta)]$$ (32)

$$V_{FT} = M_{FT}g[y - \ell_{TRM} \cos\theta - \ell_{TH} \cos(\gamma - \theta)$$

$$- \ell_{SH} \cos(\gamma - \theta - \beta) - \ell_{FTM} \sin(\theta - \gamma$$

$$+ \beta + \alpha)]$$ (33)

$$V_{UA} = M_{UA}g[y + (\ell_{TR} - \ell_{TRM})\cos\theta$$

$$- \ell_{UAM} \cos(\theta - \delta)]$$ (34)

$$V_{FA} = M_{FA}g[y + (\ell_{TR} - \ell_{TRM})\cos\theta$$

$$- \ell_{UA} \cos(\theta - \delta) - \ell_{FAM} \cos(\theta - \delta - \epsilon)]$$
    (35)

$$V_{HD} = M_{HD}g[y + (\ell_{TR} - \ell_{TRM}) \cos\theta$$

$$+ \ell_{HDM} \cos(\theta + \zeta)]$$ (36)

and the total system potential energy is

$$V = V_{TR} + V_{TH} + V_{SH} + V_{FT} + V_{UA} + V_{FA} + V_{HD}$$
    (37)

which can be grouped as

$$V = \{M_{TR} + M_{TH} + M_{SH} + M_{FT} + M_{UA} + M_{FA}$$

$$+ M_{HD}\}gy - \{[M_{TH} + M_{SH} + M_{FT}]\ell_{TRM}$$

$$- [M_{UA} + M_{FA} + M_{HD}](\ell_{TR} - \ell_{TRM})\} g \cos\theta$$

$$- \{M_{TH}\ell_{THM} + [M_{SH} + M_{FT}]\ell_{TH}\}g \cos(\gamma - \theta)$$

$$- \{M_{SH}\ell_{SHM} + M_{FT}\ell_{SH}\}g \cos(\gamma - \theta - \beta)$$

$$- \{M_{FT}\ell_{FTM}\}g \sin(\theta - \gamma + \beta + \alpha)$$

$$- \{M_{UA}\ell_{UAM} + M_{FA}\ell_{UA}\}g \cos(\theta - \delta)$$

$$- \{M_{FA}\ell_{FAM}\}g\cos(\theta - \delta - \epsilon)$$

$$+ \{M_{HD}\ell_{HDM}\}g\cos(\theta + \zeta) \qquad (38)$$

or

$$\begin{aligned}
V &= M_{gy} - V_1\cos\theta - V_2\cos(\gamma - \theta) \\
&\quad - V_3\cos(\gamma - \theta + \beta) - V_4\sin(\theta - \gamma + \beta \\
&\quad + \alpha) - V_5\cos(\theta - \delta) - V_6\cos(\theta - \delta + \epsilon) \\
&\quad + V_7\cos(\theta + \zeta) \qquad (39)
\end{aligned}$$

where M is the total mass of the stick man, g is the gravitational acceleration, and the V_i are constants obtained by comparison of equations (38) and (39).

Lagrange's equations, in the form

$$\frac{d}{dt}\left(\frac{\partial T}{\partial \dot{q}_i}\right) - \frac{\partial T}{\partial q_i} + \frac{\partial V}{\partial q_i} = Q_i \qquad (40)$$

where the q_i are the system generalized coordinates and the Q_i are the generalized forces arising from muscular contraction, require partial differentiation of the system kinetic energy as given by equation (29) with respect to all the generalized coordinates and their derivatives and partial differentiation of the system potential energy as given by equation (39) with respect to the generalized coordinates. With no approximations, the resulting expressions are too lengthy for inclusion here; digital computer symbolic processing techniques to assist in carrying out the more laborious and error-prone calculations with greater reliability are being investigated.

Conclusion

Successful completion of the derivation would provide a pitch-axis model of the human postural control system, valid for large angular deflections of the joints, which could be simulated by standard analog or digital simulation techniques.

This simulation would include the dynamic force-velocity characteristics of the muscles in addition to the dynamics of the controlled object. It would then be possible to investigate the design of control laws [29] which, when incorporated into the simulation, could be tested for agreement with experimental data on human subjects performing the same tasks.

In this paper, the derivation of the postural control system equations of motion has been carried to the point where it clearly is advisable to utilize a digital computer to do the bookkeeping involved in the coordinate transformations and the subsequent partial differentiation required by Lagrange's equations. Certainly the possibility of ever extending the model to the

full number of degrees of freedom of the human body would require such an organized "infallible" approach. Computer techniques for assisting in this problem are currently being investigated in terms of the present problem.

Subscript Convention

TR	↔	TRunk, CG thereof
TH	↔	THigh, CG thereof
SH	↔	SHank, CG thereof
FT	↔	FooT, CG thereof
HD	↔	HeaD, CG thereof
UA	↔	Upper Arm, CG thereof
FA	↔	Fore Arm, CG thereof
H	↔	Hip
K	↔	Knee
A	↔	Ankle
T	↔	Toe
S	↔	Shoulder
E	↔	Elbow
N	↔	Neck

List of Symbols

J_{TR}	=	Moment of inertia of trunk, slug-ft^2
J_{HD}	=	Moment of inertia of head, slug-ft^2
J_{UA}	=	Moment of inertia of upper arm, slug-ft^2
J_{FA}	=	Moment of inertia of fore arm slug-ft^2
J_{TH}	=	Moment of inertia of thigh, slug-ft^2
J_{FT}	=	Moment of inertia of foot, slug-ft^2
M_{TR}	=	Mass of trunk, slugs
M_{HD}	=	Mass of head, slugs
M_{UA}	=	Mass of upper arm, slugs
M_{FA}	=	Mass of fore arm, slugs
M_{TH}	=	Mass of thigh, slugs
M_{FT}	=	Mass of foot, slugs

ℓ_{TR}	=	Length of trunk, ft
ℓ_{UA}	=	Length of upper arm, ft
ℓ_{TH}	=	Length of thigh, ft
ℓ_{SH}	=	Length of shank, ft
ℓ_{FT}	=	Length of foot, ft
ℓ_{TRM}	=	Distance from hip to trunk CG, ft
ℓ_{HDM}	=	Distance from shoulder to head CG, ft
ℓ_{UAM}	=	Distance from shoulder to upper arm CG, ft
ℓ_{FAM}	=	Distance from elbow to fore arm CG, ft
ℓ_{THM}	=	Distance from hip to thigh CG, ft
ℓ_{SHM}	=	Distance from knee to shank CG, ft
ℓ_{FTM}	=	Distance from ankle to foot, CG, ft
$\dot{X}_{A/0}$	=	Absolute velocity of ankle CG wrt origin, ft/sec
$\dot{X}_{FT/0}$	=	Absolute velocity of foot CG wrt origin, ft/sec
$\dot{X}_{FT/A}$	=	Relative velocity of foot CG wrt ankle, ft/sec
$\dot{X}_{S/0}$	=	Absolute velocity of shoulder wrt origin, ft/sec
$\dot{X}_{S/TR}$	=	Relative velocity of shoulder wrt trunk CG, ft/sec
$\dot{X}_{UA/0}$	=	Absolute velocity of upper arm CG wrt origin, ft/sec
$\dot{X}_{UA/S}$	=	Relative velocity of upper arm CG wrt shoulder, ft/sec
$\dot{X}_{E/0}$	=	Absolute velocity of elbow wrt shoulder, ft/sec
$\dot{X}_{FA/0}$	=	Absolute velocity of fore arm CG wrt origin, ft/sec
$\dot{X}_{FA/E}$	=	Relative velocity of fore arm CG wrt elbow, ft/sec
$\dot{X}_{HD/0}$	=	Absolute velocity of head CG wrt origin, ft/sec
$\dot{X}_{HD/S}$	=	Relative velocity of head CG wrt shoulder, ft/sec
$\dot{X}_{TR/0}$	=	Absolute velocity of trunk CG wrt origin, ft/sec
$\dot{X}_{H/TR}$	=	Relative velocity of hip wrt trunk CG, ft/sec
$\dot{X}_{H/0}$	=	Absolute velocity of hip wrt origin, ft/sec
$\dot{X}_{TH/0}$	=	Absolute velocity of thigh CG wrt origin, ft/sec
$\dot{X}_{TH/H}$	=	Relative velocity of thigh CG wrt hip, ft/sec

$\dot{X}_{K/0}$	=	Absolute velocity of knee wrt origin, ft/sec
$\dot{X}_{K/H}$	=	Relative velocity of knee wrt hip, ft/sec
$\dot{X}_{SH/0}$	=	Absolute velocity of shank CG wrt origin, ft/sec
$\dot{X}_{SH/K}$	=	Relative velocity of shank CG wrt knee, ft/sec
θ	=	Angle of trunk with respect to vehicle, radians, positive CW
δ	=	Angle of upper arm with respect to trunk, radians, positive CCW
ζ	=	Angle of head with respect to trunk, radians, positive CW
ε	=	Angle of fore arm with respect to upper arm, radians, positive CCW
γ	=	Angle of thigh with respect to trunk, radians, positive CCW
β	=	Angle of shank with respect to thigh, radians, positive CCW
α	=	Angle of foot with respect to perpendicular to shank, radians, positive CW
x	=	Horizontal displacement of trunk CG, ft
y	=	Verticle displacement of trunk CG, ft
$\underset{\sim}{u}_x$	=	Unit vector in positive x direction
$\underset{\sim}{u}_y$	=	Unit vector in positive y direction
$\underset{\sim}{u}_{TR}$	=	Unit vector directed from hip to trunk CG
$\underset{\sim}{u}_{TH}$	=	Unit vector directed from hip to thigh CG
$\underset{\sim}{u}_{SH}$	=	Unit vector directed from knee to shank CG
$\underset{\sim}{u}_{FT}$	=	Unit vector directed from ankle to foot CG
$\underset{\sim}{u}_H$	=	Unit vector directed from shoulder to head CG
$\underset{\sim}{u}_{UA}$	=	Unit vector directed from shoulder to upper arm CG
$\underset{\sim}{u}_{FA}$	=	Unit vector directed from elbow to fore arm CG
$\underset{\sim}{u}_\theta$	=	Unit vector in direction of increasing θ
$\underset{\sim}{u}_\gamma$	=	Unit vector in direction of increasing γ
$\underset{\sim}{u}_\beta$	=	Unit vector in direction of increasing β
$\underset{\sim}{u}_\alpha$	=	Unit vector in direction of increasing α

159

$\mathcal{H}_\delta$ = Unit vector in direction of increasing δ

$\mathcal{H}_\varepsilon$ = Unit vector in direction of increasing ε

$\mathcal{H}_\zeta$ = Unit vector in direction of increasing ζ

V = Potential energy, slug-ft

V_{TR} = Potential energy of trunk, slug-ft

V_{TH} = Potential energy of thigh, slug-ft

V_{SH} = Potential energy of shank, slug-ft

V_{FT} = Potential energy of foot, slug-ft

V_{UA} = Potential energy of upper arm, slug-ft

V_{FA} = Potential energy of fore arm, slug-ft

V_{HD} = Potential energy of head, slug-ft

$V_1, V_2 \ldots V_7$ = Constants in potential energy expression, slug-ft

T = Kinetic energy, slug-ft

T_{TR} = Kinetic energy of trunk, slug-ft

T_{TH} = Kinetic energy of thigh, slug-ft

T_{SH} = Kinetic energy of shank, slug-ft

T_{FT} = Kinetic energy of foot, slug-ft

T_{UA} = Kinetic energy of upper arm, slug-ft

T_{FA} = Kinetic energy of fore arm, slug-ft

T_{HD} = Kinetic energy of head, slug-ft

g = Gravitational acceleration, 32.18 ft/sec^2

M = Total system mass, slugs

References

1. Milhorn, H.T., Jr., "The Application of Control Theory to Physiological Systems", W.B. Saunders Co., Chapter 17: "The Stretch Reflex in Human Muscle Systems", pp. 283-316.
2. Houk, J.C., "A Mathematical Model of the Stretch Reflex in Human Muscle Systems," M.A. Thesis, Massachusetts Institute of Technology, Cambridge, 1963.
3. Fenn, W.O., and Marsh, B.S., "Muscular Force at Different Speeds of Shortening", Journal of Physiology (London), Vol. 85, pp. 277ff, 1935.
4. Bahler, A.S., "Modeling of Mammalian Skeletal Muscle", I.E.E.E. Transactions on Bio-Medical Engineering, Vol. BME-15, No. 4, pp. 249-257, October, 1968.
5. Vickers, W.H., and Sheridan, T.B., "A Dynamic Model of an Agonist-Antagonist Muscle Pair", I.E.E.E. Transactions on Man-Machine Systems, March, 1968.

6. Galiana, H.L., "Modeling the Human Leg in Walking", Master of Engineering Thesis, Department of Electrical Engineering, McGill University, Montreal, Canada, August, 1968.
7. Magdaleno, R.E., and McRuer, D.T., "A Closed-Loop Neuromuscular System Explanation of Force Disturbance Regulation and Tremor Data" Fourth Annual NASA-University Conference on Manual Control, University of Michigan, Ann Arbor, March 21-23, 1968.
8. Dewhurst, D.J., "Neuromuscular Control System", I.E.E.E. Transactions on Bio-Medical Engineering, Vol. BME-14, No. 3, pp. 167-171, July, 1967.
9. Miery, J.L., "The Vestibular System and Human Dynamic Space Orientation", Doctor of Science Thesis, M.I.T., June, 1965.
10. Young, L.R., "A Control Model of the Vestibular System", I.F.A.C. Symposium on Technical and Biological Problems in Cybernetics, Yerivan, Armenia, U.S.S.R., September, 1968.
11. Gottlieb, G.L., Agarwal, G.C., and Stark, L., "Stretch Receptor Models, I-Single-Efferent Single Affevent Innovation", I.E.E.E. Transactions on Man-Machine Systems, Vol. MMS-10, No. 1, pp. 17-27, March, 1969.
12. McRuer, D.T., and Magdaleno, R.E., "Human Pilot Dynamics with Various Manipulators", Technical Report No. AFFDL-TR-66-138, Air Force Flight Dynamics Laboratory, Research and Technology Division, Air Force Systems Command, Wright-Patterson AFB, Ohio; December, 1966.
13. Wasicko, R.J., McRuer, D.T., and Magdaleno, R.E., "Human Pilot Dynamic Response in Single-loop Systems with Compensatory and Pursuit Displays", Technical Report AFFDL-TR-66-137, Air Force Flight Dynamics Laboratory, Research and Technology Division, Air Force Systems Command, Wright-Patterson AFB, Ohio; December, 1966.
14. Magdaleno, R.E. and McRuer, D.T., "Effects of Manipulator Restraints on Human Operator Performance", Technical Report AFFDL-TR-66-72, Air Force Flight Dynamics Laboratory, Research and Technology Division, Air Force Systems Command, Wright-Patterson AFB, Ohio; December, 1966.
15. McRuer, D.T., Graham, D., Kvendal, E., and Reisener, W., Jr., "Human Pilot Dynamics in Compensatory Systems: Theory, Models, and Experiments with Controlled Element and Forcing Function Variations", Technical Report No. AFFDL-TR-65-15, Air Force Flight Dynamics Laboratory, Research and Technology Division, Air Force Systems Command, Wright-Patterson AFB, Ohio; December, 1966.
16. Shirley, R.S., and Young, L.R., "Motion Cues in Man-Vehicle Control", Fourth Annual NASA-University Conference on Manual Control, University of Michigan, Ann Arbor, March 21-23, 1968.
17. Adams, J.J., "Synthesis of Human Response in Closed-Loop Control Tasks", Fourth Annual NASA-University Conference on Manual Control, University of Michigan, Ann Arbor, March 21-23, 1968.

18. Wier, D.H., and McRuer, D.T., "Models for Steering Control of Motor Vehicles", Fourth Annual NASA-University Conference on Manual Control, University of Michigan, Ann Arbor, March 21-23, 1968.

19. Crossman, E.R.F.W., "Man-Machine Models for Car Steering", Fourth Annual NASA-University Conference on Manual Control, University of Michigan, Ann Arbor, March 21-23, 1968.

20. Agarwal, G.C., Berman, G., Hogins, M.T., Lohnberg, P., and Stark, L., "Effect of External Loading on Human Motor Reflexes", Fourth Annual NASA-University Conference on Manual Control, University of Michigan, Ann Arbor, March 21-23, 1968.

21. McGhee, R.B., "Some Finite State Aspects of Legged Locomotion", Mathematical Biosciences, Vol. 2, No. 2, pp. 67-84, 1968.

22. McGhee, R.B., "Finite State Control of Quadruple Locomotion", Simulation, Vol 9, No. 3, pp. 135-140, September, 1967.

23. McGhee, R.B., and Frank, A.A., "On the Stability Properties of Quadruped Creeping Gaits", Mathematical Biosciences, December, 1968.

24. Frank, A.A., and McGhee, R.B., "Some Considerations Relating to the Design of Autopilots for Legged Vehicles", Symposium on Aids to Human Motion, January 21,22, 1968, sponsored by the General Electric Company, and the U.S. Army Tank and Automotive Command, Warren, Michigan.

25. Tomovic, R., and McGhee, R.B., "A Finite State Approach to the Synthesis of Bioengineering Control Systems", I.E.E.E. Transactions on Human Factors in Electronics Vol. HFE-7, No. 2, June 1966, pp. 65-69.

26. Gibson, J.E., di Tada, E.G., Hill, J.C. and Ibrahim, E.S., "Describing Function Inversion: Theory and Computational Techniques", Technical Report TR-EE62-10, Purdue University School of Electrical Engineering, December, 1962.

27. Mosher, Ralph S., "Exploring the Potential of a Quadruped", S.A.E. Paper No. 690191, International Automotive Engineering Conference, Detroit, Michigan, January 13-17, 1969.

28. Blackmer, R.H., Interian, A., and Clodfelter, R.G., "The Role of Space Manipulator Systems for Extravehicular Tasks", Second National Conference on Space Maintenance and Extravehicular Activities, Las Vegas, Nevada, August 6-8, 1968.

29. Whitney, Daniel E., "Resolved Motion Rate Control of Manipulators and Human Prostheses", I.E.E.E. Transactions on Man-Machine Systems, Vol. MMS-10, No. 2, June, 1969, pp. 47-53.
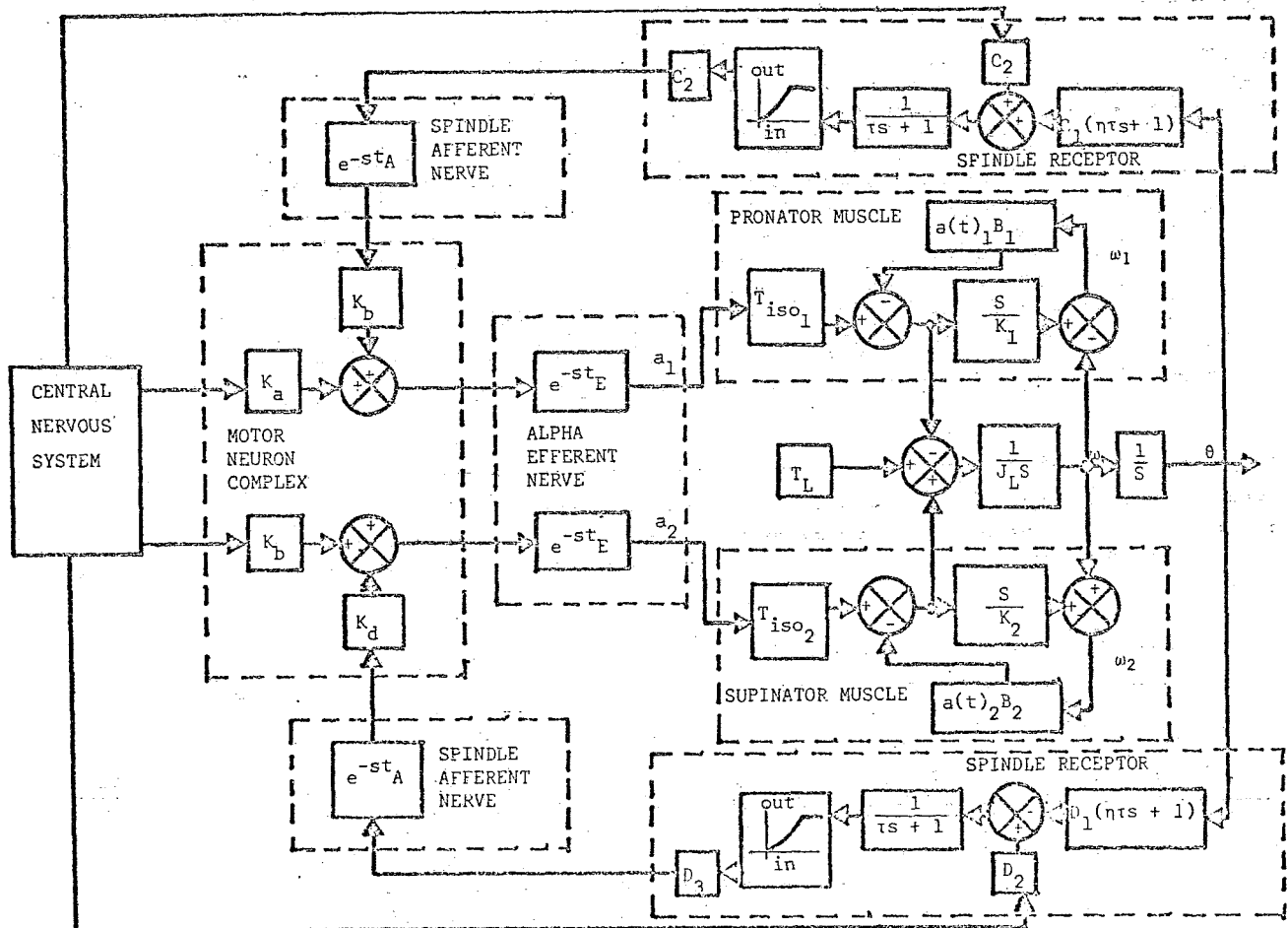
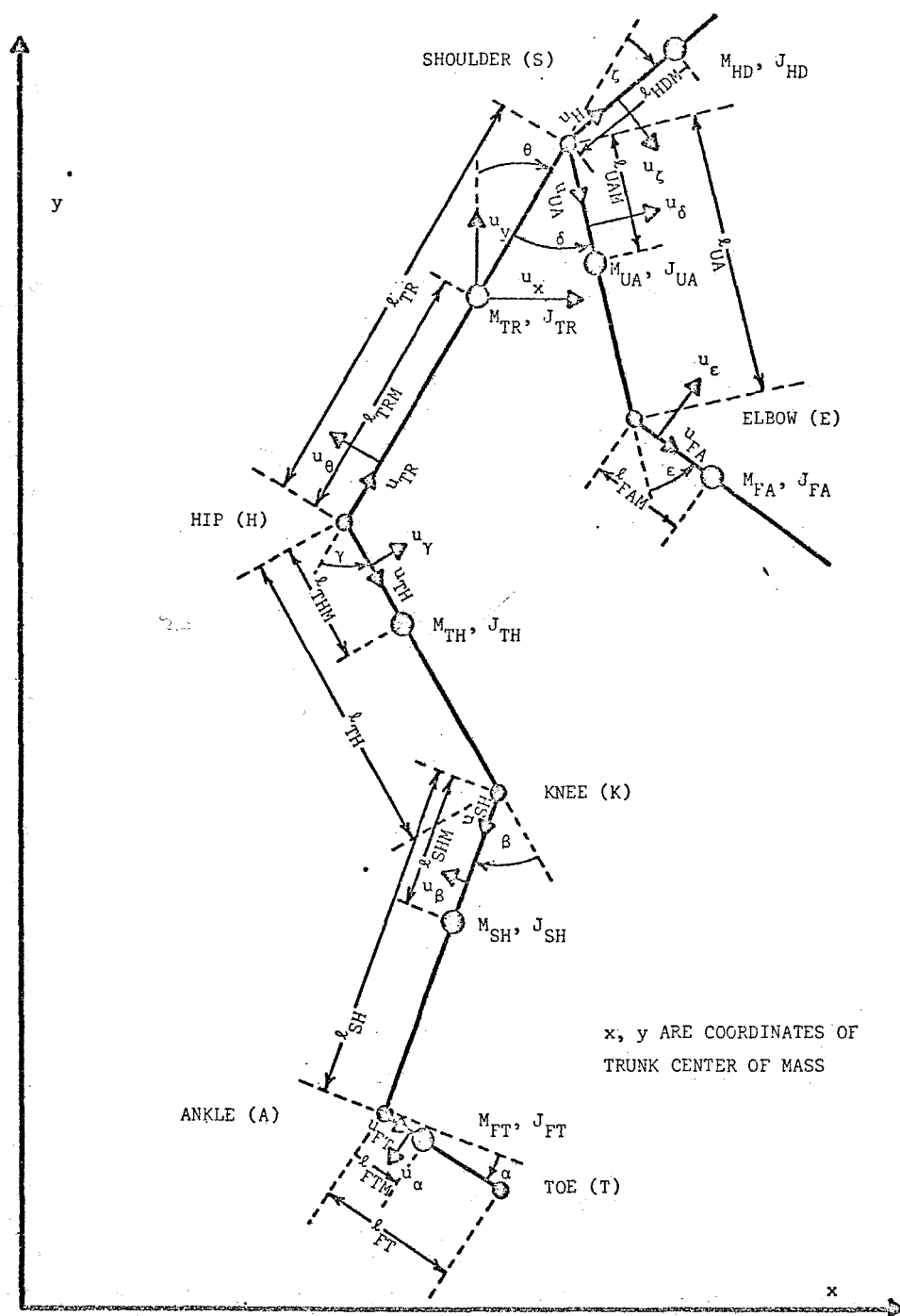FIGURE 1. Postural Control System Block Diagram (From Milhorn, after Houk)

FIGURE 2. Coordinate System for Postural Control System Model

APPENDIX II

FORMAC Source Program Generating the Equations

of Motion of the Seven Element Stick Man

```
INPUT TO FORMAC PREPROCESSOR
DERIP: PROCEDURE OPTIONS(MAIN);
FORMAC_OPTIONS;
    LET(VTRSO=DX*UX+DY*UY);
    LET(VHSOA=LTRM*DTHTA*UTHTA+VTRSO);
    LET(VHSB=EVAL(VHSOA,UX,UTR*SIN(THETA)-UTHTA*COS(THETA)));
    LET(VHSO=EVAL(VHSB,UY,UTR*COS(THETA)+UTHTA*SIN(THETA)));
ATOMIZE(VHSB);
    LET(VTHSOA=LTHM*DGAMA*UGAMA+VHSO);
    LET(VTHSA=EVAL(VTHSOA,UTHTA,-UTH*SIN(GAMMA)-UGAMA*COS(GAMMA)));
    LET(VTHSO=EVAL(VTHSA,UTR,-UTH*COS(GAMMA)+UGAMA*SIN(GAMMA)));
ATOMIZE(VTHSA);
    LET(VKSO=EVAL(VTHSO,LTHM,LTH));
    LET(VSHSOA=LSHM*DBETA*UBETA+VKSO);
    LET(VSHSA=EVAL(VSHSOA,UTH,USH*COS(BETA)-UBETA*SIN(BETA)));
    LET(VSHSO=EVAL(VSHSA,UGAMA,-UBETA*COS(BETA)-USH*SIN(BETA)));
ATOMIZE(VSHSA);
    LET(VASO=EVAL(VSHSO,LSHM,LSH));
    LET(VFTSOA=LFTM*DALFA*UALFA+VASO);
    LET(VFTSA=EVAL(VFTSOA,USH,UALFA*COS(ALPHA)+UFT*SIN(ALPHA)));
    LET(VFTSO=EVAL(VFTSA,UBETA,-UFT*COS(ALPHA)+UALFA*SIN(ALPHA)));
ATOMIZE(VFTSA);
    LET(VSSOA=-(LTR-LTRM)*DTHTA*UTHTA+VTRSO);
    LET(VSSA=EVAL(VSSOA,UX,UTR*SIN(THETA)-UTHTA*COS(THETA)));
    LET(VSSO=EVAL(VSSA,UY,UTR*COS(THETA)+UTHTA*SIN(THETA)));
ATOMIZE(VSSA);
    LET(VUASOA=LUAM*DDLTA*UDLTA+VSSO);
    LET(VUASA=EVAL(VUASOA,UTHTA,-UDLTA*COS(DELTA)-UUA*SIN(DELTA)));
    LET(VUASO=EVAL(VUASA,UTR,UDLTA*SIN(DELTA)-UUA*COS(DELTA)));
ATOMIZE(VUASA);
    LET(VESO=EVAL(VUASO,LUAM,LUA));
    LET(VFASOA=LFAM*DEPSN*UEPSN+VESO);
    LET(VFASA=EVAL(VFASOA,UDLTA,UEPSN*COS(EPSN)+UFA*SIN(EPSN)));
    LET(VFASO=EVAL(VFASA,UUA,-UEPSN*SIN(EPSN)+UFA*COS(EPSN)));
ATOMIZE(VFASA);
    LET(VHDSOA=LHDM*DZETA*UZETA+VSSO);
    LET(VHDSA=EVAL(VHDSOA,UTR,UHD*COS(ZETA)-UZETA*SIN(ZETA)));
    LET(VHDSO=EVAL(VHDSA,UTHTA,-UHD*SIN(ZETA)-UZETA*COS(ZETA)));
ATOMIZE(VHDSA);
    OPTSET(EXPND);
    LET(T1R=(1/2)*JTR*DTHTA**2+(1/2)*MTR*(COEFF(VTRSO,UX)**2));
    LET(TTR=T1R+(1/2)*MTR*(COEFF(VTRSO,UY)**2));
ATOMIZE(T1R);
    ATOMIZE(VTRSO;VHSOA;VHSO);
    LET(TTR1=DERIV(TTR,X));
    LET(TTR2=DERIV(TTR,Y));
    LET(TTR3=DERIV(TTR,THETA));
    LET(TTR4=DERIV(TTR,GAMMA));
    LET(TTR5=DERIV(TTR,BETA));
    LET(TTR6=DERIV(TTR,DELTA));
    LET(TTR7=DERIV(TTR,ALPHA));
    LET(TTR8=DERIV(TTR,EPSN));
    LET(TTR9=DERIV(TTR,ZETA));
    LET(TTR10=DERIV(TTR,DX));
    LET(TTR11=DERIV(TTR,DY));
    LET(TTR12=DERIV(TTR,DTHTA));
    LET(TTR13=DERIV(TTR,DGAMA));
    LET(TTR14=DERIV(TTR,DBETA));
    LET(TTR15=DERIV(TTR,DDLTA));
    LET(TTR16=DERIV(TTR,DALFA));
```

```
        LET(TTR17=DERIV(TTR,DEPSN));
        LET(TTR18=DERIV(TTR,DZETA));
      LET(TTR10A=REPLACE(TTR10,DX,DX.(T)));
      LET(TTR11A=REPLACE(TTR11,DY,DY.(T)));
      LET(TTR12A=REPLACE(TTR12,DTHTA,DTHTA.(T)));
        LET(TTR19=DERIV(TTR10A,T));
        LET(TTR20=DERIV(TTR11A,T));
        LET(TTR21=DERIV(TTR12A,T));
    ATOMIZE(TTR10A;TTR11A;TTR12A);
    ATOMIZE(TTR19;TTR20;TTR21);
    ATOMIZE(TTR;TTR1;TTR2;TTR3;TTR4;TTR5;TTR6;TTR7;TTR8;TTR9);
    ATOMIZE(TTR10;TTR11;TTR12;TTR13;TTR14;TTR15;TTR16;TTR17;TTR18);
  LET(T1H=(1/2)*JTH*(DTHTA-DGAMA)**2+(1/2)*MTH*(COEFF(VTHSO,UTH)**2));
      LET(TTH=T1H+(1/2)*MTH*(COEFF(VTHSO,UGAMA)**2));
      ATOMIZE(VTHSO;VTHSOA);
    ATOMIZE(T1H);
        LET(TTH1=DERIV(TTH,X));
        LET(TTH2=DERIV(TTH,Y));
        LET(TTH3=DERIV(TTH,THETA));
        LET(TTH4=DERIV(TTH,GAMMA));
        LET(TTH5=DERIV(TTH,BETA));
        LET(TTH6=DERIV(TTH,DELTA));
        LET(TTH7=DERIV(TTH,ALPHA));
        LET(TTH8=DERIV(TTH,EPSN));
        LET(TTH9=DERIV(TTH,ZETA));
        LET(TTH10=DERIV(TTH,DX));
        LET(TTH10A=REPLACE(TTH10,GAMMA,GAMMA.(T),THETA,THETA.(T)));
    LET(TTH10A=REPLACE(TTH10A,DGAMA,DGAMA.(T),DX,DX.(T),DTHTA,DTHTA.(T)));
        ATOMIZE(TTH10);
        LET(TTH11=DERIV(TTH,DY));
    LET(TTH11A=REPLACE(TTH11,GAMMA,GAMMA.(T),THETA,THETA.(T)));
    LET(TTH11A=REPLACE(TTH11A,DGAMA,DGAMA.(T),DY,DY.(T),DTHTA,DTHTA.(T)));
        ATOMIZE(TTH11);
        LET(TTH12=DERIV(TTH,DTHTA));
    LET(TTH12A=REPLACE(TTH12,DGAMA,DGAMA.(T),DTHTA,DTHTA.(T)));
    LET(TTH12A=REPLACE(TTH12A,GAMMA,GAMMA.(T),THETA,THETA.(T)));
    LET(TTH12A=REPLACE(TTH12A,DX,DX.(T),DY,DY.(T)));
        ATOMIZE(TTH12);
        LET(TTH13=DERIV(TTH,DGAMA));
    LET(TTH13A=REPLACE(TTH13,DGAMA,DGAMA.(T),DTHTA,DTHTA.(T),DX,DX.(T)));
    LET(TTH13A=REPLACE(TTH13A,GAMMA,GAMMA.(T),THETA,THETA.(T),DY,DY.(T)));
        ATOMIZE(TTH13);
        LET(TTH14=DERIV(TTH,DBETA));
        LET(TTH15=DERIV(TTH,DDLTA));
        LET(TTH16=DERIV(TTH,DALFA));
        LET(TTH17=DERIV(TTH,DEPSN));
        LET(TTH18=DERIV(TTH,DZETA));
        LET(TTH19=DERIV(TTH10A,T));
        LET(TTH20=DERIV(TTH11A,T));
        LET(TTH21=DERIV(TTH12A,T));
        LET(TTH22=DERIV(TTH13A,T));
      ATOMIZE(TTH19;TTH20;TTH21;TTH22;TTH23);
    ATOMIZE(TTH;TTH1;TTH2;TTH3;TTH4;TTH5;TTH6;TTH7;TTH8;TTH9);
    ATOMIZE(TTH10;TTH11;TTH12;TTH13;TTH14;TTH15;TTH16;TTH17;TTH18);
        LET(T5H=(1/2)*JSH*(DTHTA-DGAMA+DBETA)**2);
        LET(T6H=(1/2)*MSH*(COEFF(VSHSO,USH)**2));
        LET(TSH=T5H+T6H+(1/2)*MSH*(COEFF(VSHSO,UBETA)**2));
    ATOMIZE(T5H;T6H);
      ATOMIZE(VSHSO;VKSO;VSHSOA);
        LET(TSH1=DERIV(TSH,X));
```

```
        LET(TSH2=DERIV(TSH,Y));
        LET(TSH3=DERIV(TSH,THETA));
        LET(TSH4=DERIV(TSH,GAMMA));
        LET(TSH5=DERIV(TSH,BETA));
        LET(TSH6=DERIV(TSH,DELTA));
        LET(TSH7=DERIV(TSH,ALPHA));
        LET(TSH8=DERIV(TSH,EPSN));
        LET(TSH9=DERIV(TSH,ZETA));
        LET(TSH10=DERIV(TSH,DX));
    LET(TSH10A=REPLACE(TSH10,GAMMA,GAMMA.(T),THETA,THETA.(T)));
    LET(TSH10A=REPLACE(TSH10A,BETA,BETA.(T),DGAMA,DGAMA.(T)));
    LET(TSH10A=REPLACE(TSH10A,DBETA,DBETA.(T),DX,DX.(T),DTHTA,DTHTA.(T)));
        ATOMIZE(TSH10);
        LET(TSH11=DERIV(TSH,DY));
    LET(TSH11A=REPLACE(TSH11,GAMMA,GAMMA.(T),THETA,THETA.(T)));
    LET(TSH11A=REPLACE(TSH11A,BETA,BETA.(T),DGAMA,DGAMA.(T)));
    LET(TSH11A=REPLACE(TSH11A,DBETA,DBETA.(T),DY,DY.(T),DTHTA,DTHTA.(T)));
        ATOMIZE(TSH11);
        LET(TSH12=DERIV(TSH,DTHTA));
    LET(TSH12A=REPLACE(TSH12,GAMMA,GAMMA.(T),BETA,BETA.(T)));
    LET(TSH12A=REPLACE(TSH12A,DGAMA,DGAMA.(T),DBETA,DBETA.(T),DX,DX.(T)));
    LET(TSH12A=REPLACE(TSH12A,THETA,THETA.(T),DY,DY.(T),DTHTA,DTHTA.(T)));
        ATOMIZE(TSH12);
        LET(TSH13=DERIV(TSH,DGAMA));
    LET(TSH13A=REPLACE(TSH13,BETA,BETA.(T),DBETA,DBETA.(T),DX,DX.(T)));
    LET(TSH13A=REPLACE(TSH13A,GAMMA,GAMMA.(T),THETA,THETA.(T),DY,DY.(T)));
    LET(TSH13A=REPLACE(TSH13A,DTHTA,DTHTA.(T),DGAMA,DGAMA.(T)));
        ATOMIZE(TSH13);
        LET(TSH14=DERIV(TSH,DBETA));
    LET(TSH14A=REPLACE(TSH14,BETA,BETA.(T),DGAMA,DGAMA.(T),DX,DX.(T)));
    LET(TSH14A=REPLACE(TSH14A,GAMMA,GAMMA.(T),THETA,THETA.(T),DY,DY.(T)));
    LET(TSH14A=REPLACE(TSH14A,DTHTA,DTHTA.(T),DBETA,DBETA.(T)));
        ATOMIZE(TSH14);
        LET(TSH15=DERIV(TSH,DDLTA));
        LET(TSH16=DERIV(TSH,DALFA));
        LET(TSH17=DERIV(TSH,DEPSN));
        LET(TSH18=DERIV(TSH,DZETA));
        LET(TSH19=DERIV(TSH10A,T));
        LET(TSH20=DERIV(TSH11A,T));
        LET(TSH21=DERIV(TSH12A,T));
        LET(TSH22=DERIV(TSH13A,T));
        LET(TSH23=DERIV(TSH14A,T));
        ATOMIZE(TSH19;TSH20;TSH21;TSH22;TSH23);
    ATOMIZE(TSH;TSH1;TSH2;TSH3;TSH4;TSH5;TSH6;TSH7;TSH8;TSH9);
    ATOMIZE(TSH10;TSH11;TSH12;TSH13;TSH14;TSH15;TSH16;TSH17;TSH18);
    OPTSET(LINELENGTH=72);   OPTSET(PRINT);
        LET(T1T=(1/2)*JFT*(DTHTA-DGAMA+DBETA+DALFA)**2);
        LET(T2T=(1/2)*MFT*(COEFF(VFTSO,UALFA)**2));
        LET(TFT=T1T+T2T+(1/2)*MFT*(COEFF(VFTSO,UFT)**2));
        ATOMIZE(VFTSO;VFTSOA;VASO);
    ATOMIZE(T1T;T2T);
        LET(TFT1=DERIV(TFT,X));
        LET(TFT2=DERIV(TFT,Y));
        LET(TFT3=DERIV(TFT,THETA));
        LET(TFT4=DERIV(TFT,GAMMA));
        LET(TFT5=DERIV(TFT,BETA));
        LET(TFT6=DERIV(TFT,DELTA));
        LET(TFT7=DERIV(TFT,ALPHA));
        LET(TFT8=DERIV(TFT,EPSN));
        LET(TFT9=DERIV(TFT,ZETA));
```

```
LET(TFT10=DERIV(TFT,DX));
LET(TFT10A=REPLACE(TFT10,GAMMA,GAMMA.(T),THETA,THETA.(T)));
ATOMIZE(TFT10);
LET(TFT10A=REPLACE(TFT10A,BETA,BETA.(T),ALPHA,ALPHA.(T)));
LET(TFT10A=REPLACE(TFT10A,DBETA,DBETA.(T),DALFA,DALFA.(T)));
LET(TFT10A=REPLACE(TFT10A,DGAMA,DGAMA.(T),DY,DX.(T),DTHTA,DTHTA.(T)));
LET(TFT11=DERIV(TFT,DY));
LET(TFT11A=REPLACE(TFT11,GAMMA,GAMMA.(T),THETA,THETA.(T)));
ATOMIZE(TFT11);
LET(TFT11A=REPLACE(TFT11A,BETA,BETA.(T),ALPHA,ALPHA.(T)));
LET(TFT11A=REPLACE(TFT11A,DBETA,DBETA.(T),DALFA,DALFA.(T)));
LET(TFT11A=REPLACE(TFT11A,DGAMA,DGAMA.(T),DY,DY.(T),DTHTA,DTHTA.(T)));
LET(TFT12=DERIV(TFT,DTHTA));
LET(TFT12A=REPLACE(TFT12,DALFA,DALFA.(T),DBETA,DBETA.(T)));
ATOMIZE(TFT12);
LET(TFT12A=REPLACE(TFT12A,DGAMA,DGAMA.(T),DTHTA,DTHTA.(T)));
LET(TFT12A=REPLACE(TFT12A,GAMMA,GAMMA.(T),BETA,BETA.(T),DX,DX.(T)));
LET(TFT12A=REPLACE(TFT12A,ALPHA,ALPHA.(T),THETA,THETA.(T),DY,DY.(T)));
LET(TFT13=DERIV(TFT,DGAMA));
LET(TFT13A=REPLACE(TFT13,DALFA,DALFA.(T),DBETA,DBETA.(T)));
ATOMIZE(TFT13);
LET(TFT13A=REPLACE(TFT13A,DGAMA,DGAMA.(T),DTHTA,DTHTA.(T)));
LET(TFT13A=REPLACE(TFT13A,BETA,BETA.(T),ALPHA,ALPHA.(T),DX,DX.(T)));
LET(TFT13A=REPLACE(TFT13A,GAMMA,GAMMA.(T),THETA,THETA.(T),DY,DY.(T)));
LET(TFT14=DERIV(TFT,DBETA));
LET(TFT14A=REPLACE(TFT14,DALFA,DALFA.(T),DBETA,DBETA.(T)));
ATOMIZE(TFT14);
LET(TFT14A=REPLACE(TFT14A,DGAMA,DGAMA.(T),DTHTA,DTHTA.(T)));
LET(TFT14A=REPLACE(TFT14A,ALPHA,ALPHA.(T),BETA,BETA.(T),DX,DX.(T)));
LET(TFT14A=REPLACE(TFT14A,GAMMA,GAMMA.(T),THETA,THETA.(T),DY,DY.(T)));
LET(TFT15=DERIV(TFT,DDLTA));
LET(TFT16=DERIV(TFT,DALFA));
LET(TFT16A=REPLACE(TFT16,DALFA,DALFA.(T),DBETA,DBETA.(T)));
ATOMIZE(TFT16);
LET(TFT16A=REPLACE(TFT16A,DGAMA,DGAMA.(T),DTHTA,DTHTA.(T)));
LET(TFT16A=REPLACE(TFT16A,ALPHA,ALPHA.(T),BETA,BETA.(T),DX,DX.(T)));
LET(TFT16A=REPLACE(TFT16A,GAMMA,GAMMA.(T),THETA,THETA.(T),DY,DY.(T)));
LET(TFT17=DERIV(TFT,DEPSN));
LET(TFT18=DERIV(TFT,DZETA));
LET(TFT19=DERIV(TFT10A,T));
LET(TFT20=DERIV(TFT11A,T));
LET(TFT21=DERIV(TFT12A,T));
LET(TFT22=DERIV(TFT13A,T));
LET(TFT23=DERIV(TFT14A,T));
LET(TFT25=DERIV(TFT16A,T));
ATOMIZE(TFT19;TFT20;TFT21;TFT22;TFT23;TFT25);
ATOMIZE(TFT;TFT1;TFT2;TFT3;TFT4;TFT5;TFT6;TFT7;TFT8;TFT9);
ATOMIZE(TFT10;TFT11;TFT12;TFT13;TFT14;TFT15;TFT16;TFT17;TFT18);
LET(T1A=(1/2)*JUA*(DTHTA-DDLTA)**2);
LET(T2A=(1/2)*MUA*(COEFF(VUASO,UDLTA)**2));
LET(TUA=T1A+T2A+(1/2)*MUA*(COEFF(VUASO,UUA)**2));
ATOMIZE(VUASO;VUASOA);
ATOMIZE(T1A;T2A);
LET(TUA1=DERIV(TUA,X));
LET(TUA2=DERIV(TUA,Y));
LET(TUA3=DERIV(TUA,THETA));
LET(TUA4=DERIV(TUA,GAMMA));
LET(TUA5=DERIV(TUA,BETA));
LET(TUA6=DERIV(TUA,DELTA));
LET(TUA7=DERIV(TUA,ALPHA));
```

```
      LET(TUA8=DERIV(TUA,EPSN));
      LET(TUA9=DERIV(TUA,ZETA));
      LET(TUA10=DERIV(TUA,DX));
   LET(TUA10A=REPLACE(TUA10,THETA,THETA.(T),DELTA,DELTA.(T)));
      ATOMIZE(TUA10);
   LET(TUA10A=REPLACE(TUA10A,DTHTA,DTHTA.(T),DDLTA,DDLTA.(T)));
   LET(TUA10A=REPLACE(TUA10A,DX,DX.(T),DTHTA,DTHTA.(T)));
      LET(TUA11=DERIV(TUA,DY));
   LET(TUA11A=REPLACE(TUA11,THETA,THETA.(T),DELTA,DELTA.(T)));
      ATOMIZE(TUA11);
   LET(TUA11A=REPLACE(TUA11A,DTHTA,DTHTA.(T),DDLTA,DDLTA.(T),DY,DY.(T)));
      LET(TUA12=DERIV(TUA,DTHTA));
   LET(TUA12A=REPLACE(TUA12,DDLTA,DDLTA.(T),DTHTA,DTHTA.(T),DX,DX.(T)));
      ATOMIZE(TUA12);
   LET(TUA12A=REPLACE(TUA12A,DELTA,DELTA.(T),THETA,THETA.(T),DY,DY.(T)));
      LET(TUA13=DERIV(TUA,DGAMA));
      LET(TUA14=DERIV(TUA,DBETA));
      LET(TUA15=DERIV(TUA,DDLTA));
   LET(TUA15A=REPLACE(TUA15,DDLTA,DDLTA.(T),DTHTA,DTHTA.(T),DX,DX.(T)));
      ATOMIZE(TUA15);
   LET(TUA15A=REPLACE(TUA15A,DELTA,DELTA.(T),THETA,THETA.(T),DY,DY.(T)));
      LET(TUA16=DERIV(TUA,DALFA));
      LET(TUA17=DERIV(TUA,DEPSN));
      LET(TUA18=DERIV(TUA,DZETA));
      LET(TUA19=DERIV(TUA10A,T));
      LET(TUA20=DERIV(TUA11A,T));
      LET(TUA21=DERIV(TUA12A,T));
      LET(TUA24=DERIV(TUA15A,T));
      ATOMIZE(TUA19;TUA20;TUA21;TUA24);
   ATOMIZE(TUA;TUA1;TUA2;TUA3;TUA4;TUA5;TUA6;TUA7;TUA8;TUA9);
   ATOMIZE(TUA10;TUA11;TUA12;TUA13;TUA14;TUA15;TUA16;TUA17;TUA18);
      LET(T5A=(1/2)*JFA*(DTHTA-DDLTA-DEPSN)**2);
      LET(T6A=(1/2)*MFA*(COEFF(VFASO,UEPSN)**2));
      LET(TFA=T5A+T6A+(1/2)*MFA*(COEFF(VFASO,UFA)**2));
      ATOMIZE(VFASO;VFASOA;VESO);
   ATOMIZE(T5A;T6A);
      LET(TFA1=DERIV(TFA,X));
      LET(TFA2=DERIV(TFA,Y));
      LET(TFA3=DERIV(TFA,THETA));
      LET(TFA4=DERIV(TFA,GAMMA));
      LET(TFA5=DERIV(TFA,BETA));
      LET(TFA6=DERIV(TFA,DELTA));
      LET(TFA7=DERIV(TFA,ALPHA));
      LET(TFA8=DERIV(TFA,EPSN));
      LET(TFA9=DERIV(TFA,ZETA));
      LET(TFA10=DERIV(TFA,DX));
   LET(TFA10A=REPLACE(TFA10,THETA,THETA.(T),DELTA,DELTA.(T)));
      ATOMIZE(TFA10);
   LET(TFA10A=REPLACE(TFA10A,EPSN,EPSN.(T),DDLTA,DDLTA.(T),DX,DX.(T)));
   LET(TFA10A=REPLACE(TFA10A,DEPSN,DEPSN.(T),DTHTA,DTHTA.(T)));
      LET(TFA11=DERIV(TFA,DY));
   LET(TFA11A=REPLACE(TFA11,THETA,THETA.(T),DELTA,DELTA.(T)));
      ATOMIZE(TFA11);
   LET(TFA11A=REPLACE(TFA11A,EPSN,EPSN.(T),DDLTA,DDLTA.(T),DY,DY.(T)));
   LET(TFA11A=REPLACE(TFA11A,DEPSN,DEPSN.(T),DTHTA,DTHTA.(T)));
      LET(TFA12=DERIV(TFA,DTHTA));
   LET(TFA12A=REPLACE(TFA12,DEPSN,DEPSN.(T),DDLTA,DDLTA.(T)));
      ATOMIZE(TFA12);
   LET(TFA12A=REPLACE(TFA12A,DTHTA,DTHTA.(T),DELTA,DELTA.(T),DX,DX.(T)));
   LET(TFA12A=REPLACE(TFA12A,EPSN,EPSN.(T),THETA,THETA.(T),DY,DY.(T)));
```

```
        LET(TFA13=DERIV(TFA,DGAMA));
        LET(TFA14=DERIV(TFA,DBETA));
        LET(TFA15=DERIV(TFA,DDLTA));
  LET(TFA15A=REPLACE(TFA15,DEPSN,DEPSN.(T),DDLTA,DDLTA.(T)));
        ATOMIZE(TFA15);
  LET(TFA15A=REPLACE(TFA15A,DTHTA,DTHTA.(T),EPSN,EPSN.(T),DX,DX.(T)));
  LET(TFA15A=REPLACE(TFA15A,DEPSN,DEPSN.(T),DELTA,DELTA.(T)));
  LET(TFA15A=REPLACE(TFA15A,THETA,THETA.(T),DY,DY.(T)));
        LET(TFA16=DERIV(TFA,DALFA));
        LET(TFA17=DERIV(TFA,DEPSN));
  LET(TFA17A=REPLACE(TFA17,DEPSN,DEPSN.(T),DDLTA,DDLTA.(T)));
        ATOMIZE(TFA17);
  LET(TFA17A=REPLACE(TFA17A,DTHTA,DTHTA.(T),EPSN,EPSN.(T),DX,DX.(T)));
  LET(TFA17A=REPLACE(TFA17A,DELTA,DELTA.(T),THETA,THETA.(T),DY,DY.(T)));
        LET(TFA18=DERIV(TFA,DZETA));
        LET(TFA19=DERIV(TFA10A,T));
        LET(TFA20=DERIV(TFA11A,T));
        LET(TFA21=DERIV(TFA12A,T));
        LET(TFA24=DERIV(TFA15A,T));
        LET(TFA26=DERIV(TFA17A,T));
        ATOMIZE(TFA19;TFA20;TFA21;TFA24;TFA26);
  ATOMIZE(TFA;TFA1;TFA2;TFA3;TFA4;TFA5;TFA6;TFA7;TFA8;TFA9);
  ATOMIZE(TFA10;TFA11;TFA12;TFA13;TFA14;TFA15;TFA16;TFA17;TFA18);
        LET(T1D=(1/2)*JHD*(DTHTA+DZETA)**2);
        LET(T2D=(1/2)*MHD*(COEFF(VHDSO,UHD)**2));
        LET(THD=T1D+T2D+(1/2)*MHD*(COEFF(VHDSO,UZETA)**2));
        ATOMIZE(VHDSO;VHDSOA);
  ATOMIZE(T1D;T2D);
        LET(THD1=DERIV(THD,X));
        LET(THD2=DERIV(THD,Y));
        LET(THD3=DERIV(THD,THETA));
        LET(THD4=DERIV(THD,GAMMA));
        LET(THD5=DERIV(THD,BETA));
        LET(THD6=DERIV(THD,DELTA));
        LET(THD7=DERIV(THD,ALPHA));
        LET(THD8=DERIV(THD,FPSN));
        LET(THD9=DERIV(THD,ZETA));
        LET(THD10=DERIV(THD,DX));
  LET(THD10A=REPLACE(THD10,THETA,THETA.(T),ZETA,ZETA.(T)));
        ATOMIZE(THD10);
  LET(THD10A=REPLACE(THD10A,DZETA,DZETA.(T),DTHTA,DTHTA.(T),DX,DX.(T)));
        LET(THD11=DERIV(THD,DY));
  LET(THD11A=REPLACE(THD11,THETA,THETA.(T),ZETA,ZETA.(T)));
        ATOMIZE(THD11);
  LET(THD11A=REPLACE(THD11A,DZETA,DZETA.(T),DTHTA,DTHTA.(T),DY,DY.(T)));
        LET(THD12=DERIV(THD,DTHTA));
  LET(THD12A=REPLACE(THD12,DZETA,DZETA.(T),DTHTA,DTHTA.(T),DX,DX.(T)));
        ATOMIZE(THD12);
  LET(THD12A=REPLACE(THD12A,ZETA,ZETA.(T),THETA,THETA.(T),DY,DY.(T)));
        LET(THD13=DERIV(THD,DGAMA));
        LET(THD14=DERIV(THD,DBETA));
        LET(THD15=DERIV(THD,DDLTA));
        LET(THD16=DERIV(THD,DALFA));
        LET(THD17=DERIV(THD,DEPSN));
        LET(THD18=DERIV(THD,DZETA));
  LET(THD18A=REPLACE(THD18,DZETA,DZETA.(T),DTHTA,DTHTA.(T),DX,DX.(T)));
        ATOMIZE(THD18);
  LET(THD18A=REPLACE(THD18A,ZETA,ZETA.(T),THETA,THETA.(T),DY,DY.(T)));
        LET(THD19=DERIV(THD10A,T));
        LET(THD20=DERIV(THD11A,T));
```

```
      LET(THD21=DERIV(THD12A,T));
      LET(THD27=DERIV(THD18A,T));
    ATOMIZE(THD19;THD20;THD21;THD22);
  ATOMIZE(THD;THD1;THD2;THD3;THD4;THD5;THD6;THD7;THD8;THD9);
  ATOMIZE(THD10;THD11;THD12;THD13;THD14;THD15;THD16;THD17;THD18);
  OPTSET(NOPRINT);
  OPTSET(EXPND);
  END DERIP;
```

APPENDIX III

Calculation of the dielectric constant

of a suspension of symmetric ellipsoids

in a simple shear flow.

APPENDIX III

Calculation of the dielectric constant of a suspension of symmetric ellipsoids in a simple shear flow.

Flow Analysis

In sheared suspensions at steady state in couette flows the motion of ellipsoids has been mathematically described by Jeffreys[5] and experimentally verified by Mason.[6,7,8] These descriptions give the motion in terms of the angles ϕ and λ shown in Figure 1. If steady state is assumed, then in rotational diffusion the probability density functions for distribution in the angles ϕ and λ are inversely proportional to the angular velocity w of the particles. Hence

$$p(\phi) \;=\; \frac{const}{w\phi}$$

$$p(\lambda) \;=\; \frac{const}{w\lambda}$$

Now given that the particle is orientated somewhere in the field

$$\int_o^\pi \int_o^{2\pi} p(\phi)p(\lambda)d\phi d\lambda \;=\; 1; \qquad (A1)$$

the conductivity in a given direction may be then found as

$$\overline{K}_\alpha = \int\limits_0^\pi \int\limits_0^{2\pi} p(\phi)p(\lambda)K_{\alpha\alpha}^{1}(\phi,\lambda)\,d\phi d\lambda. \quad \text{(no sum)} \quad \text{(A2)}$$

If the particles are randomly distributed then $p(\phi) = \frac{1}{2\pi}$ and $p(\lambda) = \frac{1}{\pi}$. From geometry the angle θ_3 can be written in terms of ϕ and λ since

$$\cos^2\theta_3 = \frac{\tan^2\lambda}{\tan^2\phi}. \qquad \text{(A3)}$$

Then

$$\overline{K}_r = \int\limits_0^\pi \int\limits_0^{2\pi} \left[K_b + (K_a - K_b)\cos^2\theta_3 \right] \frac{1}{2\pi}\frac{1}{\pi}\,d\phi d\lambda \qquad \text{(A4)}$$

$$\overline{K}_r = \frac{K_a + K_b}{2} \qquad \text{(A5)}$$

Given the random uniform dispersion of ellipsoids the dielectric constant measured will be assumed to be $\overline{K}_r$ given by this equation. It should be noted that the dielectric constant of a suspension of axially symmetric ellipsoids which are uniformly dispersed at random orientations is the average of the dielectric constant when aligned. This is independent of whether they are oblate or prolate ellipsoids. This average quantity which is easily measured can be used for determining the shape of particles and for estimating K_a and K_b and hence the relative dimensions of particles.

In a shear flow the particles are not randomly distributed in orientation and do not rotate at a constant angular velocity. The calculation of the dielectric constants then requires a knowledge of the distribution probabilities $p(\phi)$ and $p(\theta)$. These probabilities can be calculated from Jeffreys analysis by using the relation between the angles or orientation and the orbits constant C, for a particle.

$$\tan \theta_2 = \frac{C\, r_e}{(r_e^2 \cos^2\phi + \sin^2\phi)^{1/2}} \tag{A6}$$

Where r_e is the axis ratio of the ellipsoid of revolution. The constant (C) of the orbit is determined by the angle at which the axis of the ellipsoid is orientated to the plane of shear and its distribution in a random dispersion would be uniform. In a shear situation there is no theoretical reason, in the limit of Stokes flow, that this will change.

The conductivity for a fixed orbit constant C may then be calculated as follows:

If the effect of Brownian motion on the particle distribution is neglected, then in the steady state

$$p(\phi) = \frac{const}{w\phi}$$

$$p(\theta_2) = \frac{const}{w_{\phi2}}$$

The angular velocity of particles in Couette shear flow (derived theoretically by Jeffreys using Stokes flow approximations) may be expressed for the shear flow shown in Figure 1 as:

$$w_{\theta_2} = \frac{G}{4} \frac{re^2 - 1}{re^2 + 1} \sin 2\theta_2 \sin 2\phi \qquad \text{(A7a)}$$

$$w_{\phi} = \frac{G}{re^2 + 1} \left[re^2 \cos^2 \phi + \sin^2 \phi \right] \qquad \text{(A7b)}$$

for a symmetrical ellipsoid. Using the condition from Equation (A1) together with Equation (A7b) gives

$$p(\phi) = \frac{r_e}{2\pi(r_e^2 \cos^2\phi + \sin^2\phi)} \qquad \text{(A8)}$$

Let us first consider the dielectric constant in the X_2^1 direction (parallel to shear planes, perpendicular to the flow).

From Equation (8b)

$$K_{22}^1 = K_b + (K_a - K_b) \cos^2 \theta_2$$

this can be expressed as a function of the angle ϕ by using Equation (A6) expressed in the form:

$$\cos \theta_2 = \left(1 - \frac{\dfrac{c^2 \, re^2}{re^2 - 1}}{\dfrac{re^2 (1 + c^2)}{re^2 - 1} - \sin^2 \phi} \right)^{1/2} \qquad \text{(A9)}$$

Then for a fixed C the dielectric constant $K_{11}{}^1$ can be expressed as

$$\left. K_{22}{}^1 \right)_C = \int_0^{2\pi} p(\phi) \, K_{22}{}^1 \, d\phi$$

Integrating using $p(\phi)$ from Equation (38) gives:

$$\left. K_{22}{}^1 \right)_C = K_b + (K_a - K_b) \left(\frac{1}{(1 + C^2)[1 + (Cre)^2]} \right)^{1/2}$$

$$= K_b + (K_a - K_b) \, F_2. \tag{A10}$$

The dielectric constant for a suspension with the orbits (C) distributed with a probability distribution $p(C)$ can be found as

$$\overline{K_{22}{}^1} = \int_0^\infty p(C) \left. K_{22}{}^1 \right)_C dC$$

$$= K_b + (K_a - K_b) \, \overline{F_2} \tag{A11}$$

where

$$\overline{F_2} \equiv \int_0^\infty p(C) \, F_2 \, dC$$

Similarly the dielectric constant in the X_3^1 direction can be found using the relations that

$$\tan \phi = re \tan \frac{2\pi t}{T} \qquad (A12)$$

and

$$\tan \lambda = Cre \sin \frac{2\pi t}{T} \qquad (A13)$$

Note: T is the period of revolution of a particle.

By solving for $\tan^2 \lambda$ in terms of $\tan^2 \phi$

$\tan^2 \lambda$ may be shown to be equal to

$$\tan^2\lambda = \frac{(Cre)^2 \tan^2 \phi}{(Cre)^2 + \tan^2 \phi} . \qquad (A14)$$

Now from geometry

$$\cos^2 \theta_3 = \frac{\tan^2 \lambda}{\tan^2 \phi} = \frac{c^2 re^2}{(Cre)^2 + \tan^2 \phi} , \qquad (A15)$$

then

$$K_{33}^{\ 1} = K_b + (K_a - K_b) \cos^2 \theta_3$$

$$= K_b + (K_a - K_b) \frac{(c^2 re)^2}{(Cre)^2 + \tan^2 \phi} \qquad (A16)$$

$$K_{33}^{\ 1}\Bigg)_C = K_b + (K_a - K_b) \int_0^{2\pi} p(\phi) \frac{c^2 re^2}{(Cre)^2 + \tan^2 \phi} d\phi \qquad (A17)$$

$$= K_b + (K_a - K_b) \frac{C}{1 + C} \quad \text{and} \qquad (A18)$$

$$\overline{K_{33}^{\ 1}} = K_b + (K_a - K_b) \int_0^{\infty} p(C) \frac{C}{1 + C} dC \equiv K_b + (K_a - K_b)\overline{F_3} \qquad (A19)$$

The dielectric constant in the X_1^1 direction is found using the relations

$$K_{11}^1 = K_b + (K_a - K_b) \cos^2 \theta_1 .$$

From geometry

$$\cos \theta_1 = \cos \theta_2 \tan \lambda$$

Then using Equation (A9) for θ_2 and Equation (A14) for $\tan \lambda$

$$K_{11}^1\bigg)_C = K_b + (K_a - K_b) \int_0^{2\pi} \frac{[(re^2-1)\cos^2\phi+1][(Cre)^2\sin^2\phi]p(\phi)d\phi}{[(Cre)^2+(re^2-1)\cos^2\phi+1][(Cre)^2-1)\cos^2\phi+1]}$$

$$(A20)$$

Integrating with $p(\phi)$ from Equation (38) gives:

$$K_{11}^1\bigg)_C = K_b + (K_a - K_b) \frac{2(Cre)^2 r_e}{[2(Cre)^2+r_e^2+1]} \frac{3}{[(Cre)^2+1][H-D]} \left[\frac{H+1}{(1-H^2)^{1/2}} \right.$$

$$\left. - \frac{D+1}{(1-D^2)^{1/2}} \right] \qquad (A21)$$

$$K_{11}^1\bigg)_C = K_b + (K_a - K_b) F_1$$

where

$$D \equiv \frac{(Cre)^2 - 1}{(Cre)^2 + 1} , \qquad H \equiv \frac{re^2 - 1}{2(Cre)^2 + re^2 + 1}$$

then

$$\overline{K_{11}{}^1} = \int_0^\infty p(C) \left. K_{11}{}^1 \right)_C dC .$$

Since K_a and K_b are independent of C and $\int_0^\infty p(C) = 1$ this may be written as

$$\overline{K_{11}{}^1} = K_b + (K_a - K_b) \overline{F_1}$$

where

$$\overline{F_1} \equiv \int_0^\infty p(C) F_1 dC . \qquad (A21a)$$

The evaluation of the distribution p(C) of the orbit constant for a suspension is next required to determine the dielectric constant. The parameter C may range from 0 to ∞. C = 0 corresponds to the symmetric axis of the ellipsoid being perpendicular to the shear planes and C = ∞ corresponds to the symmetry axis of the ellipsoid rotating in the plane of the flow which corresponds to the ellipsoid having the angle $\theta_2 = 90°$.

No theoretical prediction of the distribution of C with flow rate have been made. Two hypotheses have been proposed, however.

1. Jeffreys assumed that the ellipsoids would eventually rotate in such a way as to minimize the energy disipation. This theory predicts that

   $$p(C) = 1 \text{ for } C = 0$$
   $$p(C) = 0 \text{ for } C > 0$$

All the ellipsoids would be alligned with their symmetrical axes perpendicular to the shear planes if a/b < 1 or parallel to the shear planes if a/b > 1. The conductivity with time across shear planes would approach K_a with $\frac{a}{b} < 1$ or K_b with $\frac{a}{b} > 1$ using this assumption.

2. Eisenshitz[9] assumed that P (C) remained the same whether at rest or in motion, so that every orbital constant C was equally probably.

The first assumption gives the results shown in Figure 3 curve (A). Since it has been demonstrated that Jeffrey's hypotheses is not correct, we will assume a uniform distribution of the orbital constant (the Eisenschitz assumption). In this case the probability that a particle axis is between C = 0 and C is

$$P(C) = \frac{2}{\pi} \int_0^{\pi/2} [1 - \cos \theta_2 (\phi)] \, d\phi \qquad (A22)$$

Substituting Equation (A7) into Equation (A22) gives

$$P(C) = 1 - \frac{2}{\pi} \int_0^{\frac{\pi}{2}} \left(\frac{1 - \frac{re^2 - 1}{re^2} \sin^2 \phi}{1 + C^2 - \frac{re^2 - 1}{re^2} \sin^2 \phi} \right)^{1/2} d\phi \ . \qquad (A23)$$

Since the probability density distribution $p(C) \equiv \frac{dP(C)}{dC}$ is needed, differentiation gives

$$P(C) = \frac{2}{\pi} \frac{C}{(1 + C^2)^{3/2}} \int_0^{\frac{\pi}{2}} \frac{\left(1 - \frac{re^2 - 1}{re^2} \sin^2 \phi\right)^{1/2}}{\left(1 - \frac{re^2 - 1}{re^2(1 + C^2)} \sin^2 \phi\right)^{3/2}} d\phi.$$

(A24)

This equation is of the form of an elliptic integral if the coefficients of the $\sin^2 \phi$ terms range between 0 and 1. For re < 1 this is not true and a change in form must therefore be made. First the numerator is expanded as:

$$P(C) = \frac{2}{\pi} \frac{C}{(1 + C^2)^{3/2}} \int_0^{\frac{\pi}{2}} \frac{\left(1 - \sin^2 \phi + \frac{\sin^2 \phi}{re^2}\right)^{1/2}}{\left(1 - \frac{re^2 - 1}{re^2(1 + C^2)} \sin^2 \phi\right)^{3/2}} d\phi$$

Changing the variable by letting $\phi = \frac{\pi}{2} - \psi$ gives:

$$P(C) = \frac{2}{\pi} \frac{C \, re^2}{[(Cre)^2 + 1]^{3/2}} \int_0^{\frac{\pi}{2}} \frac{[1 - (1 - re^2) \sin^2 \psi]^{1/2}}{\left(1 - \frac{1 - re^2}{1 + (Cre)^2} \sin^2 \psi\right)^{3/2}} d\psi$$

(A25)

This is a complete elliptic integral of the second kind.

$$P(C) = \frac{2}{\pi} \frac{Cre^2}{[(Cre)^2 + 1]^{3/2}} \left[\frac{1}{\left(1 - \frac{1 - re^2}{1 + (Cre)^2}\right)^{1/2}} E\left[\left[\frac{\pi}{2}, C\left(\frac{1 - re^2}{1 + C^2}\right)^{1/2}\right]\right]\right]$$

$$= \frac{2}{\pi} \frac{2\,Cre}{[(Cre)^2 + 1](1 + C^2)^{1/2}} \left[E\left[\frac{\pi}{2}, C\left(\frac{1 - re^2}{1 + C^2}\right)^{1/2}\right]\right] \tag{A26}$$

The other case of interest, i.e., re > 1 are found directly from Equation (A26) as:

$$P(C) = \frac{2}{\pi} \frac{Cre}{(1 + C^2)[(Cre)^2 + 1]^{1/2}} E\left[\frac{\pi}{2}, \left[\frac{C^2(re^2 - 1)}{(Cre)^2 + 1}\right]^{1/2}\right] \tag{A27}$$

There are two cases where these integrals can be expressed as simple closed solutions.

1. The first is the case where re = 1. This corresponds to a sphere (Hydrodynamically). For this case

$$P(C) = \frac{C}{(1 + C^2)^{3/2}} \tag{A28}$$

2. For the second case re = ∞ (an infinitely long rod).

$$P(C) = \frac{2}{\pi(1 + C^2)} \tag{A29}$$

The factors F_i are then calculated using the probability distributions with Equations (A11), (A19) and (A21a). The results are shown plotted in Figure 3.

References

1. Campbell, W. F. and G. Westheimer, "Dynamics of Accommodation Responses of the Human Eye", J. Physiology, Vol. 151, p. 285, (1960).

2. Young, L. R. and Stark, L., "Variable Feedback Experiments Testing a Sampled Data Model for Eye Tracking", IEEE Transactions, Prof. Tech. Group on Human Factors in Electronics, HFE-4:39, 1963.

3. Edgerton, R. H., "Conductivity of Sheared Suspensions of Ellipsoidal Particles with Application to Blood Flow", (in preparation).

4. Fricke, H., "The Electric Conductivity and Capacity of Disperse Systems", Physics, Vol. 1, p. 106, 1931.

5. Jeffrey, G. B.: Proc. Roy. Soc. (London), H 102, 161, 1932.

6. Anczurowski, E. and Mason, S. G., J. Colloid and Interface Science, Vol. 23, p. 522, 1967.

7. Mason, S. G. and Manley, R. St. J., Proc. Roy Soc. (London) A 238, 117, 1956.

8. Anczurowski, E. and Mason, S. G., J. Colloid and Interface Science, 23, 535, 1967.

9. Eisenschitz, R., Z. Physik Chem. (Leipzig) a 158, 85, 1932.

APPENDIX IV

TERMINAL REPORT

Research Sponsored by the
National Science Foundation
Under Grant No. GK-3490

TERMINAL REPORT

Determination of the Error Cost Functional
Used by Human Operators While Controlling
Certain Compensatory Systems

Research Sponsored by the

National Science Foundation

Under Grant No.
GK-3490

September 30, 1969

Oakland University

Rochester, Michigan 48063

Glenn A. Jackson, Principal Investigator

TABLE OF CONTENTS

I. SUMMARY

The purpose of this research was to determine the error cost func-
tional used by human operators while controlling low order compensatory
control systems. The systems investigated were limited to those cases
where the model of the forward loop of the control system -- including
human operator and controlled element -- was satisfactorily represented
by the McRuer crossover model. This forward loop model consists entirely
of a gain K, a time-delay τ, and a single integration. This simple model
is applicable for a fairly wide range of low-order controlled elements.

It was shown that when the crossover model is applicable, the two
model parameters, K and τ, are effectively adjusted to minimize the cost
functional

$$ J = \overline{e^2(t)} + \overline{\alpha c^2(t)} $$

with the constraint

$$ \tau = \beta K, \quad 0.01 \le \beta \le 0.12 \text{ seconds}^2. $$

$\overline{e^2}$ is the mean squared control system error and $\overline{c^2}$ is the mean squared
value of control effort. β is inversely proportional to a subject's
closed loop bandwidth, and thus varies between subjects, and even within
the same subject at various stages of training. For a given control
system, α is a constant that doesn't change either between subjects or

with subject practice. However, α does change with the type of system being controlled and becomes smaller as the control task becomes more difficult.

The conclusion is drawn that all subjects optimize the same cost functional when given the same control task. They perform differently, however, due to their varying abilities in processing high frequency signals. The subjects penalize control effort to a greater extent on easier tasks, than on harder tasks.

II. FINAL REPORT

A. Introduction

Since the start of World War II interest in manual control systems

has been rapidly increasing [1]. A considerable amount of the research

done in this area has been aimed at determining the characteristics of

the human operator while he is functioning as the controller in a basic

compensatory control task [2]. In this type of task the operator is

placed into a control system described by the block diagram in Figure 1.

The signal N(t) is Gaussian white noise, and the input filter is low

pass with a cut-off frequency of 1 to 4 radians per second. The con-

trolled element, $Y_c(s)$, is of low order, usually second or less.

Through the efforts of many different researchers, and by such

diverse experimental techniques as random input describing functions

[3], parameter tracking [4,5], and orthogonal filtering [6], several

facts pertaining to the human operator have been verified. One of the

more important of these findings, and one which is directly related to

the research being reported, involves the human operator's describing

function. For low order controlled elements (second or less), the

human operator adjusts his mode of operation so that the entire forward

loop of the compensatory system has the form [7]

$$\frac{\theta_0}{e}(s) = \frac{K\varepsilon^{-\tau s}}{s} .$$

It appears that whenever the system characteristics are changed, the

human operator immediately changes his describing function so that the

forward-loop describing function retains the form given above. The
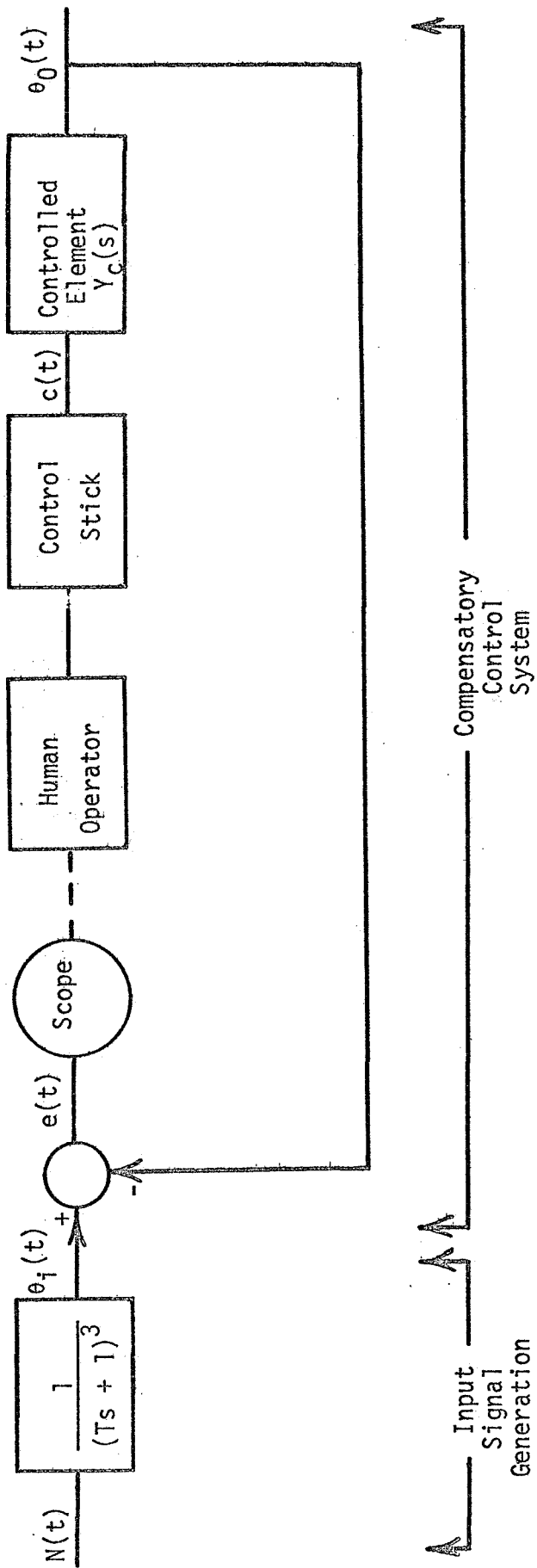
3.

Figure 1 Typical Compensatory Tracking Task

4.

magnitudes of K and τ depend upon $\theta_i(t)$, the controlled element, and the subject being tested.

This simple forward-loop model, called the "crossover model" by McRuer et. al. [7], fits the human operator describing function data extremely well over that portion of the frequency spectrum where input power is significant, and in the region where the absolute magnitude of the forward-loop describing function is unity. Since this latter region mainly determines closed-loop response, the closed-loop crossover model is a very realistic approximation to the compensatory system.

In 1967 Jackson [8] published the results of a parameter tracking study that indicated the compensatory control system of Figure 1 could be adequately modeled by the approximate crossover model of Figure 2. In this study the parameters K and τ were directly measured, and were found to change in definite patterns as a function of input badnwidth, subject practice, and order of the controlled element [9].

B. Purpose of the Present Research

In pre-test orientation, the subjects to be tested in a compensatory control task are simply told to "keep the error e(t) as small as possible at all times." The question investigated in this research was: Exactly what cost functional is the human trying to minimize when he "keeps the error as small as possible?" It is natural to assume that he is optimum in some sense, or at least trying to be. The present research is intended to determine this optimizing functional, and to determine how this functional can be used in both the mathematical description of the human operator's control actions, and in manual control system design.
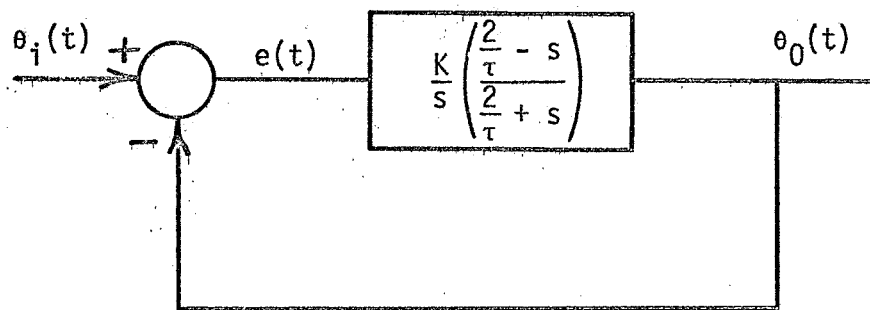
5.

Figure 2   Approximate Crossover Model of The Compensatory System

There appear to be few results in the literature that are directly related to this problem.

(1) McRuer, et. al. [6,10] have postulated that the human minimizes the mean squared error subject to stability constraints on the compensatory control system. However, the constraints are given verbally in very general terms so that no mathematical form for the minimizing functional and associated constraints is given.

(2) It has been shown [11] that for Gaussian input systems when the mean squared error is minimized several other error scores are also minimized, indicating that the determination of a unique minimizing functional is probably not possible.

(3) Systems Technology, Inc. (STI) recently published a summary of new techniques which they hope to use in determining the functional which shows why the form of the crossover model is used by the operator [12].

The present research is different from the STI approach in that it is assumed from the start that the approximate crossover model is a good compensatory system model. (In fact, the only cases analyzed were those in which the approximate crossover model had proven to be exceptionally good.) The optimal policy sought was that policy which explained: why particular subjects adjust the K and τ parameters to the values they do; why K and τ change with input bandwidth; why K and τ differ between subjects; and why K and τ change with practice.

The data used in this analysis are from previous tests outlined in detail in reference [8].

C. A Unique Property of K and τ.

In the parameter tracking tests reported in reference [8], the K and τ paramaters of the model of Figure 2 were directly measured. This was done for six subjects: three controlling a 5/s element and three controlling a $5/s^2$ element. In each case input filter time constants of 1, 1/2, and 1/4 seconds were all used, and K and τ values determined for each condition during each day of training.

One important property of these data, which was not discussed in the previous analysis, is that in the cases where the approximate cross-over model was exceptionally good*, K and τ are highly correlated. This correlation exists at a given test condition, between subjects and even for the same subject on different days during the training period.

In Tables 1 and 2 in the Appendix the daily average values of K and τ are given for each subject at each of the test conditions where the approximate crossover model was exceptionally good. These test conditions are

(1) $Y_c(s) = 5/s$, T = 1 second,

(2) $Y_c(s) = 5/s$, T = 1/2 second,

(3) $Y_c(s) = 5/s^2$, T = 1 second.

In Figure 3 the data points for these conditions are plotted along with the linear regression line for each condition. The correlation coefficients are also given in the figure.

---

*"Exceptionally good" is taken to be those cases where the power in the error between model output and compensatory system output is less than 10% of the power out of the compensatory system. The Power Match [8] is thus > 90%. This indicates that the model is accurate and that the human operator is fairly linear.

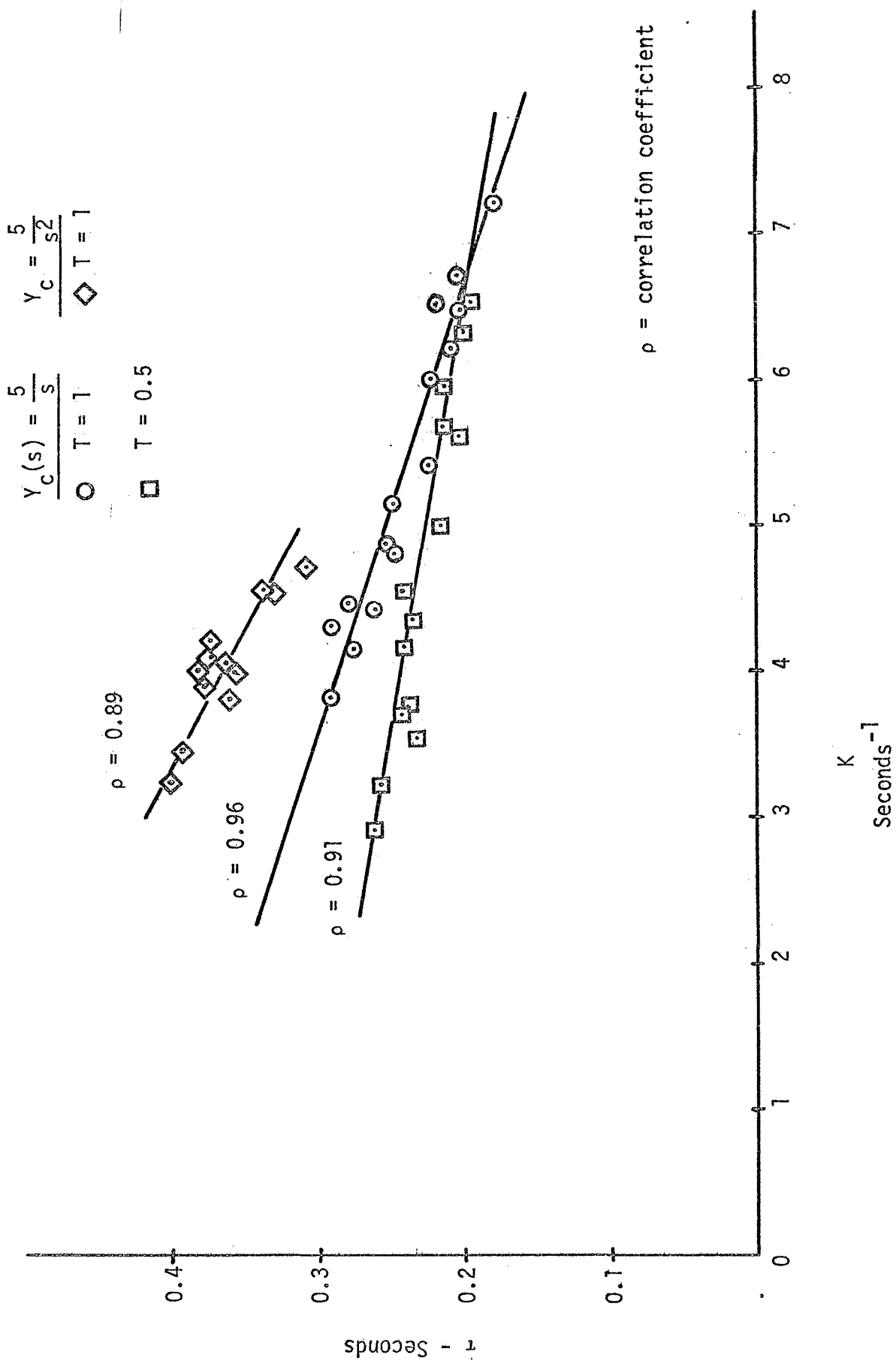Figure 3 Correlation of K and τ

9.

It is important to re-emphasize at this point that K and τ are linearly related, in spite of the fact that the data involves different subjects and various intervals in each subject's training period.

In the remainder of this report it will be shown that the correlation existing between K and τ can be attributed to an apparent parameter optimization of the approximate crossover model. It will be shown that when K and τ of the model are adjusted to minimize a realistic performance index at a given test condition, the optimum values of K and τ fall on essentially the same linear regression lines as found in Figure 3.

D. Development of an Optimal Policy

When the compensatory portion of Figure 1 is replaced by the approximate crossover model of Figure 2, the normalized mean squared control system error (NMSE) for the model is as shown in Figures 4 and 5 for input filter time constants of 1 and 1/2 seconds, respectively. Each set of curves has NMSE as a function of K with τ as a parameter. Superimposed on each of these sets of curves is the location of the associated K-τ regression line from Figure 3. From a casual study of Figures 4 and 5 it is not evident that the subjects have adjusted K and τ to optimize NMSE in any recognizable manner.

To account for the correlation existing in the experimental values of K and τ, three postulates are developed.

Rationale for Postulate 1: At any stage of training, each subject undoubtedly has the capability of operating the closed loop compensatory system at some maximum bandwidth. Further, the closed loop bandwidth can be approximated by the natural frequency of the compensatory system.
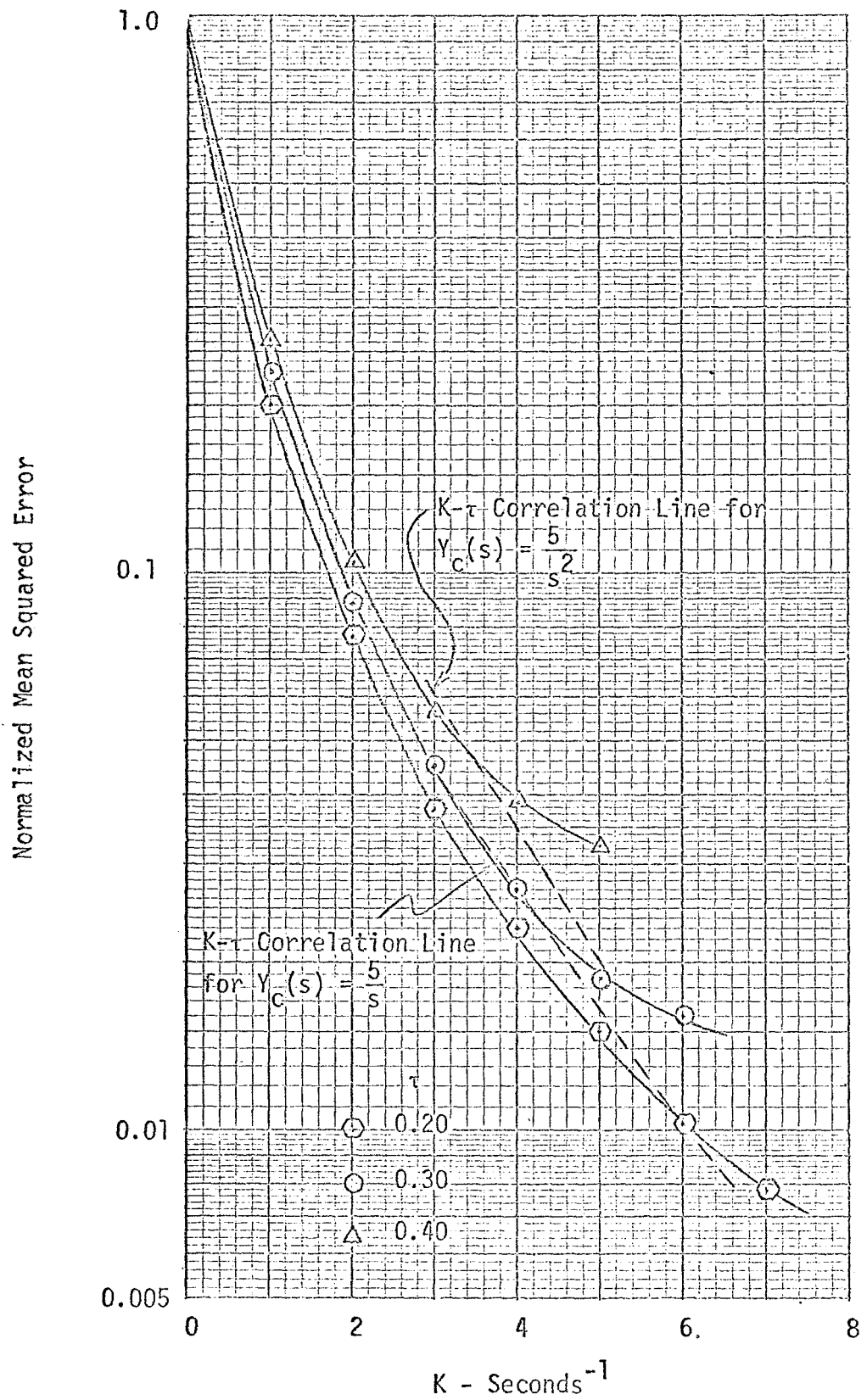
Figure 4   Normalized Mean Squared Error for the Approximate Crossover Model
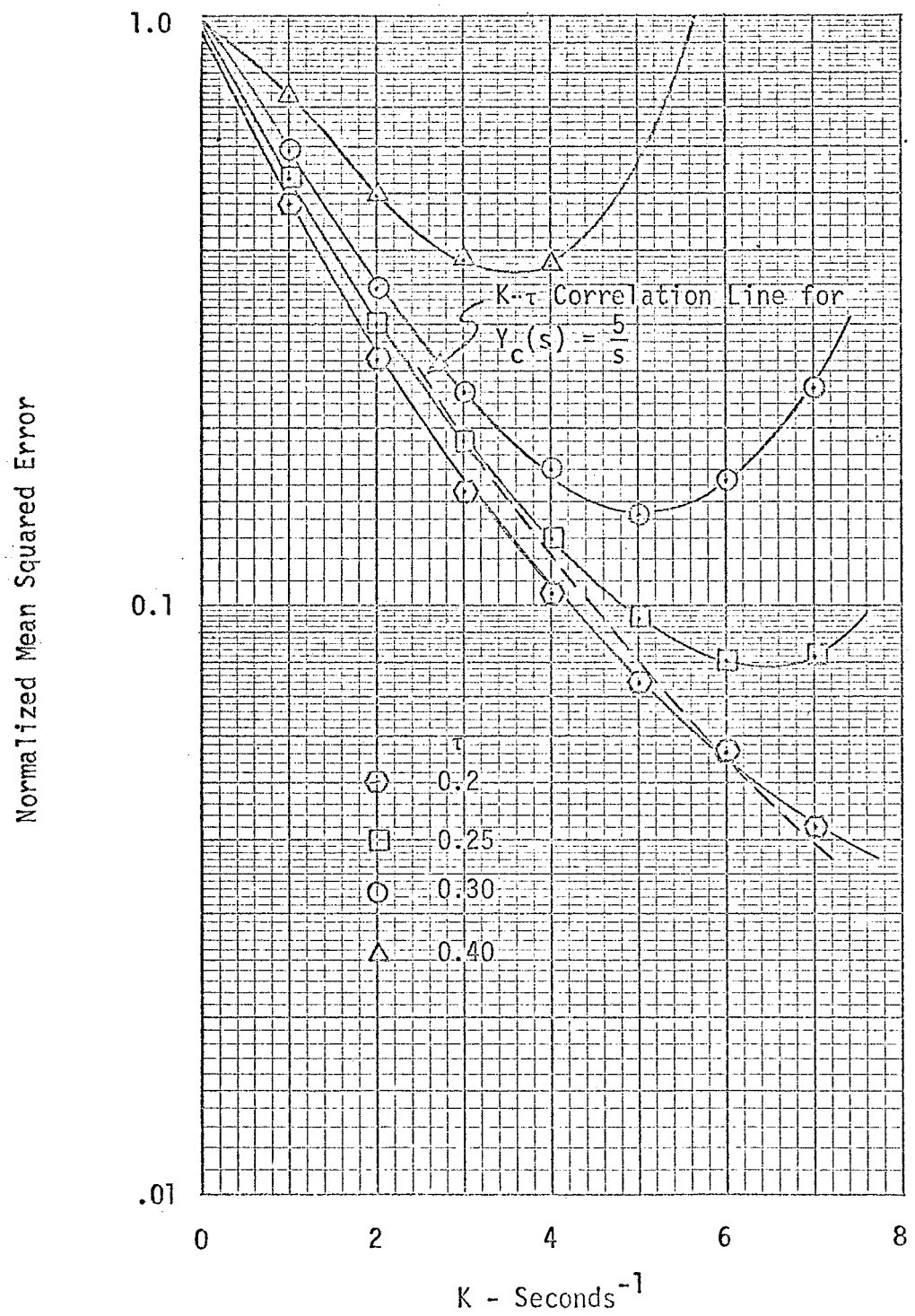with an Input Filter of $1/(s + 1)^3$.

Figure 5   Normalized Mean Squared Error for the Approximate Crossover Model
with an Input Filter of $1/(\tfrac{1}{2}s + 1)^3$.

This approximation is reasonable since the input power at frequencies above the natural frequency is extremely low [8]. In terms of the cross-over model the closed loop natural frequency, ω_n, is

$$\omega_n = \sqrt{\frac{2K}{\tau}} \quad .$$

If it is assumed that each subject runs the compensatory system at his maximum bandwidth, and that this maximum is fixed during a given interval of his training, then

$$\sqrt{\frac{2K}{\tau}} = \text{constant} = B = \text{Bandwidth in radians/second.}$$

$$\frac{2K}{\tau} = B^2$$

$$\tau = \frac{2}{B^2} K$$

or

$$\tau = \beta K \ . \tag{1}$$

Under the conditions assumed, Equation (1) can be considered as a constraint on any optimal adjustment of the parameters K and τ which might be taking place. It should be emphasized that "β" in Equation (1) will be different for different subjects, and different for the same subject during various intervals of his training period. Emperically, β can be determined to be in the range $0.01 \leq \beta \leq 0.12$ seconds^2.

Postulate 1: Any parameter optimization of the approximate crossover model (compensatory control system) is constrained by Equation (1): $\tau = \beta K$, $0.01 \leq \beta \leq 0.12$. β is fixed for a given subject, at a given point in training, on a given tracking task.

Rationale for Postulate 2:   A general performance index in optimal control theory, and one that seems intuitively reasonable for the human operator, involves the combination of control system error and control effort.   Using the notation of Figure 1, one form of this index is

$$J = E\left\{\lim_{t_f \to \infty} \frac{1}{t_f} \int_o^{t_f} \left[e^2(t) + \alpha c^2(t)\ dt\right]\right\}$$

or

$$J = \overline{e^2} + \alpha \overline{c^2} \tag{2}$$

where $E\ \{\cdot\}$ is the statistical average, $\overline{e^2}$ is the mean squared value of the tracking error, $e(t)$, and $\overline{c^2}$ is the mean squared value of the controlled variable, $c(t)$. α is a constant.

Postulate 2:   The performance index being minimized by the human operator is Equation (2): $J = \overline{e^2} + \alpha \overline{c^2}$.

Postulate 3:   The control strategy of the human operator while controlling one of the elements discussed in Section C is a two-step process consisting of:

(1)   Forcing the compensatory system into the form of the approximate crossover model.

(2)   Minimizing the performance index

$$J = \overline{e^2} + \alpha \overline{c^2}$$

via a parameter adjustment that is constrained by the relation

$$\tau = \beta K.$$

It should be noted that part (1) of Postulate 3 has already been proven, while part (2) has not.

14.

E. Analysis of the Postulated Strategy

To evaluate the optimal strategy postulated above, and to determine the value of α for each test condition, a digital computer program was developed to generate J for the approximate crossover model. This was done for the following conditions:

Condition 1: $Y_c(s) = 5/s$ and $T = 1$ second.

Condition 2: $Y_c(s) = 5/s$ and $T = 1/2$ second.

In these cases the transfer function relating $c(t)$ to $e(t)$ must be

$$\frac{c}{e}(s) = \frac{K(2/\tau - s)}{5(2/\tau + s)}$$

so that the entire forward loop remains as the approximate crossover model.

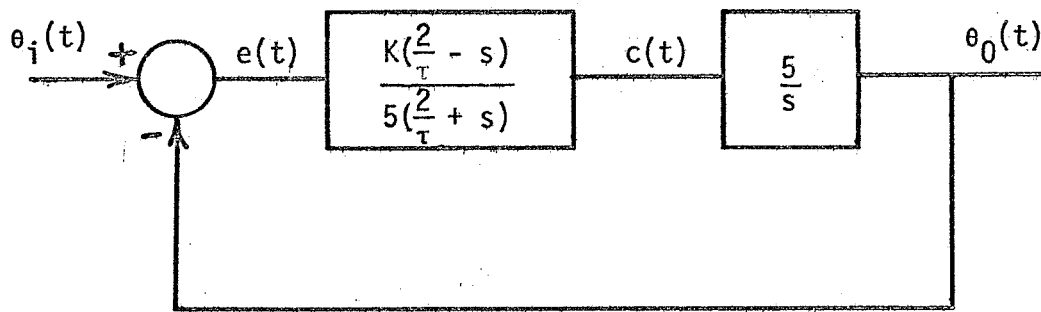Condition 3: $Y_c(s) = 5/s^2$ and $T = 1$ second.

Here,

$$\frac{c}{e}(s) = \frac{Ks(2/\tau - s)}{5(2/\tau + s)} .$$

so the approximate crossover model is retained. Figures 6a and 6b show the compensatory system models for the three conditions.

In terms of the block diagrams of Figure 6, the performance index can be reduced to the following integral forms.

$$J = \overline{e^2} + \alpha \overline{c^2}$$

$$= \frac{1}{2\pi j} \left\{ \int_{-j\infty}^{j\infty} \left| \frac{\theta_i}{N}(s) \right|^2 \left| \frac{e}{\theta_i}(s) \right|^2 \Phi_{NN}(s) \, ds \right.$$

$$\left. + \alpha \int_{-j\infty}^{j\infty} \left| \frac{\theta_i}{N}(s) \right|^2 \left| \frac{c}{\theta_i}(s) \right|^2 \Phi_{NN}(s) \, ds \right\} .$$

15.
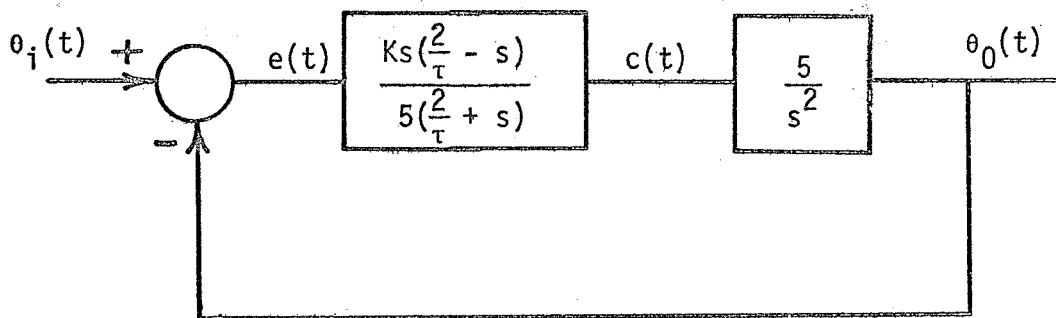
$$\text{(a)} \quad Y_c(s) = \frac{5}{s}$$

$$\text{(b)} \quad Y_c(s) = \frac{5}{s^2}$$

Figure 6 Compensatory System Models for Two Controlled Elements
Based on Approximate Crossover Model

$\Phi_{NN}(j\omega)$ is the power spectral density of the signal N(t). Assuming $\Phi_{NN}(j\omega) = 1$,

$$J = \frac{1}{2\pi j}\left\{\int_{-j\infty}^{j\infty}\left|\frac{1}{(Ts+1)^3}\right|^2 \cdot \left|\frac{s(2/\tau+s)}{s^2+(2/\tau-K)s+2K/\tau}\right|^2 ds\right.$$

$$\left. + \alpha \cdot \int_{-j\infty}^{j\infty}\left|\frac{1}{(Ts+1)^3}\right|^2 \cdot \left|\frac{Ks/5(2/\tau-s)}{s^2+(2/\tau-K)s+2K/\tau}\right|^2 ds\right\} \qquad (3)$$

when $Y_c(s) = 5/s$ (Conditions 1 and 2), and

$$J = \frac{1}{2\pi j}\left\{\int_{-j\infty}^{j\infty}\left|\frac{1}{(Ts+1)^3}\right|^2 \cdot \left|\frac{s(2/\tau+s)}{s^2+(2/\tau-K)s+2K/\tau}\right|^2 ds\right.$$

$$\left. + \alpha \cdot \int_{-j\infty}^{j\infty}\left|\frac{1}{(Ts+1)^3}\right|^2 \cdot \left|\frac{Ks^2/5(2/\tau-s)}{s^2+(2/\tau-K)s+2K/\tau}\right|^2 ds\right\} \qquad (4)$$

when $Y_c(s) = 5/s^2$ (Condition 3). These equations were also normalized by dividing by $\overline{e^2}$ at K = 0. The normalization factor happens to be 3/16T in all cases, under the assumption that N(t) is a white noise source with unity power level. The solution of these equations was accomplished by use of tabulated solutions of Parseval's Theorem [13], under the constraint, $\tau = \beta K$.

A programmed search of the solutions to Equations (3) and (4) was made in the following manner. With α, β and T fixed, $\min_{K,\tau} J$ was determined. This was done for various values of α, β and T in order to find that value of α which, for a given $Y_c(s)$ and T, would yield K and τ values equivalent to those present on the subject regression lines in Figure 3. If the postulated strategy is correct, and if all subjects are minimizing the same functional at a given test condition, then the optimum values of K

17.

and τ should fall on the regression lines of Figure 3, regardless of the value to which β is fixed. This was indeed shown to be the case.

The results of the computer analysis may be summarized as follows:

For Condition 1: $Y_c(s) = 5/s$ and $T = 1$ second, $\alpha = 2.5$.

The $\min_{K,\tau} J$ with $J = \overline{e^2} + 2.5\overline{c^2}$ and $\tau = \beta K$, where β is any fixed value $0.01 \le \beta \le 0.08$, occurs at values of K and τ which fall essentially on the subject's $Y_c(s) = 5/s$, $T = 1$ regression line of Figure 3.

For Condition 2: $Y_c(s) = 5/s$ and $T = 1/2$ second, $\alpha = 0.25$.

The $\min_{K,\tau} J$ with $J = \overline{e^2} + 0.25\overline{c^2}$ and $\tau = \beta K$, where β is any fixed value $0.01 \le \beta \le 0.08$, occurs at values of K and τ which fall essentially on the subject's $Y_c(s) = 5/s$, $T = 1/2$ regression line of Figure 3.

For Condition 3: $Y_c(s) = 5/s^2$ and $T = 1$ second, $\alpha = 0$.

The $\min_{K,\tau} J$ with $J = \overline{e^2}$ and $\tau = \beta K$, where β is any fixed value $0.07 \le \beta \le 0.12$, occurs at values of K and τ which fall essentially on the subject's $Y_c(s) = 5/s^2$, $T = 1$ regression line of Figure 3.

The optimum values of K and τ for several values of β are given in Figures 7, 8 and 9 for Conditions 1, 2 and 3, respectively. These figures indicate the strong relationship between the K-τ regression lines of Figure 3 and the optimum K-τ values derived from the postulated performance index.

F. Conclusions and Extensions

Conclusions

From the data summarized in Figures 7-9 several tentative conclusions can be drawn.
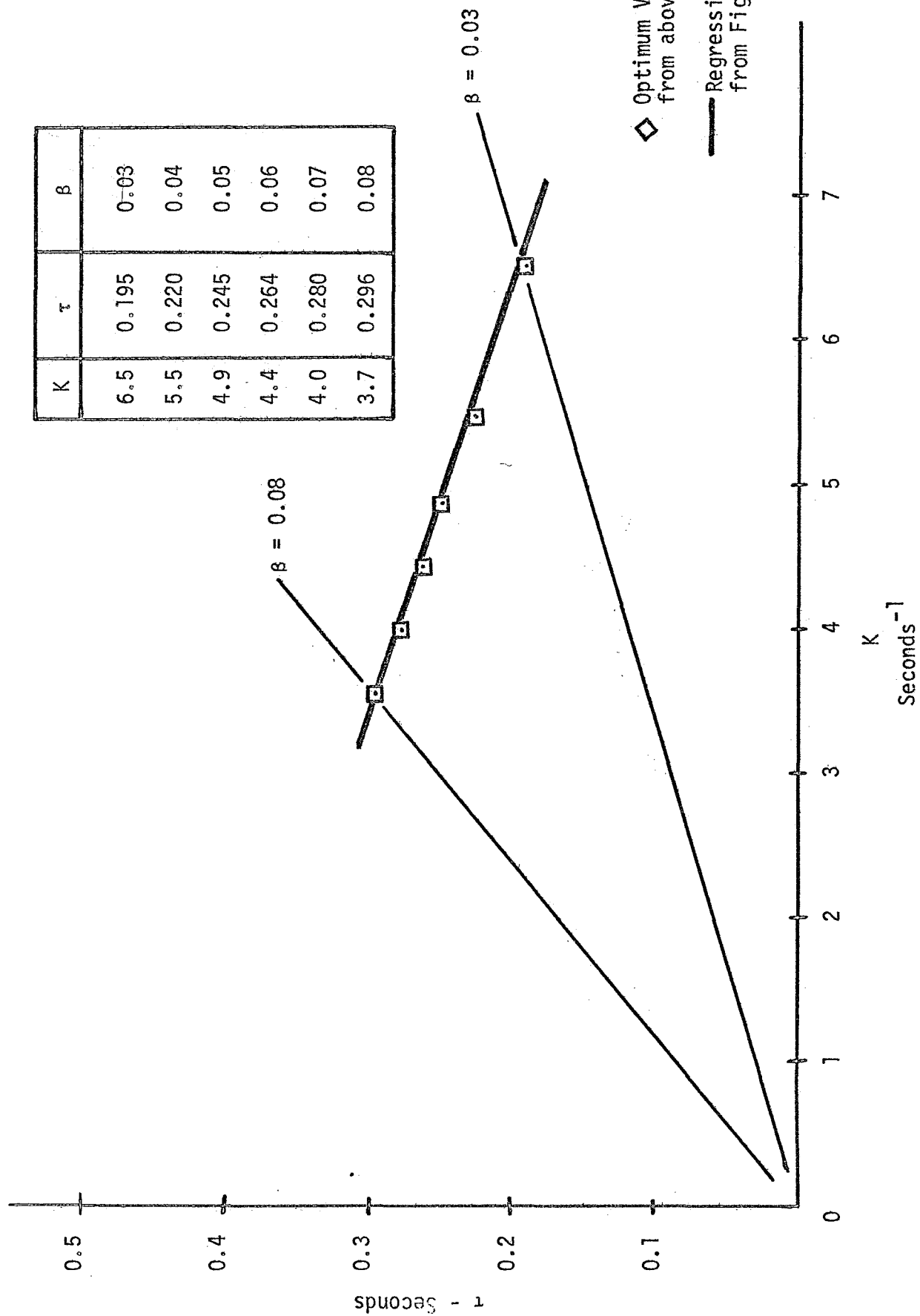
Figure 7 Optimum K and τ Values, $J = MSE + 2.5(MSC)$, $Y_C(s) = \frac{5}{s}$, $T = 1$

K	τ	β
6.5	0.195	0.03
5.5	0.220	0.04
4.9	0.245	0.05
4.4	0.264	0.06
4.0	0.280	0.07
3.7	0.296	0.08

◇ Optimum Values
   from above

━━ Regression line
   from Figure 3

$\beta = 0.03$

$\beta = 0.08$

K
Seconds^{-1}

τ - seconds

K	τ	β
6.3	0.189	0.03
5.3	0.212	0.04
4.5	0.225	0.05
4.0	0.240	0.06
3.6	0.252	0.07
3.2	0.256	0.08

$\beta = 0.08$

$\beta = 0.3$

O Optimum values from above

— Regression line from Figure 3

K
Seconds^{-1}

τ - Seconds
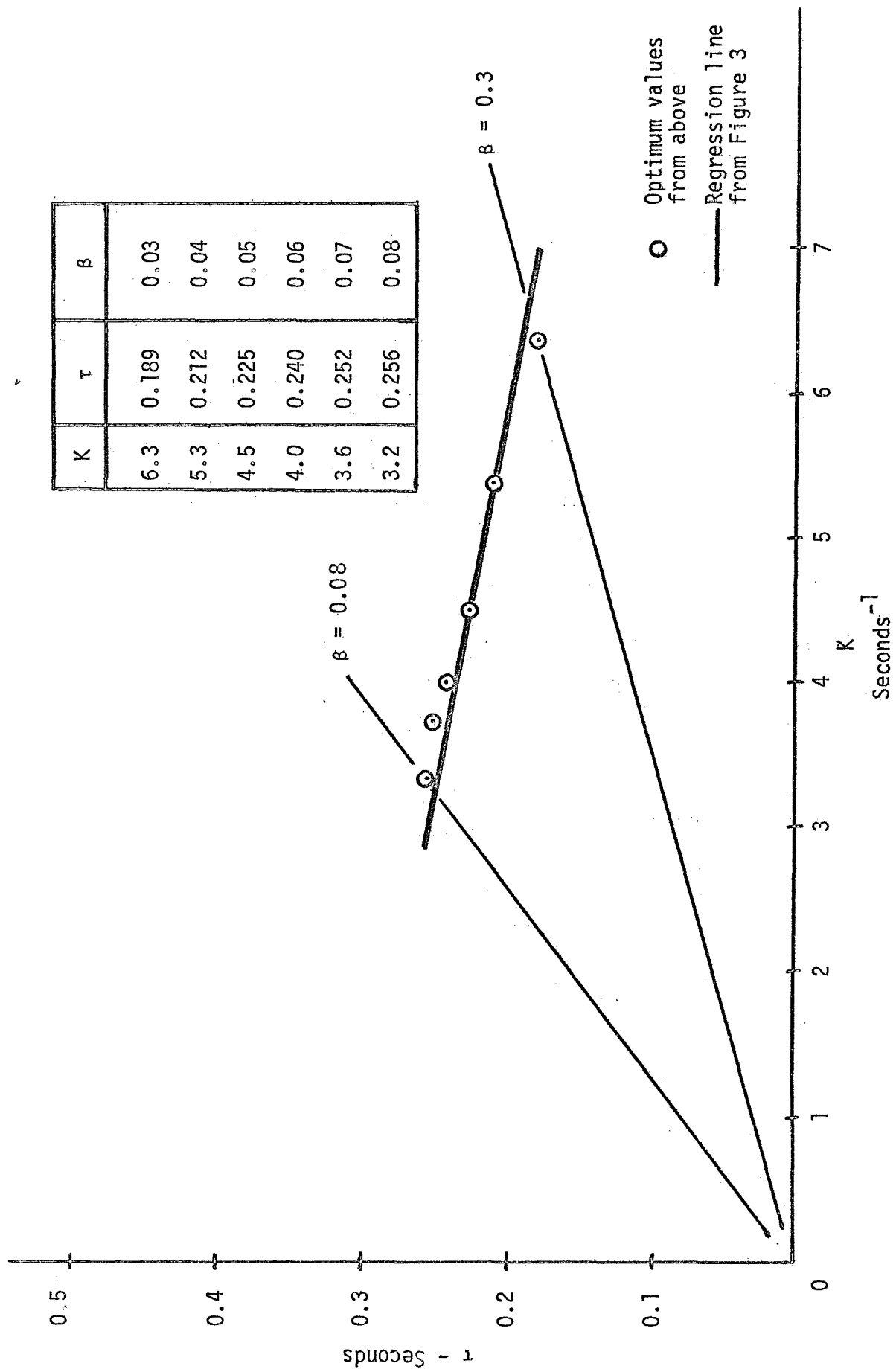
Figure 8 Optimum K and τ Values, $J = MSE + 0.25(MSC)$, $Y_c(s) = \frac{5}{s}$, $T = 0.5$

20.

K	τ	β
5.1	0.306	0.06
4.7	0.329	0.07
4.3	0.344	0.08
4.0	0.360	0.09
3.8	0.380	0.10
3.6	0.398	0.11
3.4	0.408	0.12

◇ Optimum values
    from above

—— Regression line
    from Figure 3

Figure 9 Optimum K and τ Values, J = MSE, $Y_c(s) = \frac{5}{s^2}$, T = 1

21.

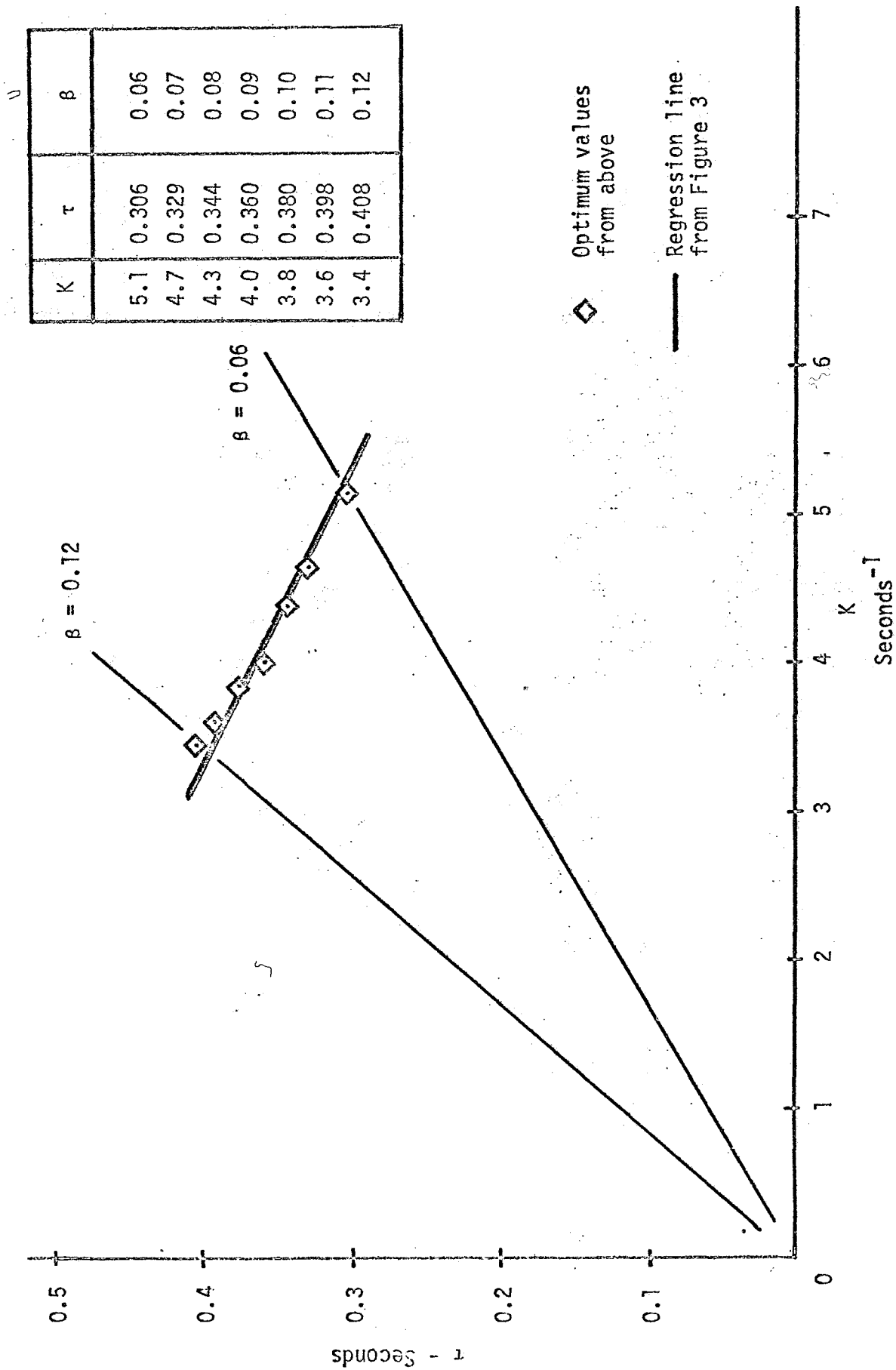(1) The postulated optimum strategy yields crossover model parameters which are in close agreement with the data obtained from six subjects and two controlled elements which were available for analysis. Thus, the hypothesis that subjects in compensatory control systems essentially minimize the performance index $J = \overline{e^2} + \alpha \overline{c^2}$ for their associated crossover model, under the constraint $\tau = \beta K$, appears valid and warrants further experimental analysis.

(2) For a given test condition a unique value of α in the performance index $J = \overline{e^2} + \alpha \overline{c^2}$ exists which is the same for all subjects. The β's in the constraint $\tau = \beta K$, however, vary between subjects. The conclusion can be drawn that all subjects minimize the same performance index, but arrive at different parameter values due to the subject's varying abilities in controlling higher frequency components.

(3) Test Conditions 1, 2 and 3 are arranged in order of increasing task difficulty. The value of α shows a definite tendency to decrease as task difficulty increases. This implies that subjects penalize control effort more on easier tasks than they do for harder tasks. They can "keep the error small" and still conserve control energy when the task is easy. However, as the task becomes harder this is not true, and they thus trade off control effort in favor of reducing the system error, which is the assigned task.

22.

Extensions:

(1) Since only six subjects were used in obtaining the experimental data from which the postulates were drawn and evaluated, several additional subjects should be run to see if their model coefficients fall on the same regression lines as found for the first subjects. This extension has been started, and is making extensive use of both the equipment purchased under this grant, and Oakland University's new Hybrid computer facility.

(2) If the postulates are correct, the changes in the values of K and τ for a given trained subject, due to small variations in the spectrum of the input signal, should be predictable. An interesting area of research would be to see if this prediction can indeed be made.

23.

G. <u>References</u>

1. Summers, L. G. and Ziedman, K.: A Study of Manual Control Methodology with Annotated Bibliography. NASA CR-125, November 1964.

2. McRuer, D. T. and Krendel, E. S.: Dynamic Response of Human Operators. WADC-TR-56-524, October 1957.

3. McRuer, D. T. and Graham, D.: Analysis of Nonlinear Control Systems. John Wiley and Sons, Inc., 1961.

4. Bekey, G. A., Meissinger, H. F., and Rose, R. E.: A Study of Model Matching Techniques for the Determination of Parameters in Human Pilot Models. TRW-STL-8426-6006-RUOO, May 1964.

5. Adams, J. J.: A Simplified Method for Measuring Human Performance. NASA TN-1782, 1963.

6. Elkind, J. I.: Further Studies of Multiple Regression Analysis of Human Pilot Dynamic Response; A Comparison of Analysis Techniques and Evaluation of Time-Varying Measurements. ASK-TDR-63-618, March 1964.

7. McRuer, D. T., Graham, D., Krendel, E. S., and Reisener, W. Jr.: Human Pilot Dynamics in Compensatory Systems. AFFDL-TR-65-15, July 1965.

8. Jackson, G. A.: Measuring Human Performance with a Parameter Tracking Version of the Crossover Model. NASA-CR-910, October 1967.

9. Jackson, G. A.: A Method for the Direct Measurement of Crossover Model Parameters. IEEE Transactions on Man-Machine Systems, Vol. MMS-10, No. 1, pp. 27-33, March 1969.

10. McRuer, D. T. and Jex, H. R.: A Review of Quasi-linear Pilot Models. IEEE Transactions on HFE, Vol. HFE-8, No. 3, pp. 231-249, September 1967.

11. Wolkovitch, J., and Magdaleno, R.: Performance Criteria for Linear Constant Coefficient Systems with Random Inputs: ASD-TDR-62-470, January 1963.

12. McRuer, D. T., Hofmann, L. G., Jex, H. R., Moore, G. P., Phatak, A. V., Weir, D. H., and Wolkovitch, J.: New Approaches to Human-Pilot/ Vehicle Dynamic Analysis. AFFDL-TR-67-150, February 1968.

13. Eveleigh, V. W.: Adaptive Control and Optimization Techniques. McGraw-Hill Book Company, Appendix A., 1967.

H. Appendix

Subject Tracking Data

Each K and τ value in the following tables was determined by averaging over those K-τ values determined in 5 two-minute tracking tasks. These experimental tests are discussed at length in references [8,9].

Table 1

$$Y_c(s) = 5/s$$

Subject No.	Day of Training	Input Filter Time Constant (Seconds)	K (seconds^{-1})	τ (seconds)
1	2	1.0	4.92	0.240
	2	0.5	3.63	0.221
	4	1.0	5.23	0.240
	4	0.5	4.61	0.234
	6	1.0	5.52	0.215
	6	0.5	5.08	0.201
	8	1.0	6.55	0.194
	8	0.5	5.70	0.198
	10	1.0	6.79	0.198
	10	0.5	6.05	0.206
2	2	1.0	4.95	0.245
	2	0.5	4.24	0.231
	4	1.0	6.10	0.216
	4	0.5	5.75	0.206
	6	1.0	6.61	0.210
	6	0.5	6.30	0.205
	8	1.0	7.28	0.172
	8	0.5	6.39	0.192
	10	1.0	6.31	0.202
	10	0.5	6.62	0.188
3	2	1.0	3.93	0.282
	2	0.5	3.01	0.249
	4	1.0	4.42	0.281
	4	0.5	3.33	0.246
	6	1.0	4.25	0.266
	6	0.5	3.75	0.233
	8	1.0	4.50	0.253
	8	0.5	4.45	0.234
	10	1.0	4.54	0.273
	10	0.5	3.83	0.229

25.

Table 2

$$Y_c(s) = 5/s^2$$

Subject No.	Day of Training	Input Filter Time Constant (Seconds)	K (seconds^{-1})	τ (seconds)
4	3	1.0	3.32	0.392
	5		4.12	0.347
	7		3.90	0.353
	9		4.80	0.301
5	3	1.0	4.19	0.365
	5		4.30	0.367
	7		4.14	0.357
	9		4.65	0.329
6	3	1.0	3.56	0.384
	5		4.03	0.369
	7		4.10	0.373
	9		4.64	0.325

III. GRANT ACTIVITIES

Publication: The results of this research will be submitted for presen-tation at the 6th Annual Manual Control Conference to be held in March 1970. After the extensions to this research have been completed, the material will be submitted for publication in the IEEE Transactions on Man-Machine Systems.

Personnel Supported by the Grant

Glenn A. Jackson, Principal Investigator.

Robert White, Undergraduate Research Assistant.